

**NASA TECHNICAL
MEMORANDUM**

November 1974

NASA TM X-64881



MSFC INTEGRATED EXPERIMENTS PRELIMINARY REPORT

Skylab Program Office

PROPERTY OF
NASA
MARSHALL SPACE FLIGHT CENTER

NASA

*George C. Marshall Space Flight Center
Marshall Space Flight Center, Alabama*

1. REPORT NO. NASA TM X-64881	2. GOVERNMENT ACCESSION NO.	3. RECIPIENT'S CATALOG NO.
4. TITLE AND SUBTITLE MSFC INTEGRATED EXPERIMENTS PRELIMINARY REPORT		5. REPORT DATE November 1974
		6. PERFORMING ORGANIZATION CODE
7. AUTHOR(S)		8. PERFORMING ORGANIZATION REPORT #
9. PERFORMING ORGANIZATION NAME AND ADDRESS George C. Marshall Space Flight Center Marshall Space Flight Center, Alabama 35812		10. WORK UNIT NO.
		11. CONTRACT OR GRANT NO.
12. SPONSORING AGENCY NAME AND ADDRESS National Aeronautics and Space Administration Washington, D. C. 20546		13. TYPE OF REPORT & PERIOD COVERED Technical Memorandum
		14. SPONSORING AGENCY CODE

15. SUPPLEMENTARY NOTES

16. ABSTRACT

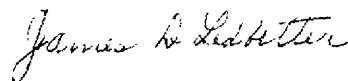
This Technical Memorandum describes the Skylab experiments integrated by the Marshall Space Flight Center, Experiment Development and Payload Evaluation Project Office and presents the preliminary results. Where preliminary results are not yet available, the scientific data collected and returned to the respective Principal Investigator for analyses have been identified. Results of the data analyses will be presented at a later date in the Principal Investigators' final reports.

The Apollo Telescope Mount, Science Demonstrations, the pre- and postflight Medical (M110 series) and Student experiments are not covered in this report.

17. KEY WORDS

18. DISTRIBUTION STATEMENT

Unclassified-unlimited



19. SECURITY CLASSIF. (of this report)

Unclassified

20. SECURITY CLASSIF. (of this page)

Unclassified

21. NO. OF PAGES

145

22. PRICE

NTIS

TABLE OF CONTENTS

	Page
TABLE OF CONTENTS.	iii
LIST OF ILLUSTRATIONS.	v
LIST OF TABLES	vi
DEFINITION OF SYMBOLS.	vii
NONSTANDARD ABBREVIATIONS.	viii
SECTION I. SUMMARY	1
SECTION II. INTRODUCTION.	2
SECTION III. SKYLAB EXPERIMENTS.	5
A. Biomedical.	5
1. M071 Mineral Balance.	7
2. M073 Bioassay of Body Fluids.	7
3. M074 Specimen Mass Measurement.	8
4. M092 In-Flight Lower Body Negative Pressure	8
5. M093 Vectorcardiogram	9
6. M131 Human Vestibular Function.	10
7. M133 Sleep Monitoring	11
8. M151 Time and Motion Study.	11
9. M171 Metabolic Activity	12
10. M172 Body Mass Measurement.	13
B. Earth Resources	14
1. S190A Multispectral Cameras	15
2. S190B Earth Terrain Camera.	18
3. S191 Infrared Spectrometer.	18
4. S192 Multispectral Scanner.	20
5. S193 Microwave Radiometer/Scatterometer and Altimeter	22
6. S194 Microwave L-Band Radiometer.	24
C. Space Physics	26
1. S009 Nuclear Emulsion	26
2. S019 UV Stellar Astronomy	28
3. S020 UV/X-Ray Solar Photography	29
4. S063 UV Airglow Horizon Photography	31
5. S073 Gegenschein/Zodiacal Light	32
6. S149 Particle Collection.	33
7. S150 Galactic X-Ray Mapping	34

	Page
8. S183 Ultraviolet Panorama.	35
9. S201 Far UV Electronographic Camera.	36
10. S228 Trans-Uranic Cosmic Rays.	39
11. S230 Magnetospheric Particle Composition	41
12. S233 Kohoutek Photometric Photography.	42
13. Proton Spectrometer.	42
D. Materials Processing	44
1. M512 Materials Processing Facility	44
2. M479 Zero-Gravity Flammability	51
3. M551 Metals Melting.	54
4. M552 Exothermic Brazing.	57
5. M553 Sphere Forming.	60
6. M555 GaAs Crystal Growth	61
7. M518 Multipurpose Electric Furnace System. . . .	64
8. M556 Vapor Growth of IV-VI Compounds	66
9. M557 Immiscible Alloy Composition.	70
10. M558 Radioactive Tracer.	76
11. M559 Microsegregation in Germanium	80
12. M560 Growth of Spherical Crystals.	81
13. M561 Whisker-Reinforced Composites	86
14. M562 Indium Antimonide Crystal Growth.	88
15. M563 Mixed III-V Crystal Growth.	93
16. M564 Halide Eutectics.	100
17. M565 Silver Grids Melted in Space.	101
18. M566 Aluminum-Copper Eutectics	110
E. Engineering/Operations	112
1. D024 Thermal Control Coating	112
2. M415 Thermal Control Coatings.	114
3. M487 Habitability/Crew Quarters.	119
4. M509 Astronaut Maneuvering Equipment	121
5. T002 Manual Navigation Sightings	122
6. T003 In-Flight Aerosol Analysis.	125
7. T013 Crew/Vehicle Disturbance.	126
8. T020 Foot-Controlled Maneuvering Unit.	127
F. Contamination.	128
1. T025 Coronagraph Contamination Measurement . .	128
2. T027 Contamination Measurement	129
REFERENCES.	134
APPROVAL.	137

LIST OF ILLUSTRATIONS

Figure	Title	Page
1.	Skylab S190A Resolution Comparison	17
2.	Typical S190B Photography.	19
3.	Typical S191 Spectra Data	20
4.	S192 Multispectral Scanner Imagery of Holt County, Nebraska	21
5.	Imagery from the Yuma, Arizona Region obtained with the Improved Thermal Detector	21
6.	Radiometer/Scatterometer Data from Hurricane Ava . . .	23
7.	SL-2 Groundtrack for Altimeter Data	23
8.	Altimeter Range Measurements	24
9.	Example of Data Produced by the S194 Sensor	25
10.	Large Magellanic Cloud (SL-2 DAC Photograph)	37
11.	Comet Kohoutek and Target Stars (SL-4 Photograph) . .	38
12.	M512 Materials Processing Facility	47
13.	Experiment Operational Configuration (M551, M553) . .	49
14.	Experiment Operational Configuration (M552, M479) . .	50
15.	Returned M479 Samples	52
16.	Burning of Polyurethane Foam on SL-4	53
17.	Metals Melting Assembly	55
18.	Skylab Stainless Steel Sample	56
19.	Exothermic Brazing Package	58
20.	Sphere Forming Assembly	62
21.	Photographs of M553 Samples	63
22.	Multipurpose Electric Furnace	65
23.	M518 MEFS Installed on M512 MPF	67
24.	Deposition of GeSe Crystals	71
25.	Largest GeSe Crystal Growth	72
26.	Gold-Germanium Dispersion	74
27.	Lead-Zinc-Antimony Dispersion	75
28.	M558 Ground Based Sample A-13	77
29.	M558 Ground Based Sample B-13	77
30.	M558 Ground Based Sample A-1	78
31.	M558 Flight Sample A-6	78
32.	M558 Flight Sample B-5	79
33.	M558 Flight Sample A-7	79
34.	X-Ray Shadowgraphs of SL-3 Cartridges	83
35.	X-Ray Shadowgraphs of Ground Test Sample after Thermal Testing	83
36.	Sample Processed During SL-3	84
37.	Sample Processed During SL-4	84
38.	Microstructure of SL-3 Samples	89
39.	Microstructure of SL-4 Samples	90
40.	Crystalline Homogeneity Improvement	92

Figure	Title	Page
41.	SL-3 Free Surface Configuration	92
42.	SL-4 Free Surface Configuration	94
43.	Intentional Crystal Growth Discontinuity	94
44.	Photograph of Casting	97
45.	Photographs of Cast Ingots	97
46.	SL-3 Ingots	98
47.	SL-4 Ingots	99
48.	Continuous Sodium Fluoride Fibers	102
49.	Sodium Fluoride Fibers	102
50.	Side Views of Skylab-Tested Fibre Specimens	105
51.	Sectioned Samples	106
52.	Polished Section through Skylab Sample X6	107
53.	Ampoule X-rays	108
54.	Skylab Sample 1BP6 Showing Piping and Substructure X92	109
55.	Skylab Sample 1BP7-8 Showing Cellular Solidification Substructure X20	109
56.	Experiment D024 Polymer Film Strip	115
57.	Reflectance Versus Wavelength for S230 Aluminum Foil 4-2	131

LIST OF TABLES

Table	Title	Page
I.	Skylab Flight Experiments/Instrument Integrated by SL-DP	3
II.	Biomedical Experiment Performances	6
III.	Accomplishment of Experiment Functional Objectives	27
IV.	Experiment S020 Operations	30
V.	Ultraheavy Cosmic Rays found in First Scan	40
VI.	Accomplishment of Experiment Functional Objectives	45
VII.	Transport Reactions and Experimental Conditions	69
VIII.	Summary of NASA Experiments	96
IX.	Accomplishment of Experiment Functional Objectives	113
X.	D024 Thermal Control Materials Listing	116
XI.	Polymeric Film Strip Materials	119
XII.	Sample Characteristics	119
XIII.	T002 SL-3 Mission Results	124

DEFINITION OF SYMBOLS

<u>SYMBOL</u>	<u>DEFINITION</u>
\AA	Angstroms
$^{\circ}\text{C}$	Degree Celcius
H^3	Tritium - hydrogen isotope
${}^3_2\text{He}$	Helium isotope
${}^4_2\text{He}$	Alpha particle - helium isotope
i.e.	That is
$^{\circ}\text{K}$	Degree Kelvin
OH	Hydroxyl ion
μ	Micro

NONSTANDARD ABBREVIATIONS

AMS	Articulated mirror system
amu	Atomic mass unit
ARC	Ames Research Center
ATM	Apollo Telescope Mount
AU	Astronomical unit
CM	Command Module
CMG	Control moment gyro
cm	Centimeter
CSM	Command and Service Module
DA	Deployment Assembly
DAC	Data acquisition camera
DOY	Day of year
etc	Etcetera
EREP	Earth Resource Experiment Package
EVA	Extravehicular Activity
FCMU	Foot controlled maneuvering unit
FO	Functional Objectives
GBT	Ground Base Test
G/R	Temperature gradient/growth rate
hr	Hour
IR	Infrared
JSC	Lyndon B. Johnson Space Center
kev	Thousand electron volts
km	Kilometers

KW	Kilowatt
ma	Milliamperes
MDA	Multiple Docking Adapter
Mev	Million electron volt
mm	Millimeter
MPF	Multi-Purpose Furnace
MSFC	George C. Marshall Space Flight Center
NASA	National Aeronautics and Space Administration
nm	Nautical miles
NRL	Naval Research Laboratories
PI	Principal Investigator
PS	Photometer system
rpm	Revolutions per minute
SA	Sample array
SAL	Scientific Airlock
SI	Solar inertial
v	Volts

TECHNICAL MEMORANDUM X-64881

MSFC INTEGRATED EXPERIMENTS

PRELIMINARY REPORT

SECTION I. SUMMARY

The Experiment Development and Payload Evaluation Project Office at the George C. Marshall Space Flight Center (MSFC) integrated fifty-six experiments on Skylab that supported investigations in six scientific disciplines. There were ten medical experiments to assist in understanding man's ability to live and operate efficiently during extended space flights. Six earth resource experiments provided information fundamental to the effective use and conservation of natural resources. Twelve experiments and one operational instrument were flown on Skylab to provide data for space physics studies that cannot be observed effectively through the earth's shielding atmosphere. Eighteen experiments were performed to study material processing in the absence of the earth's environmental characteristics, i.e., atmosphere and gravity. Eight engineering/operations experiments provided spacecraft design knowledge to enhance living and working in space. Two experiments were to determine surface deposition and sunlight scattering by spaceborne contaminants.

This document provides the preliminary results of the MSFC integrated experiments if available, or a definition of the return data that is being analyzed and evaluated by the Principal Investigator (PI).

The experiment program was a success in spite of the early anomaly, i.e., the meteoroid shield and solar panel loss which resulted in available power reduction and the non-availability of the solar scientific airlock (SAL) for experiment operations. This success was attributed to the work-arounds that were developed and executed by the ground support personnel and the Skylab flight crews. In addition, the real-time flight planning effort proved to be a significant contribution to the high percent of experimental program accomplishments.

SECTION II. INTRODUCTION

The Experiment Development and Payload Evaluation Project Office (SL-DP) was responsible for integrating 75 experiments and the Proton Spectrometer, an operational instrument.

This report provides a single reference source of the existing preliminary experiment data results. Part of the data included has been extracted from the available published documents and technical papers which have been presented to various societies. The sources, where available, are noted in the subject material and listed in the Reference Section. Preliminary results contained herein have been coordinated with PIs and appropriate NASA personnel.

This report identifies the PI, his organizational affiliation, the experiment objective, the preliminary data results or the type of data collected during the Skylab missions for each SL-DP integrated experiments.

The preliminary results for the nineteen student experiments, which were integrated by SL-DP, are presented in the "MSFC Skylab Student Project Report". Table I lists the experiments and indicates the NASA center development and integration responsibilities.

TABLE I. SKYLAB FLIGHT EXPERIMENTS/INSTRUMENT INTEGRATED BY SL-DP

NUMBER	EXPERIMENT TITLE	DEVELOPMENT RESPONSIBILITY		INTEGRATION RESPONSIBILITY
		MSFC	JSC	MSFC
D024	Thermal Control Coatings	X(DOD)		X
M071	Mineral Balance		X	X
M073	Bioassay of Body Fluids		X	X
M074	Specimen Mass Measurement		X	X
M092	Inflight Lower Body Negative Pressure		X	X
M093	Vectorcardiogram		X	X
M131	Human Vestibular Function		X	X
M133	Sleep Monitoring		X	X
M151	Time and Motion Study		X	X
M171	Metabolic Activity		X	X
M172	Body Mass Measurement		X	X
M415	Thermal Control Coatings	X		X
M479	Zero Gravity Flammability	X		X
M487	Habitability/Crew Quarters	X		X
M509	Astronaut Maneuvering Equipment		X	X
M512	Materials Processing Facility	X		X
M518	Multipurpose Electric Furnace System	X		X
M551	Metals Melting	X		X
M552	Exothermic Brazing	X		X
M553	Sphere Forming	X		X
M555	GaAs Crystal Growth (Not Launched)	X		X
M556	Vapor Growth of IV-VI Compounds	X		X
M557	Immiscible Alloy Composition	X		X
M558	Radioactive Tracer	X		X
M559	Microsegregation in Germanium	X		X
M560	Growth of Spherical Crystals	X		X
M561	Whisker-Reinforced Composites	X		X
M562	Indium Antimonide Crystal Growth	X		X
M563	Mixed III-V Crystal Growth	X		X
M564	Halide Eutectics	X		X
M565	Silver Grids Melted in Space	X		X

TABLE I. SKYLAB FLIGHT EXPERIMENTS/INSTRUMENTS INTEGRATED BY SL-DP (Concluded)

NUMBER	EXPERIMENT TITLE	DEVELOPMENT RESPONSIBILITY		INTEGRATION RESPONSIBILITY
		MSFC	JSC	MSFC
M566	Aluminum-Copper Eutectic			
S009	Nuclear Emulsion	X		X
S019	UV Stellar Astronomy		X	X
S020	UV/X-Ray Solar Photography		X	X
S063	UV Airglow Horizon Photography		X	X
S073	Gegenschein/Zodiacal Light	X		X
S149	Particle Collection		X	X
S150	Galactic X-Ray Mapping	X		X
S183	Ultraviolet Panorama	X(FRANCE)		X
S190A	Multispectral Cameras		X	X
S190B	Earth Terrain Camera		X	X
S191	Infrared Spectrometer		X	X
S192	Multispectral Scanner		X	X
S193	Microwave Radiometer/Scatterometer & Altimeter		X	X
S194	Microwave L-Band Radiometer		X	X
S201	Far UV Electronographic Camera		X	X
S228	Trans-Uranic Cosmic Rays	X		X
S230	Magnetospheric Particle Composition	X		X
S233	Kohoutek Photometric Photography		X	X
T002	Manual Navigation Sightings	X(ARC)		X
T003	Inflight Aerosol Analysis	X(DOT)		X
T013	Crew/Vehicle Disturbance	LaRC		X
T020	Foot-Controlled Maneuvering Unit	LaRC		X
T025	Coronagraph Contamination Measurement		X	X
T027	Contamination Measurement	X		X
	TOTAL EXPERIMENTS - 56			
OPERATIONAL INSTRUMENT				
	Proton Spectrometer	X		X

SECTION III. SKYLAB EXPERIMENTS

A. Biomedical

Pre-Skylab missions (up to 14 days duration) have shown that exposures to the space environment produce changes in the astronauts' body tissues and systems. Even though changes were expected and predicted, certain ones often differed from the predictions. Skylab offered excellent opportunities for detailed studies of extended space flight effects on man's physiological well being while providing meaningful baseline data for verifying earlier predictions and for predicting the future, longer-duration space flight effects on man.

The Skylab biomedical experiments were developed to provide systematic investigations and observations of man under controlled conditions to determine his capabilities to live and work for prolonged periods in the space environment. Experiments selected for performance on the three Skylab missions may be categorized into the following general biomedical disciplines:

- Mineral and hormonal balance,
- Hematology and immunology,
- Cardiovascular status,
- Energy expenditure,
- Neurophysiology and
- Biology.

Development responsibility for all biomedical experiments was assigned to the Lyndon B. Johnson Space Center (JSC), Houston, Texas. Integration responsibility for those experiments having total or partial dependence on carrier hardware and systems was assigned to the MSFC, Huntsville, Alabama. These experiments are:

- M071 Mineral Balance,
- M073 Bioassay of Body Fluids,
- M074 Specimen Mass Measurement,
- M092 In-Flight Lower Body Negative Pressure,
- M093 Vectorcardiogram,
- M131 Human Vestibular Function,
- M133 Sleep Monitoring,
- M151 Time and Motion Study,
- M171 Metabolic Activity and
- M172 Body Mass Measurement.

Table II provides: the total number of planned performances, the performances accomplished during each manned flight and the degree of success.

TABLE II. BIOMEDICAL EXPERIMENT PERFORMANCES

EXPERIMENT TITLE	PERFORMANCES PLANNED	PERFORMED			ACCOMPLISHMENT (Percent)
		SL-2	SL-3	SL-4	
Medical [1, 2, 3]					
M071 Mineral Balance	507	28	60	403	97
M073 Bioassay of Body Fluids	171	28	59	77	96
M074 Specimen Mass Measurement	12	4	3	3	83
M092 Inflight Lower Body Negative Pressure	153	22	50	67	91
M093 Vectorcardiogram	153	22	49	63	88
M131 Human Vestibular Function	91	14	24	43	89
M133 Sleep Monitoring	44	12	20	18	114
M151 Time and Motion Study	81	23	29	29	100
M171 Metabolic Activity	75	19	28	36	111
M172 Body Mass Measurement	9	3	3	3	100

1. M071 Mineral Balance. The PI for Experiment M071 is Dr. Donald Whedon, National Institute of Health, Bethesda, Maryland.

This experiment was to obtain data required for subsequent determinations of space flight effects on man's muscle and skeletal systems. Inflight data obtained from each crewman included: accurate food intake records (quantity and composition); accurate fluid intake records; daily body mass measurements; pooled urine samples; all feces and vomitus, if any. In addition, inflight blood samples (collected as an M110 objective) were required by M071 and M073. The records and returned samples are being analyzed and evaluated to obtain quantitative assessments of the pertinent biochemical (metabolic) constituent changes, particularly water, calcium and nitrogen during space flight.

The experiment utilized operational hardware provided by the OWS and experiment hardware provided by M074 and M172.

Data for each crewman was obtained during the mission pre-flight, inflight and postflight phases with no significant problems identified.

Preliminary experiment findings are summarized as follows: "Mineral balance studies were performed on the three Skylab visits. Results from the first two visits indicate that the composition of the body is changed during exposure to weightlessness as evidenced by significant losses of calcium, nitrogen, and other nutrients. Analysis of the third visit data are not yet complete; however, preliminary results show that the caloric requirements during exposure to zero gravity are near the one-g requirements." [3]

2. M073 Bioassay of Body Fluids. The PI for Experiment M073 is Dr. Carolyn Leach, JSC, Houston, Texas.

The experiment's purpose was to collect inflight urine samples from each crewman, preserve by freezing, and return them for postflight analysis and comparison with similar preflight and postflight data. Analytical results, along with blood analysis and dietary and fluid ingestion control data, are being used to provide an insight into the metabolic changes that occur during space flight.

The experiment utilized operational hardware (Habitability Support System) for the urine sample collection and processing and also utilized dietary and fluid ingestion control, blood and body mass data obtained from experiments M071, M110, M074 and M172 protocols. Data for each crewman was obtained during the mission preflight, inflight and postflight phases; no significant problems were identified.

Preliminary experiment findings are summarized as the following: "A preliminary review of the inflight data reveals metabolic changes in each man, suggesting a process of adaption to the space flight environment. These changes were manifested by an apparent aldosteronism that resulted in some sodium conservation and slight losses of potassium. Total body exchangeable potassium was decreased 4 to 12 percent in the three men. Cortisol was significantly elevated in the inflight and postflight samples from all three men. Epinephrine and norepinephrine were decreased in the inflight sample and increased in the postflight sample." [3]

"The data collected compare very favorably with the overall results of the first two visits with the main difference being in the early phase of each visit." [3]

3. M074 Specimen Mass Measurement. The PI for Experiment M074 is Dr. William Thornton, JSC, Houston, Texas.

The experiment's purpose was to utilize a specimen measurement device (using a linear spring/mass pendulum) for the mass determination of various objects in zero-g. The objectives were to: demonstrate mass measurement without gravity; validate theoretical characteristics of the device; and support biomedical experiments (M071 and M073) during mass determinations.

Reference calibrations (using known masses) were performed during the three missions and mass measurements of food residue and fecal samples were also performed to support experiments M071 and M073.

A summary of experiment performance follows: "The specimen mass measurement device demonstrated reasonably good stability throughout all three visits, far better than that required for operational purposes. These instruments demonstrated routine mass measurement in space (for the first time) and performed adequately for medical support purposes. In addition to the problems encountered on the third visit, an electronic package failed during the first manned visit and the package was subsequently replaced during the second Skylab visit." [3]

4. M092 In-Flight Lower Body Negative Pressure. The PI for Experiment M092 is Dr. Robert Johnson, JSC, Houston, Texas.

This experiment utilized a lower body negative pressure device, a limb volume measuring system, and a blood pressure measurement system. It was designed to determine the cardiovascular deconditioning time course during space flight and provide data for predicting the degree of orthostatic intolerance and physical capacity impairment expected following return to earth's environment. Inflight data was collected from each crewman who periodically performed as the test subject, with a second crewman in attendance as observer.

Experiment data was collected, as planned, throughout the Skylab missions. An experiment vacuum source modification was necessary early in the third visit. This modification allowed the vacuum source to be provided from the S-IVB stage liquid oxygen tank (which was not removed when the stage was converted to the Workshop). The modified system operation was satisfactory throughout the third visit.

Preliminary experiment results follow: "In almost all cases, the inflight resting heart rates of all three crewmen were elevated slightly above the preflight ranges. This characteristic was least pronounced in the Commander who sometimes demonstrated low resting heart rates early in the visit. After 6 weeks of flight, the Commander's resting and stressed heart rates were usually close to or within preflight ranges. By the end of 7 weeks, the Pilot also showed a tendency toward lowered resting and stressed heart rates.

Increases in calf volume during negative pressure, as in the first and second visit crewmen, were much higher than the preflight values. These increases, which reached to as high as 9 or 10 percent in the Scientist Pilot and Pilot, made it necessary to replace the reference band with a backup band after visit day 37. The reference band was returned to verify the authenticity of the high readings.

The loss of calf girth in the third visit crew was smaller than in either the first or second crew. Neither the initial loss nor the subsequent downward trend was as great as previously recorded, and after the first 6 or 7 weeks, no consistent downward trend occurred.

The postflight cardiovascular responses to lower body negative pressure appeared to be quite similar to those observed in the second visit crew. By the fifth day after flight, the resting and stressed heart rates were very close to the preflight ranges." [3]

5. M093 Vectorcardiogram. The PI for Experiment M093 is Dr. Newton Allebach, Naval Aerospace Medical Institute, Pensacola, Florida.

This experiment was to measure electrocardiographic potentials of each crewman during the mission preflight, inflight and postflight phases. Changes noted in the heart's electrical activity are to be correlated with prolonged weightlessness and other stress conditions and compared to changes known to occur after specific physiological interventions. In addition, vectorcardiogram measurements were taken to detect and measure significant cardiac events and cardiac system changes during space flight.

No significant protocol violations were noted during the experiment performances.

The following summarizes the preliminary results: "The initial evaluation of postflight data indicates a rapid return of the various vectorcardiogram parameters toward preflight values. Inflight and postflight vectorcardiogram alterations seem to follow the trends observed on the previous two visit crews." [3]

6. M131 Human Vestibular Function. The PI for Experiment M131 is Dr. Ashton Graybiel, Naval Aerospace Medical Institute, Pensacola, Florida.

This experiment was to determine: whether the astronaut's susceptibility to semicircular canal stimulation changes as a function of time in zero-g and whether prolonged absence of gravitational stimuli produced changes in gravity receptor activity and thus change the astronaut's judgement of spatial coordinates. The experiment was accomplished by rotating each crewman (as a test subject seated in a chair) about an axis which passes through the subject's center-of-gravity and is perpendicular to a plane passing through the lateral canals. The chair was rotated at a predetermined rotational velocity and at a predetermined programmed rotational acceleration/deceleration profile.

The following summarizes the preliminary experiment findings: "The most significant data yielded from experiment M131 was in the area of motion sickness. Five of the nine Skylab crewmen experienced some degree of discomfort that resembled motion sickness during the first several days of the visit. Following this initial period of adaptation, all crewmen became essentially immune to motion sickness as provoked by the experiment M131 protocol. This increased tolerance to vestibular stress transferred to the postflight period for all crewmen. The first and second visit crew did not return to their baseline levels of susceptibility until approximately 60 days after recovery.

No overall trends have been detected with either the oculogyral illusion or spatial localization tests; however, detailed comparisons of data from the three visits are not complete. Some crewmen tended to see the oculogyral illusion with slightly greater frequency

inflight while others saw the illusion with equal or slightly lesser frequency than preflight. The important fact is that all crewmen could see the illusion in zero gravity and this indicates that the semi-circular canals of the inner ear were intact and were functioning normally." [3]

7. M133 Sleep Monitoring. The PI for Experiment M133 is Dr. James Frost, Baylor School of Medicine and Texas Methodist Hospital, Houston, Texas.

This experiment was to evaluate sleep quantity and quality of one crewman during prolonged space flight. The evaluation was made by an automatic onboard analysis of electroencephalograph (EEG) and electro-oculograph (EOG) activity. The experiment was conducted on specified nights, and the analyzed sleep data was telemetered to the ground for comparison with the subject's preflight baseline data. Data was also recorded onboard and retrieved tapes of such data are being utilized in additional detailed analyses.

Preliminary experiment results are summarized in the following: "A preliminary analysis of the third visit data shows a marked decrease in total rest and total sleep of the Scientist Pilot during the first 35 days of the visit. After 35 days, the Scientist Pilot appeared to approach his preflight baseline level and displayed an increase in the deeper stages of sleep and a corresponding decrease in lighter stages of sleep. The very preliminary analysis indicates that the changes observed in flight on the third visit correspond to some extent with those seen during the 28-day first visit." [3]

"The alterations of the in flight sleeping patterns showed no adverse effect upon the crew performance capability." [3]

8. M151 Time and Motion Study. The PI for Experiment M151 is Dr. J. Kubis, Fordham University, Bronx, New York; Dr. Edward J. McLaughlin, NASA Headquarters, OMSF, Washington, D.C. is the co-investigator.

"The purpose of experiment M151 is to study the adaptability, mobility, and the fine and gross motor activity in work and task performance during space flight. Motion pictures were taken prior to flight and during flight to allow task evaluations." [1]

Twenty-three photographs were taken of crew activities on SL-2, 29 on SL-3 and 29 on SL-4; and these data are being analyzed.

"All photography requirements were accomplished with the exception of documenting one experiment M509 (Astronaut Manuevering Equipment) test. In addition to the requirements, four experiment M092/M093/M171 tests were photographed.

Only a partial screening of the returned 16-mm film from the third visit has been completed. A correlation of this visit voice-dump data with telemetry indicates that the third visit results will compare favorably to those of first and second visits.

The third visit data appears to support the theory that 7 to 14 days are required to fully adapt to the zero gravity environment. The time initially required depends on the nature of the task, and the type and frequency of preflight training accomplished.

The third visit crew bettered their best experiment M092 preflight performance time on their second inflight test which was performed on visit days 10 and 11. There was some variability in the performance time until visit day 30 when the crew consistently began to improve until they were bettering their best preflight time by almost 20 percent.

The importance that good fidelity preflight training has on early inflight performance was the first extravehicular activity. The third visit crew completed the task originally planned for two separate extravehicular activities in one 6 1/2-hour extravehicular activity. The increased efficiency is attributed to the neutral buoyancy training which allowed end-to-end task simulation in the same manner as in zero gravity.

The third visit is significant in that the crew continued to improve their skill working in zero gravity and they returned to earth in good mental and physical condition." [3]

9. M171 Metabolic Activity. The PI for Experiment M171 is Mr. Edward Michel, JSC, Houston, Texas.

This experiment was to measure, using a metabolic analyzer and bicycle-type ergometer, man's metabolic rate while performing mechanical work and resting in a space environment. The crew member's metabolic rates were measured in terms of oxygen consumption and carbon dioxide production. Additional data collected included respiratory exchange ratio, minute volume, vital capacity, body temperature, ergometer work rate, ergometer rpm, and total work. The experiment also afforded an opportunity to evaluate the bicycle ergometer as an exerciser for long duration missions.

Preliminary experiment results are summarized as follows:
"Crew inflight physiological responses to exercise were essentially within the preflight baseline ranges throughout the visit. A decreased vital capacity was observed inflight in all the crewmen, but the decrease did not appear to interfere with their ability to exercise. Evaluation of the postflight pulmonary function tests indicates no significant differences from values obtained preflight,

including vital capacity. Immediately postflight, however, all crewmen exhibited a significant decrement in their response to the experiment exercise protocol as compared to the preflight or inflight responses. The most obvious indications of this were in elevated heart rates and decreased cardiac output for the same workload and oxygen consumption. A significantly decreased postflight stroke volume was observed only in the Commander. All of the changes were of the same order of magnitude as noted in the previous Skylab crews, but the third visit crew returned to normal more rapidly. Preflight baseline range values for most parameters were attained 4 days after recovery." [3]

10. M172 Body Mass Measurement. The PI for Experiment M172 is Dr. William Thornton, JSC, Houston, Texas.

This experiment was to: demonstrate body mass measurement in a zero-g environment; validate theoretical behavior of the device; and support biomedical experiments (M071, M073, and M171). Body mass determinations were made using a linear spring/mass pendulum platform or seat. The mass being measured determined the pendulum period which was electronically timed and converted graphically to direct mass readings.

Preliminary experiment results are summarized as follows: "The body mass measuring experiment was conducted daily by each crewman. The device demonstrated accurate and simple mass measurement of the body in zero gravity. For human mass measurements, repeatability of ± 50 grams was demonstrated, while the absolute maximum error was estimated to be +400 grams or less." [3]

"The body mass measuring device was calibrated three times during the visit. The device had excellent performance and stability; for example, urine samples were measured to an accuracy of a few grams when adequate calibration means were available. The practicality of making mass measurements, other than the human body, was demonstrated on the most difficult material to measure using this method, namely liquids. Urine was measured during the second visit and Coolanol fluid during the third visit." [3]

B. Earth Resources

The Earth Resources Experiment Package (EREP) was a group of six remote sensing instruments, a control and display panel, and a recording system. The general objective was to provide a synoptic survey of selected areas of the earth in visible, infrared and microwave spectral wavelengths. EREP data from some areas is being correlated with information obtained from ground truth site data, data from sensor equipped aircraft underflights and the NASA Earth Resources Technology Satellite. The Skylab Program scope included data for all four seasons.

The major discipline areas that will be benefited by specific applications of the gathered natural and cultural resource data and the monitored environmental and ecological relationship data are: agriculture/range/forestry; geological applications; continental water resources; ocean investigations; atmospheric investigations; coastal zones, shoals and bays; remote sensing techniques development; regional planning and development; and cartography.

All EREP data obtained was on film and magnetic tape. Data was taken during the SL-2 mission over the United States, Mexico, Brazil, Columbia, Nicaragua, Canada and Bolivia. There were eleven earth viewing data sessions and one lunar calibration. Data was recorded on approximately: 41,000 feet of magnetic tape and 13,000 photographs, i.e., 6500 frames by S190A, 960 frames by S190B and 5,400 frames of 16mm film.

During the SL-3 mission there were 39 EREP passes plus two calibrations looking at the earth's limb and the moon. Data was obtained primarily over North and South America, the Atlantic and Pacific Oceans; however, data was obtained over South East Asia, Japan, Australia, Africa, Israel, Arabia, Europe, and the Mediterranean Sea. Data was recorded on approximately 84,000 feet of magnetic tape and 27,000 photographs, i.e., 10,000 frames by S190A, 2,000 frames by S190B and 15,000 frames of 16-mm film.

An innovation was initiated during the SL-3 mission by taking handheld photographs using a Nikon or Hasselblad camera of targets-of-opportunity. The targets that were to be photographed were selected in advance and included active volcanos, earth quake areas, tropical storms, etc. Some were scheduled and others were candidate operations when time was available.

During the SL-4 mission, there were forty EREP passes, three lunar calibrations and three earth limb calibrations. The data was obtained over the United States, and 18 other nations including Mexico, Central and South America and the North Atlantic Ocean and

the Gulf of Mexico. Selected data was obtained over Western Europe, North Africa, Iran, Nepal, Thailand, Indonesia, Australia and Japan. Data was recorded on approximately 95,000 feet of magnetic tape and 38,000 frames of photography, i.e., 18,000 frames by S190A, 3,000 frames by S190B and 17,000 frames of 16mm film. Midway through the data-taking sequences a new improved detector array was installed in the S192 Multispectral Scanner resulting in much improved thermal infrared (IR) imagery.

The SL-4 mission provided cartographic data over Gran Chaco, Paraguay, while the vehicle was in the solar inertial mode. The data obtained also included: the seasonal variations to complement earlier Skylab data; the GEO-C unmanned satellite calibration site and the wind-sea wave height and sea state over the largest storm in a decade.

The SL-4 crew provided many verbal descriptions of ground features from visual observations, such as flooding in Australia.

Data for 141 PI's was obtained and will provide an application or utility in all the stated disciplinary areas. Since the mission, NASA has had a sensor evaluation of the functional performance, geometric performance and radiometric performance conducted on flight data.

The Earth Resources Observation Data Center will provide imagery data to the general public. Their address is:

U.S. Department of the Interior
EROS Data Center
User Services
Sioux Falls, South Dakota 57198
Telephone: 1-605-594-6511

1. S190A Multispectral Cameras. This six-channel commonly boresighted camera provided multispectral photographs in six discrete wavebands from .4 to 0.88 microns. The f/2.8 lenses had a 6-inch focal length. The data will be used mainly for mapping and radiance measurements.

"Four of the cameras were operated with black-and-white film and used optical filters in front of the lens to restrict the spectral bands photographed by the camera. Two of the six camera stations were operated with special haze filters and used color-infrared film in one case and high-resolution color film in the other. Each time the camera was operated, six photographs were taken simultaneously: four with black-and-white film (through the spectral filters), one with color-infrared film, and one with normal color film." [4]

The registration capability of superimposed images from more than one camera station was better than 20 meters on the ground.

"The measured resolution capability of the camera for" the color high resolution "film was approximately 27 m per line pair for high-contrast sites. This resolution was approximately the value expected from preflight tests.

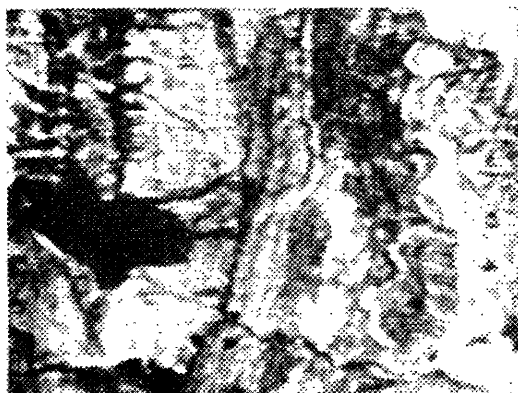
The S190A camera is a radiometric camera in that film density can be related quantitatively to the intensity of radiation incident on the lens. In-flight measurements using the ground sites and the Moon established radiometric calibrations accurate to within ± 30 percent." [4]

"The Skylab S-190A multiband camera products include film positives and prints of four black-and-white bands, color, and color infrared. Resolution of these products varies with markedly lower resolution in the infrared (Fig. 1). The Skylab S-190B color and panchromatic products show an expected resolution improvement over the S-190A with color products normally the most useful for earth resource studies.

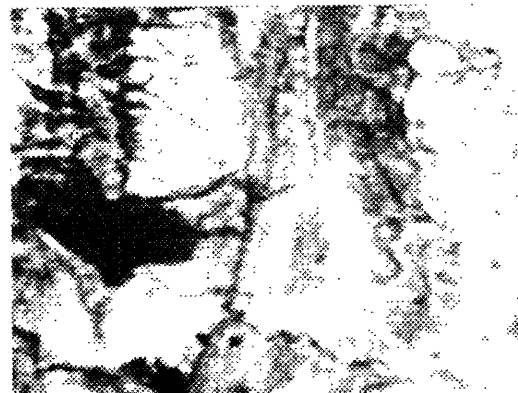
In earth resource studies selected black-and-white bands, color, and color infrared products may be used for certain topical studies. For example, black-and-white infrared is best suited for mapping surface water and water-saturated soils because of strong absorption of near infrared energy by water, whereas green-band images are useful in mapping suspended sediment in water bodies because water does not strongly absorb this wavelength and the sedimentologist can "see through" the water and pick up reflectance of suspended particles. The worker may also employ various image enhancement techniques with visual image analyses such as band combination color-additive and color-subtractive viewing, stereoscopic and pseudo-stereoscopic photo interpretation, contrast stretching, density slicing, masking and edge enhancement.

Techniques best suited for multiband photography include color addition and subtraction, image ratioing, cluster analyses, pattern recognition, and frequency analysis. The latter three processes require elaborate digitizers, computer processing, and/or laser-optical equipment.

Most of these image enhancement techniques are still experimental, but some are applied routinely to photographic products, and examples of the application of these to earth resource studies will be discussed. For geologic mapping and related studies a system that uses film positives for stereo-viewing remains the most practical technique for study. Ideally, projection of a stereo-



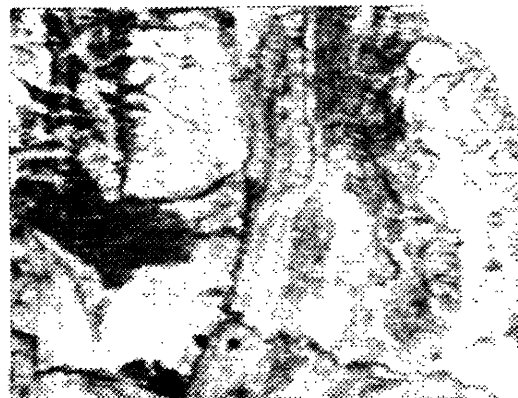
.4-.7 μ m



.5-.6 μ m



.5-.88 μ m



.6-.7 μ m



.7-.8 μ m



.8-.9 μ m

NOTE: These enlargements of each of the six S-190A bands illustrate the relative resolution of the duplicate S-190A images used by EREP investigators. The area is a small segment of the Wyoming Thrust Belt.

FIGURE 1. SKYLAB S190A RESOLUTION COMPARISON

image on a suitable topographic or planimetric base map with an instrument such as a Kern PG-2 plotter is excellent for mapping purposes. For this purpose the Skylab S-190B color stereo-pair gives the best results because it has high resolution (~ 15 -20 meters) and offers the advantage of color for discrimination of certain resources." [5]

2. S190B Earth Terrain Camera. This camera obtained high resolution photography utilizing an $f/4$ lens with an 18 inch focal length to be mainly used in support of other EREP sensors and user oriented studies. "The measured resolution limits were approximately 15 m per line pair from color film and approximately 9 m per line pair from black and white film. Performance of the camera was within expected limits for all parameters." [4]

Research personnel at the University of Wyoming have applied Skylab visual imagery to general geologic mapping, mineral exploration, tectonics, land use and vegetation mapping.

A typical S190B photograph is shown in figure 2. It is reproduced from a color infrared photograph of southern Louisiana showing the Mississippi River meandering southward from Baton Rouge. The smaller body of water is Lake Maurepas which is connected to Lake Pontchartrain by a canal.

3. S191 Infrared Spectrometer. This experiment combined an infrared spectrometer with a viewfinder tracking system. The spectrometer sensed incoming radiation from a Cassegrain optical system into a short wavelength from 0.4 to 2.5 microns and long wavelength from 6.6 to 16.0 microns. The viewfinder tracking system had a zoom controlled telescope with range from 2.25 to 22.5. The data will be used mainly for atmospheric attenuation and radiation of surface features over a broad spectral range.

"Typical spectral data obtained with the spectrometer are shown in figure 3. The lower spectrum was obtained when the Skylab spacecraft was over White Sands, New Mexico, on a foggy morning. Only the thermal region of the spectrum is shown. For comparison, the line at the top of the figure shows the spectrum measured by a similar spectrometer mounted in a helicopter. The difference between the two spectra is produced by atmospheric absorption of carbon dioxide, ozone, and water vapor. The difference observed illustrates the use of S191 data to determine atmospheric effects on data recorded from above the atmosphere. The spectrometer performed normally throughout the mission, and all its performance characteristics were within expected tolerances." [4]

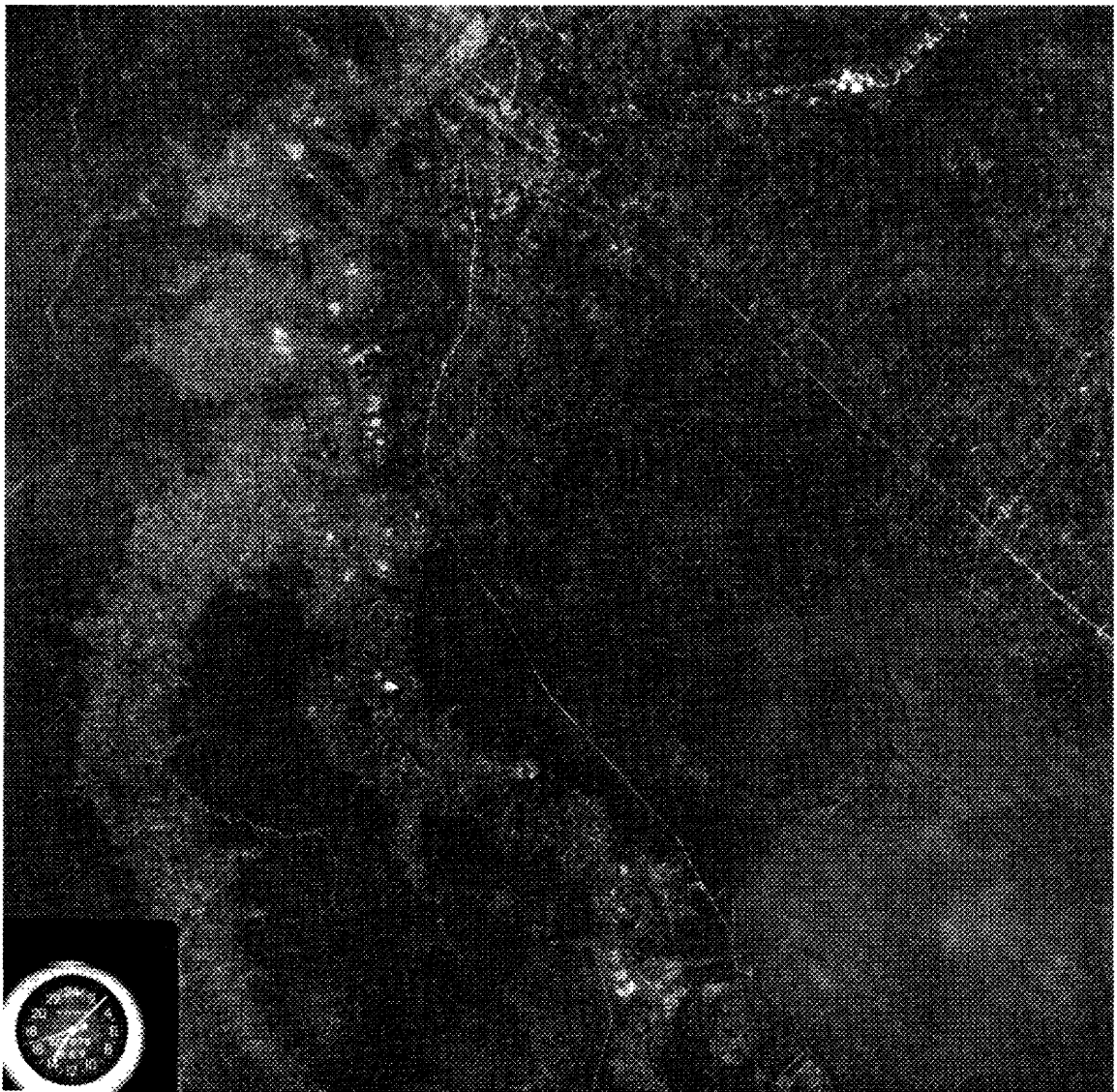


FIGURE 2. TYPICAL S190B PHOTOGRAPHY

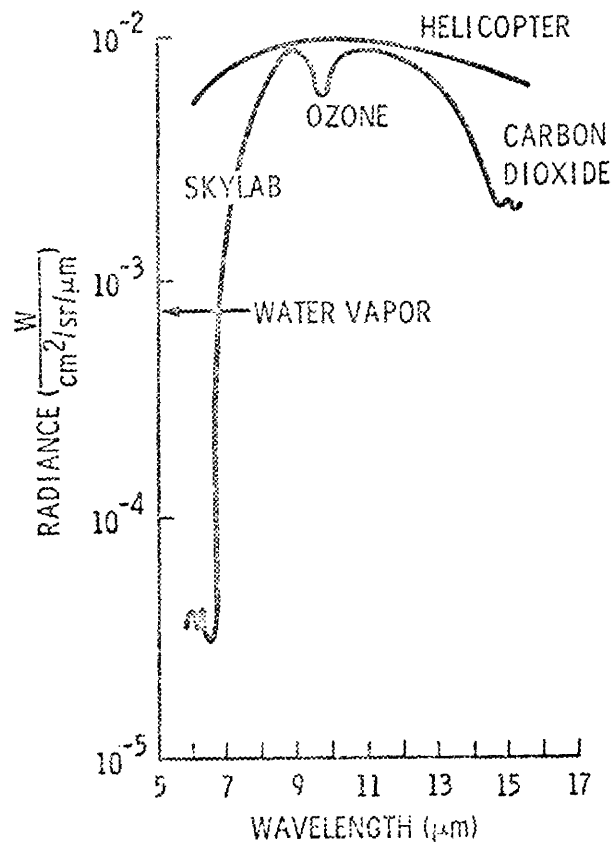


FIGURE 3. TYPICAL S191 SPECTRA DATA

4. S192 Multispectral Scanner. This experiment obtained high-spatial resolution, line scan data of reflected and emitted earth radiation into 13 discrete spectral wavebands from 0.4 to 12.5 microns.

"An example of S192 multispectral scanner imagery collected over Holt County, Nebraska, during the Skylab 2 mission is shown in Figure 4. Three of the 13 bands (2 infrared and 1 green) were superimposed to make this image. Agricultural features, such as circular irrigated fields, can be seen clearly in the imagery." [4]

Thermal "imagery (•••) is being used to evaluate the capability for remote sensing of geothermal heat sources. The radiometric performance of this thermal detector was such that temperature differences of approximately 0.8 K were equivalent to detector noise." [4] Figure 5 illustrates thermal energy obtained from Yuma, Arizona region.

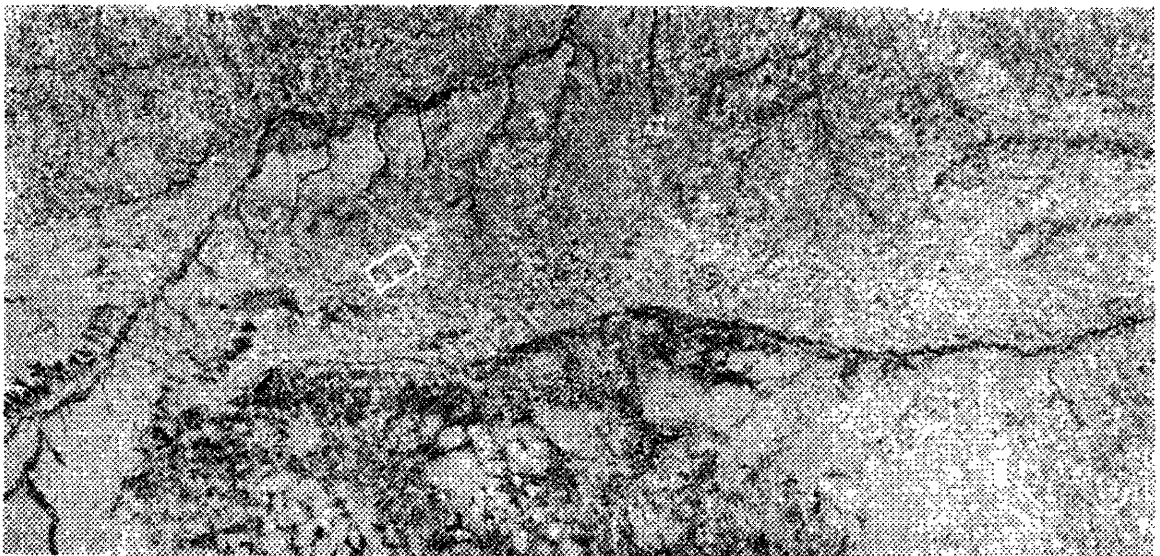


FIGURE 4. S192 MULTISPECTRAL SCANNER IMAGERY OF HOLT COUNTY, NEBRASKA

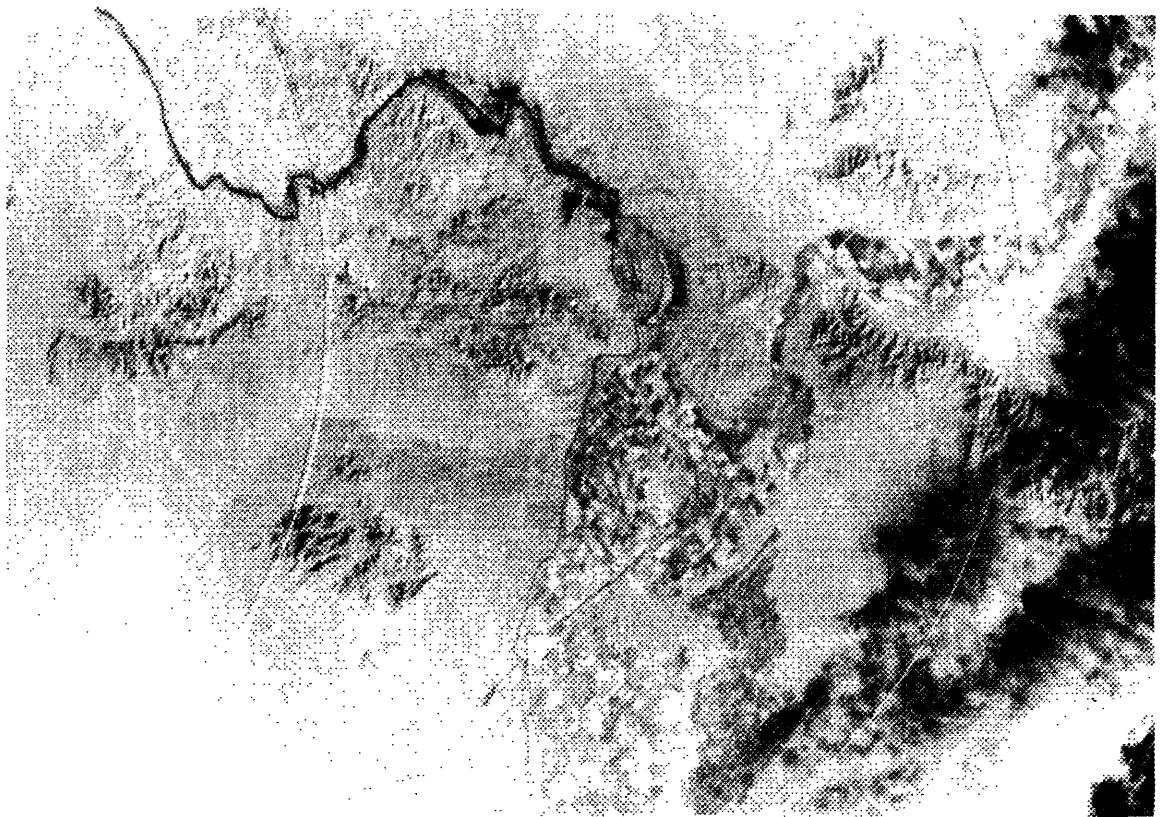


FIGURE 5. IMAGERY FROM THE YUMA, ARIZONA REGION OBTAINED WITH THE
IMPROVED THERMAL DETECTOR

The ability to perform lithographic mapping with the S192 data has great potential.

5. S193 Microwave Radiometer/Scatterometer and Altimeter.

This experiment obtained active and passive microwave radiation data for land and ocean studies at 13.9 GHz. Near simultaneous data on radar differential back scattering cross section & passive microwave thermal emission over land & ocean areas is being investigated. Also radar altimetry data will be evaluated for design of future spaceborne altimeters.

"Typical radiometer and scatterometer data collected from Hurricane Ava off the coast of Mexico are shown in Figure 6. Scatterometer and radiometer data in two polarizations are shown. The winds at the closest approach of the S193 sensors to the center of the hurricane were approximately 90 km/hr, with wave heights of 10 m. The changes of signal shown by both sensors as the spacecraft passed by the storm are caused primarily by changes in wave height, although rain clouds produced some effect. As wave height increased near the storm center, both the scattered signal intensity and the microwave brightness temperature increased by amounts approximately expected. These data are being analyzed to determine the feasibility for wave mapping of such storms.

Analysis of radiometer performance indicated that emitted radiant power was measured with an accuracy of at least 4 percent (corresponding to a brightness temperature accuracy of $\pm 7^{\circ}\text{K}$) and with a precision of at least 2 percent (or $\pm 1.5^{\circ}\text{K}$) for typical ground scenes.

The scatterometer performance was such that the reflected signal was measured within an accuracy of 4 percent for typical ground scenes, with a precision of at least 2 percent. The scatterometer was able to measure reflected signals that varied in amplitude by a factor of greater than 10,000 to 1 with the accuracy and precision given above." [4]

An example of the altimeter performance is shown in figure 7 where the "groundtrack crossed the Puerto Rican Trench, the site of a major anomaly in the Earth's gravitational field. Because of the anomaly the surface of the ocean deviates considerably from mean sea level in this region." (See figure 8) [4] The illustration shows the depression below the mean sea level corresponding to an altimeter variation of approximately 20 meters. "The altimeter measurements agree well with independent measurements of the actual sea level in this region. The altimeter performance was evaluated from measurements of sea surface in regions similar to the Puerto Rican Trench. The accuracy of the altitude measurement was ± 7 meters with a precision of ± 1 meter." [4]

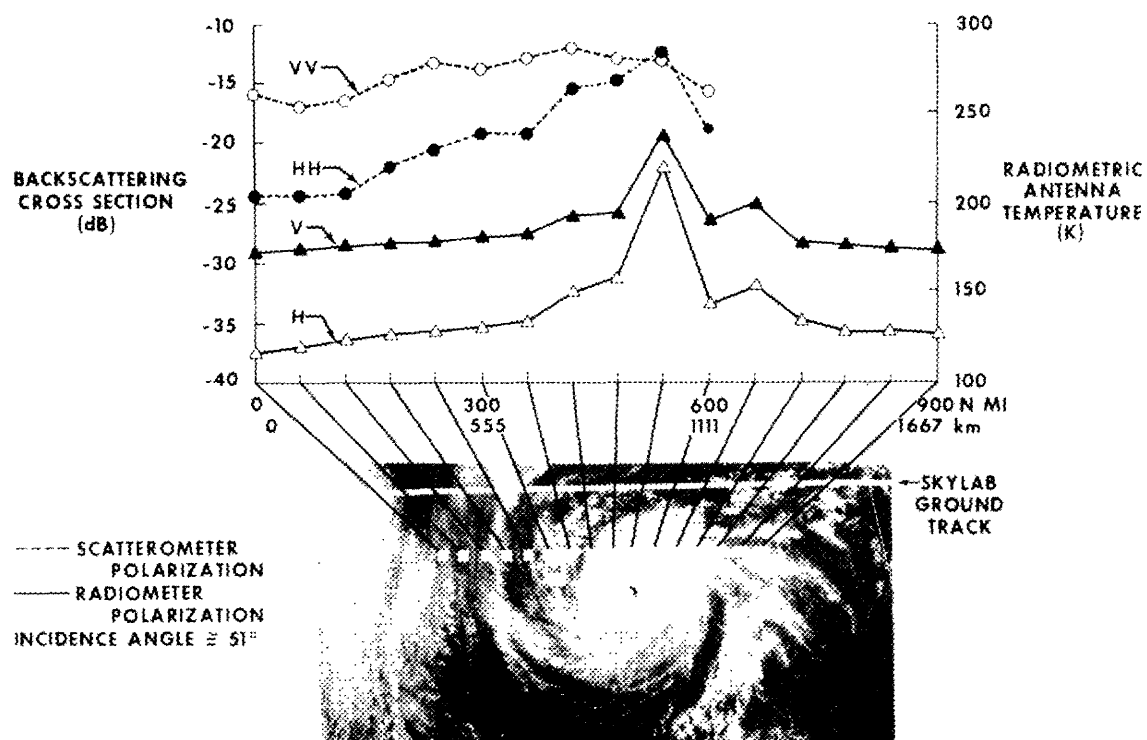


FIGURE 6. RADIOMETER/SCATTEROMETER DATA FROM HURRICANE AVA

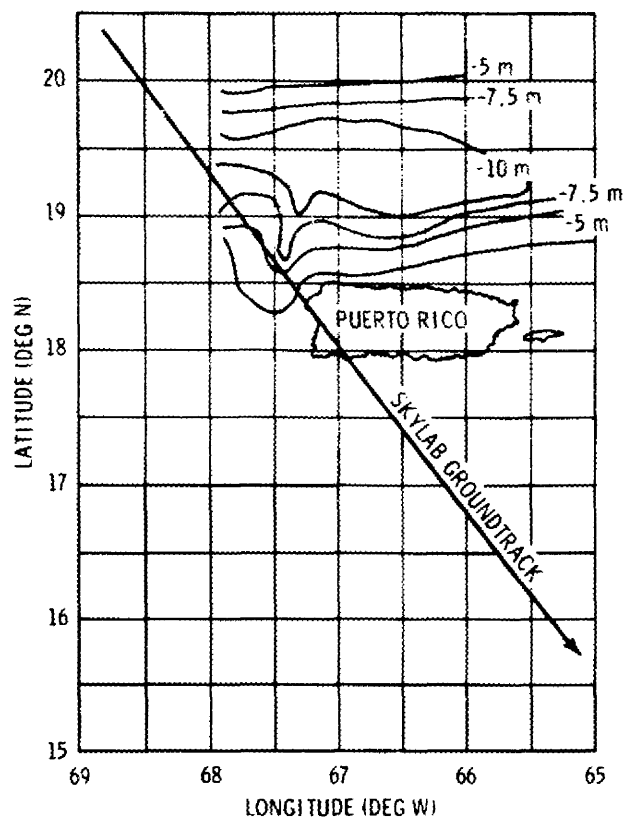


FIGURE 7. SL-2 GROUNDTRACK FOR ALTIMETER DATA

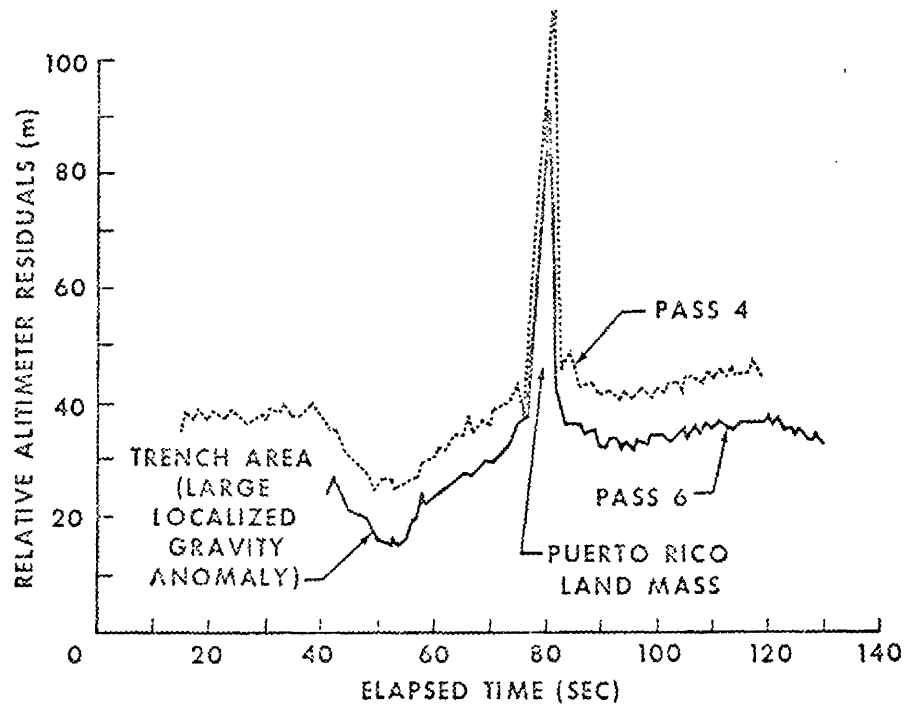


FIGURE 8. ALTIMETER RANGE MEASUREMENTS

6. S194 Microwave L-Band Radiometer. This experiment obtained passive microwave radiation data measuring earth surface brightness temperature at 1.4 GHz.

"An example of the data produced by the S194 sensor is shown in Figure 9. The spacecraft moved from Baja California across the Gulf of California and on into Mexico along the groundtrack shown in the map at the top of the figure. The antenna 'footprint' is shown as circles on the flight-path. The solid circle represents the half-power

point on the antenna pattern and corresponds to a circular area 124 km in diameter. The first null in the antenna pattern is shown by the dashed circle of 285 km in diameter.

The plot in the lower portion of Figure 9 shows the radiometer response along this groundtrack. Radiometer response is shown in terms of microwave brightness temperature, which is defined as follows. The S194 radiometer measures the intensity of microwave energy emitted from the Earth. It is conventional to express this intensity in terms of a 'temperature,' which corresponds to the temperature of a black body that would produce the observed radiation intensity. A low microwave brightness temperature could arise either from a low thermometric temperature or from a low emissivity, because either factor could reduce the emitted energy. The low 'temperature' of the sea shown in Figure 9 is caused by its low emissivity. Land surfaces have emissivities approaching that of a black body, so that the microwave 'temperatures' of Figure 9 for land surfaces are close to actual temperatures." [4]

"Correlations were obtained between moisture content of the soil and radiometric data from S193 and S194 and the S193 Scatterometer. The correlations indicate that microwave sensors may be quite useful for such measurements in the future."

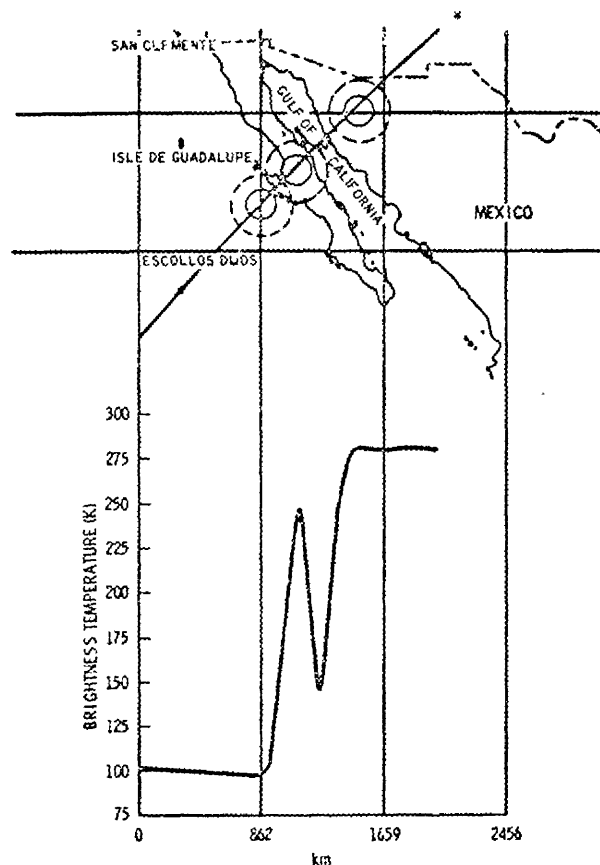


FIGURE 9. EXAMPLE OF DATA PRODUCED BY THE S194 SENSOR

C. Space Physics

The long duration Skylab mission flights above the earth's atmosphere combined with the scientific data return capability (such as film and samples) proved ideal for performing many space physics experiments.

Table III provides: the total number of planned functional objectives (FO), the numbers performed during each manned flight and the degree of success.

The ultraviolet emissions from stars and galaxies can only be studied from data obtained above the earth's atmosphere which filters ultraviolet light. Newly forming and young hot stars that emit approximately 80 percent of their light in the ultraviolet wavelengths were studied by two experiments.

One experiment also obtained data on the zodiacal light. The earth's atmosphere interferes with the low light level measurements taken by ground based instruments of the sunlight scattering from interplanetary dust particles.

Primary cosmic ray particle data was recorded during the Skylab mission before the particles interacted with molecules in the atmosphere to form secondary particle showers that have been observed from balloons.

Micrometeorite particles encountered during the Skylab mission were captured (before they burned entering the earth's atmosphere) by exposing capture surfaces on the spacecraft exterior for many days. The surfaces were returned to earth for analysis with electron microscopes.

Data on the charged particles trapped in the earth's magnetosphere, through which Skylab passed, were obtained.

Solar X-ray spectra which cannot be observed from the ground due to atmospheric absorption were recorded on film during EVAs.

1. S009 Nuclear Emulsion. The PI for Experiment S009 was Dr. Maurice M. Shapiro, Naval Research Laboratory (NRL), Washington, D. C..

The purpose was to study the charge spectrum of primary cosmic rays (extremely high-velocity atomic nuclei) approaching the earth from deep space. Emphasis was on the heavy nuclei.

The original plan was to deploy a nuclear-emulsion package (stacks of film-like material) and after 28 days return it for

TABLE III. ACCOMPLISHMENT OF EXPERIMENT FUNCTIONAL OBJECTIVES

EXPERIMENT TITLE	FO'S PLANNED	FO'S PERFORMED			ACCOMPLISHMENT (Percent)
		SL-2	SL-3	SL-4	
Space Physics [7, 8, 9]					
S009 Nuclear Emulsion	1	0	0	1	100
S019 UV Stellar Astronomy	58	3	27	26	97
S020 UV/X-Ray Solar Photography	1	0	0	3	300
S063 UV Airglow Horizon Photography	41	0	12	26	95
S073 Gegenschein/Zodiacal Light	80*	11	6	16	41
S149 Particle Collection	4	$\frac{1}{2}$	$1\frac{1}{2}$	2	100
S150 Galactic X-Ray Mapping	7	0	3	0	35
S183 Ultraviolet Panorama	60	5	14	24	72
S201 Far UV Electronographic Camera	27	0	0	24	89
S228 Trans-Uranic Cosmic Rays	5	1	1	3	100
S230 Magnetospheric Particle Composition	4	0	2	2	100
S233 Kohoutek Photometric Photography	84	0	0	74	88
*Includes T027 Contamination Measurement Joint Observing Program Function Objectives.					

analysis. This flight offered the opportunity for extended observations above the earth's atmosphere (but not sufficient to fog the emulsion) and it was expected that large quantities of new information would be obtained about the charge distribution of these primary cosmic rays.

The package was deployed on SL-1/SL-2 and returned 28 days later for analysis. Unfortunately the high-temperatures experienced on SL-1 had caused the individual emulsion layers to fuse together, making analysis impossible.

A new package was launched and successfully deployed for the full term on SL-4. It is currently under investigation at NRL. Detailed analysis and interpretation is expected to take longer than a year. However, initial examination indicates that, with optimum development and processing of the nuclear emulsion strips, a large quantity of information should be obtained. The range of nuclei where best data will be obtained is now expected to be between $Z=16$ and 28.

These investigations may be expected to yield a better understanding of cosmic ray origin and history. In addition, the studies may contribute data useful in evaluating the biological hazards of cosmic radiation in long duration space missions.

2. S019 UV Stellar Astronomy. The PI for Experiment S019 is Dr. Karl Henize, a scientist astronaut, JSC, Houston, Texas.

The purposes were: to obtain moderate dispersion stellar spectra ranging from 3000 \AA to 1400 \AA with sufficient wavelength resolution to permit the study of ultraviolet (UV) line spectra and of spectral energy distributions of early type stars; and to obtain low dispersion UV spectra in several Milky Way starfields and in nearby galaxies. The experiment used an objective prism spectrograph to record the spectra on film which was returned to earth for analysis.

The experiment was performed on all Skylab missions. One film canister was returned on SL-2. Two film canisters were returned on SL-3, and two on SL-4. Some S019 frames were used by Experiment S183 and Student Experiments ED23 and ED26.

The spectral data will permit detailed physical analysis of the UV radiation from hundreds of individual stars, nebulae, and interstellar dust. This large selection of stellar subjects will provide the statistical data for comparison against existing theoretical models. Special emphasis is being given to a search for previously unsuspected anomalies in the physics of stars and the interstellar dust.

From this spectral data, it will be possible to measure the existence and relative intensity of absorption and emission lines.

The spectral information will provide insight into the origin and composition of the stars, emission nebulae, and the interstellar dust. The temperature, pressure, and size of the star's atmosphere will be determined from the spectral data. Changes in temperature and pressure will indicate the nature of the star's energy, or luminosity. These environmental determinations will provide added information on the age, life span, nature of the mass ejection mechanisms, star formation processes, and evolution.

The exposures obtained on SL-4 included 14 exposures of Comet Kohoutek. A quick-look at the data indicates that the comet UV emissions do not occur below 3000 Å. The only UV spectral line observed thus far was the 3060 Å hydroxyl line.

3. S020 UV/X-Ray Solar Photography. The PI for Experiment S020 is Dr. R. Tousey, Naval Research Laboratories, Washington, D.C.. The objective was to obtain solar spectra in the 10 to 200 Å wavelength region. Spectra from the quiet (non-flaring) sun and during one (or more) solar flare were obtained. The spectra covered 10 to 100 Å on the upper half of each film strip and 20 to 200 Å on the lower half.

The experiment was originally planned to be operated from the solar SAL. The meteoroid shield failure and subsequent solar SAL unavailability necessitated experiment preparation for operation during EVA. The hardware to accomplish this was prepared and launched on SL-3. Two film magazines and two sets of filters were launched on SL-4.

The experiment was operated during SL-4 EVAs 2, 3 and 4. Nine exposures were taken, five from one magazine during EVA 2 and 3 and four from the other magazine during EVA 4. Table IV lists the exposures and comments on anomalies.

Generally, the spectra were far less intense than expected, by a factor of 10 to 100. This slow speed result is anomalous and not understood. On the short wavelength side of the spectrum about a half dozen very faint lines are present. When the filters were measured after return, indium, which was the short wavelength side filter, was found to be almost completely opaque; whereas the beryllium, the long wavelength side filter, transmitted the same as preflight except for some slight deterioration toward the longer wavelengths, which were outside the experiment's range. A possible explanation for the transmission loss is contamination from the spacecraft. Coolanol leakage is suspected as a contamination source, but transmittance measurements of Coolanol and the filters are inconclusive. A possible explanation for the slow speed, in addition to contamination, but one that can never be checked, is that the instrument was improperly

TABLE IV. EXPERIMENT S020 OPERATIONS

Film Magazine Number and Film Slot Number	Exposure Time (min.)	EVA Number	Filter Number	Comments
3-1	60	2	31	This and all exposures made on EVA 2 are less intense than the 7.5 min. exposure on EVA 4
3-2	30	2	31	
3-3	14	2	31	
3-4	7.5	2	31	
3-5	45	3	31	Second most intense spectrum
4-1	60	4	41	Most intense but lines are tripled, not curved, and 3Å shorter than all other spectra
4-2	30	4	41	Apparently lost during prelaunch film loading
4-3	7.5	4	41	
4-4	4	4	41	

mounted and did not point at the sun in the plane perpendicular to the slit. However, the crewman examined the boresight device several times and reported that the instrument remained pointed at the sun. Had the boresight device been misaligned during launch, the two images provided by it would probably have been displaced from each other to an extent noticeable by the crewman.

One exposed film showed tripled lines. On examination after recovery, one film strip was missing from film magazine number 4. A possible explanation is that the film strips were loose in the film drum because the film did not have the same transverse curl as normal type 101 film. This curl holds the film strip in place in the drum.

The spectral lines present in the long wavelength portion from 111 to 208 Å are more intense due to the longer exposure time than in the best rocket spectrum obtained by NRL to date, but very few, if any new lines are present on the highest contrast prints currently available.

The relative intensity differences between the S020 spectrum and the best NRL rocket spectra appear to be small in the wavelength range covered, however the contamination problem makes quantitative comparison difficult. The S020 spectrum seems to confirm the NRL rocket spectrum over the entire wavelength range covered in common.

One solar flare was recorded by S020. The flare was recorded on film strip #3-4. It began 2.5 minutes after the commencement of the 7.5 minute exposure. The lines recorded are more intense than the lines in the previous 14 minute exposure. However, all lines present are in the 170-200 Å wavelength range. These lines are predominantly from the middle ionization stages of iron, which was not expected to be enhanced greatly during a solar flare. It is tentatively concluded that reasons other than the flare account for the difference between these exposures.

4. S063 UV Airglow Horizon Photography. The PI for Experiment S063 is Dr. Donald M. Packer, Naval Research Laboratory, Washington, D.C.. The experiment was to photograph, at visible and UV wavelengths, the earth's ozone layer, twilight airglow and related targets such as noctilucent clouds, aurorae and red arcs.

Experiment S063 was not performed on SL-2. The airglow and related target data FO's were originally planned to be acquired by photography through the solar SAL. Due to the thermal shield deployment, the solar SAL was not available for experiment operations. A successful workaround was established to achieve these FO's by hand-held photography through the structural transition section or Command Module (CM) windows and by using S063 equipment mated with an adapter to the S019 Articulated Mirror System (AMS) at the anti-solar SAL.

Initially six FO's were approved in the SL-3 flight plan. As a result of the crew's desire to do more experiment work rather than have free time, 12 FO's were completed. No data was acquired on two targets-of-opportunity, the red arcs and noctilucent clouds.

The data will enable a better understanding of the ozonosphere, which protects the earth from UV radiation. The relationships between the atmospheric behavioral patterns, solar activity and earth weather patterns can be studied. An improved general understanding of atmospheric phenomena will be an additional benefit from the data collected.

Ozone data was obtained on two occasions (during the SL-3 mission) in conjunction with underflights by high altitude aircraft of the controversial jet exhaust effects on the ozonosphere.

During SL-3, 36 visible and 10 UV exposures of the airglow were obtained, 53 visible and 64 UV ozone exposures were obtained while the cluster was in the solar inertial and Z-axis local-vertical orientations. Eighty-five aurora color photographs were obtained. The exposures provided minimum data for airglow evaluation (i.e., 3 visible exposures), since the PI was establishing aperture settings during the SL-3 mission. The ozone photographs yielded 58 exposures for evaluation and the aurora photographs provided 65 exposures.

The PI believes that the number of SL-4 exposures will be adequate for scientific evaluation which includes 11 IR airglow, 202 ozone, 13 comet (11 visible and 2 UV), 3 aurora, and possibly 40 noctilucent clouds. Numerous SL-4 photographs were lost by use of the Nikon camera, which had a focusing problem.

5. S073 Gegenschein/Zodiacal Light. The PI for Experiment S073 is Dr. J. Weinberg, Director for the Space Astronomy Laboratory, State University of New York at Albany, Albany, New York.

The experiment was to measure the brightness and polarization of the skyglow (primarily zodiacal light and starlight) over as large a portion of the celestial sphere as possible. Zodiacal light is light reflected from dust in the solar system. The Gegenschein is that bright portion of the zodiacal light that appears in the anti-solar direction, where the sunlight is reflected 180 degrees.

A photometer system was extended from the anti-solar SAL during both the SL-2 and SL-3 missions to measure the brightness and polarization of the skyglow in 10 different colors. The data was telemetered to the ground for analysis. During the SL-2 mission, a simultaneous measurement of a region in the sky was made from Skylab and the ground station in Hawaii. At nearly the same time, Pioneer 10 made photoelectric measurements of this area. An area of the sky was mapped by this experiment during the SL-2 mission and by Pioneer 11 from the earth side of the asteroid belt.

Preliminary photometer data analysis indicates that the effects of atmospheric airglow and contamination can be separated from zodiacal light measurements. Results from Skylab and Pioneer indicate that the solar system dust distribution diminished linearly from the sun to the spacecraft making the observation, for distances between one astronomical unit (AU) and two AU. At distances greater than two AU, this relationship no longer applies. Indications are that the dust in

the solar system is not primarily located in the asteroid belt, but rather may be remnants or original dust remaining from the formation of the solar system or the debris from comets. The telemetry data analysis is continuing.

During the SL-3 mission, the photometer system failed to return to a retractable position which resulted in the unit being ejected from the SAL permitting the SAL to be used by other experiments. No additional photometer system operations were possible. Seven 35mm photographs of the Gegenschein were taken during the SL-3 mission from the anti-solar SAL using S063 film. Three rolls of 35mm film were used in the Nikon camera with the T025 canister and S019 AMS at the SAL to obtain photographs of zodiacal light, galaxies, cometary debris and lunar libration regions during the SL-4 mission. These photographs were obtained during seventeen night passes. The SL-4 photographs were all out-of-focus and it appears that the galactic photography cannot provide useful information; however, the other photographs are being digitized and analyzed for brightness information.

6. SL49 Particle Collection. The PI for Experiment SL49 is Dr. C. Hemenway, Director of the Dudley Observatory, Albany, New York. The SL49 experiment was to determine the mass distribution of micrometeorites in near-earth space.

Four sets of micrometeorite collection cassettes were launched on SL-1. Two sets were returned on the SL-3 CM, one on the SL-4 CM, and one was deployed on the ATM thermal shield during the last SL-4 EVA where it remained after the SL-4 mission. The present plan requires cassette retrieval by a later manned space program that includes a Skylab revisit.

One set returned on SL-3 was exposed during the unmanned period between the SL-2 and the SL-3 missions. It was deployed by the T027/S073 universal extension mechanism and faced in the anti-solar direction. The second set returned on SL-3 and the set returned on SL-4 were exposed during the manned phases of SL-3 and SL-4. These two sets were operated by manually opening and closing the cassettes for exposure during planned EVAs. The SL49 EVA operation became the prime method of deploying the experiment after the loss of the T027/S073 extension mechanism and the nonavailability of the solar SAL.

Cassette analysis indicates that the number of high velocity impact craters were about 10^{-6} particles/M² sec which is much larger than predicted from Pegasus measurements and more consistent with previous balloon flights. This difference is apparently due to the particles' fragility which penetrated the very thin gold foil on

S149 and shattered before penetrating lower layers. From the preliminary sample study there is a strong possibility that most particles in space are not solid-iron bodies but are very fragile stony bodies. These fragile particle clusters were insufficient in penetration power to be measured by Pegasus. The flux measurements on the vehicle's solar side were also very high.

Further studies are being conducted on the returned samples.

7. S150 Galactic X-Ray Mapping. The PI for Experiment S150 is Dr. William Kraushaar, Physics Department, University of Wisconsin, Madison, Wisconsin.

The experiment equipment was developed under the direction of Dr. Alan Bunner, at the University of Wisconsin.

The experiment was to detect X-rays having an energy level between 200 and 10,000 electrons volts. Its purpose was: to serve as the initial thin-window soft X-ray experiment in a satellite orbit; to examine, with high sensitivity, the diffuse soft X-ray background in selected regions of the sky; to test hypotheses that the soft X-ray background could be produced by a class of numerous point sources such as optically faint stars; and to examine the modulation of soft X-ray data by geophysical and solar-related effects peculiar to orbiting payloads.

Slot collimators defined three different fields of view, each about 1.5 by 18 degrees, and were scanned simultaneously. The experiment operated from a deployed position in the Instrument Unit on the Saturn IV-B stage after separation of the SL-2 Command and Service Module. The entire Instrument Unit/S-IVB vehicle maneuvered according to a pre-planned program to allow viewing the desired portions of the celestial sphere. Proportional counters detected the X-ray events, and discriminators and accumulators provided on-board pulse-height analysis to catalogue the events according to energy ranges. Charged-particle and cosmic-ray events were recognized and subtracted from the X-ray data. An Iron-55 radioactive source was actuated periodically to provide calibration data.

Experiment operation was successful for approximately two hours (of a hoped-for three orbits), after which a leak in the proportional counter window (2 micron "Kimfol") terminated the experiment. Among the X-ray sources identified to date are Tau X-1 (the Crab Nebula), the galaxies M87 and 7C3576, and the sun. In addition, the data from solar X-rays scattered by the earth's atmosphere and charged particles from the magnetosphere are being studied.

Since S150 is the most sensitive low-energy X-ray detector flown to date the data obtained promises to make a contribution in four major areas:

It has surveyed low-energy X-ray emissions from several point sources and can use the well-known Crab Nebula for calibration and for evaluating the density and abundances of intervening interstellar matter.

It should be possible to estimate the low-energy X-ray component of the isotropic diffused background known to exist over much of the electromagnetic spectrum and estimate how much is due to extragalactic sources or to numerous stars near our galaxy.

Occasionally, the instrument scanned the earth's horizon during daylight. It was able to measure the X-ray albedo reflected from the earth's atmosphere and after analysis it may be possible to suggest new uses for this albedo in atmosphere studies.

Since the spacecraft moved through the earth's magnetic field contours, S150 observed varying count rates due to high-energy trapped charged particles. The data will provide additional information to further understanding of this complicated phenomenon which has been a source of concern to many X-ray astronomers.

The data is currently being analyzed at the University of Wisconsin.

8. S183 Ultraviolet Panorama. The PI for Experiment S183 is Dr. George Courtes, Laboratoire d'Astronomie Spatiale, Marseilles, France.

This experiment was to obtain the color indices of stellar objects. The S183 spectrograph created two nearly superimposed images each 600 Å wide of a selected starfield on a single photographic plate. One image was centered in a spectral band about 1878 Å and the other about 2970 Å. An operational 16mm Data Acquisition Camera (DAC) attached to the spectrograph, simultaneously photographed the starfield being exposed by the spectrograph in a 360 Å bandwidth centered around 2560 Å.

The S183 experiment was performed on all three Skylab missions.

Although of scientific value, the quality of the photographs taken on SL-2 were poorer than expected. The spectrograph photographic plates exhibited sensitivity loss and latent imaging fading. Exposures obtained early in the mission were more seriously degraded than those taken later. Photographs obtained with the DAC were out of focus.

Figure 10 is a 21 minute exposure of the Large Magellanic Cloud showing hot blue stars. This is the galaxy nearest ours. Due to the focus problems that were experienced, the point sources appear as a doughnut shape, whereas, the extended sources are not as pronounced.

During SL-3, only the DAC portion of S183 was used. Although the images on the returned photographs were out of focus, the data is of good scientific value. Some stars not previously known to be strong sources of ultraviolet light, may be distinguished with further analysis and data comparison with previous observations. Color indices will be determined for star clusters, unresolved areas of the Milky Way, and selected galactic nuclei; statistical interpretation of large stellar populations will thus be possible. The data will be used in determining the light scattering of contaminant particles.

During the SL-4 mission, the DAC optics were replaced, correcting the defocused image on the 16mm film. The DAC exposed 35 frames including six frames of Comet Kohoutek before the film jammed. Two photographs are shown in figure 11. The first is of Comet Kohoutek taken on January 10, 1974. The comet tail has been added and the spectral types and magnitudes for the other stars included. The second was obtained with the DAC of stars with spectral types and magnitudes shown. Both photographs are 5 minute exposures. Approximately 3000 UV stars were classified in associations or clusters down to 12th visual magnitude at approximately 2560 Å from the DAC photographs.

Two film carrouseles were flown, one primarily for use on starfields and the other with a variety of film types useful for viewing the expected OH radiation from the Comet Kohoutek. There were 66 frames available of which 43 were used for photography of the comet and starfields; however, due to a problem with carrousel indexing, only one frame was actually extracted from the carrouseles and exposed.

9. S201 Far UV Electronographic Camera. The PI for Experiment S201 is Dr. Thornton Page, Naval Research Laboratories (NRL) at the Johnson Spacecraft Center.

The camera which was flown on Apollo 16, was modified for flight on SL-4 to study Comet Kohoutek and starfields.

The camera was to:

Photograph Comet Kohoutek's emissions of oxygen (1340-56 Å) and hydrogen Lyman-alpha (1216 Å) on a temporal basis to study evolutionary nature of these emissions.

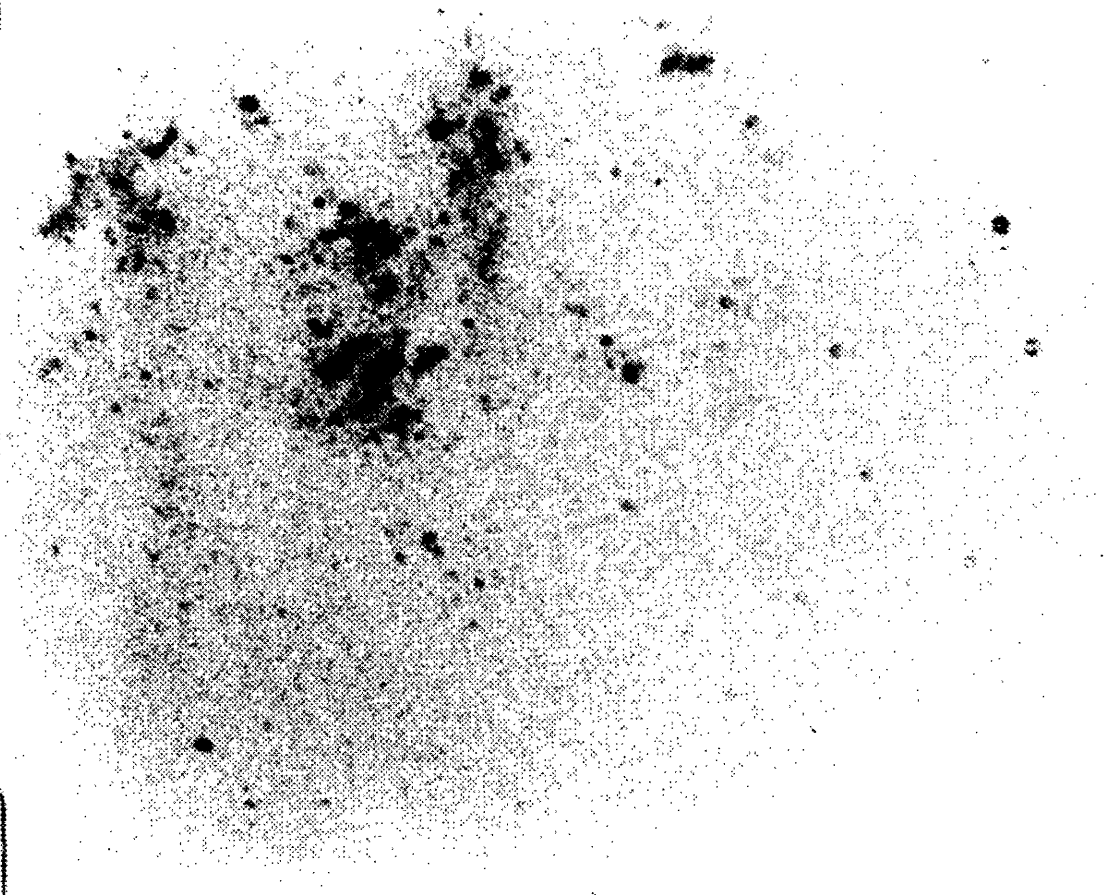


FIGURE 10. LARGE MAGELLANIC CLOUD (SL-2 DAC PHOTOGRAPH)

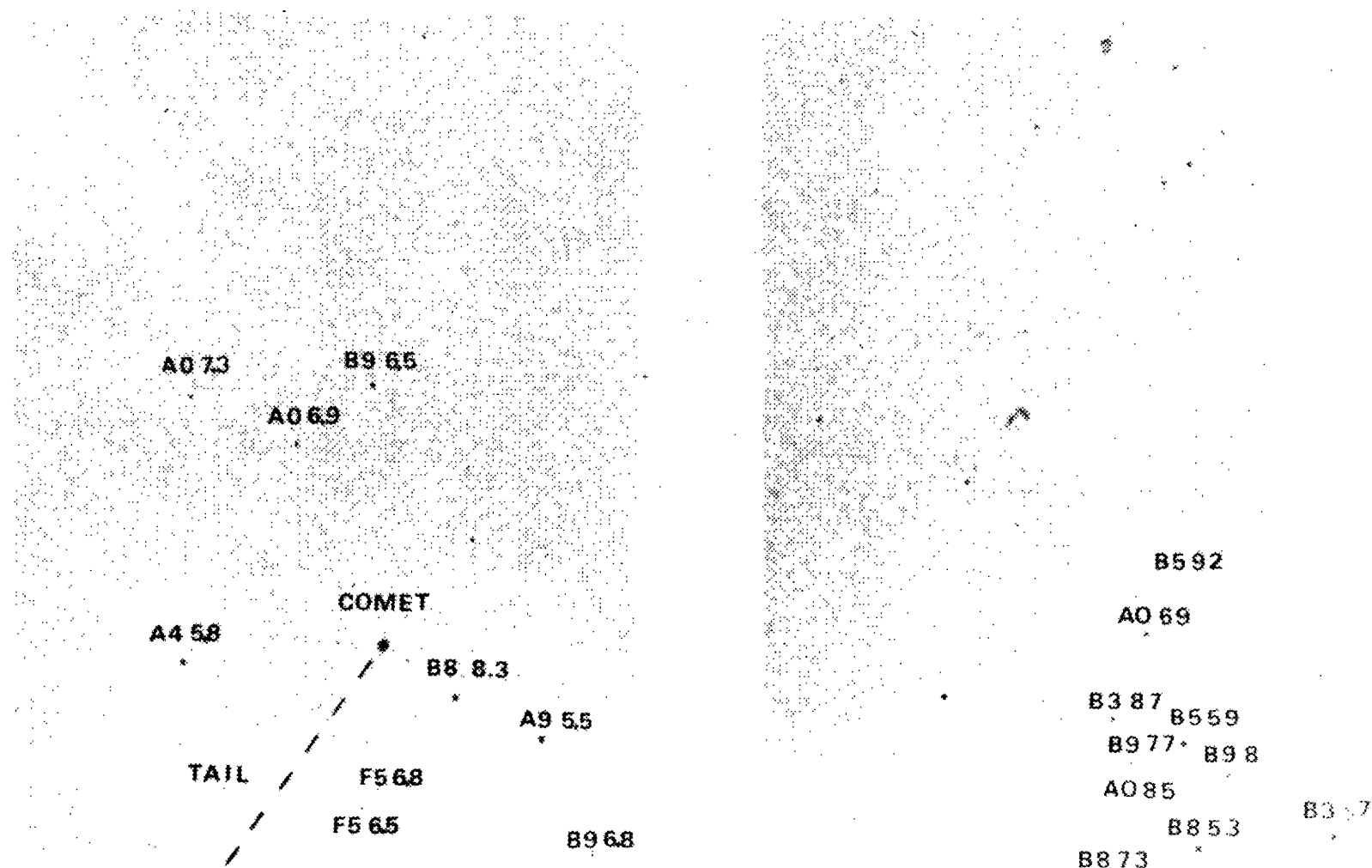


FIGURE 11. COMET KOHOUTEK AND TARGET STARS (SL-4 PHOTOGRAPH)

Confirm the following data obtained on Apollo 16:

The earth's tropical airglow bands emitting oxygen on a 1304-56 Å.

Lunar atmospheric hydrogen emitting hydrogen Lyman-alpha 1216 Å.

Interstellar material in the Large Magellanic Cloud and, possible evidence of intergalactic hydrogen in clusters of galaxies.

Measure the extent of:

Rocket exhaust trails in the atmosphere.

The earth's tropical airglow-bands emitting nascent oxygen 1304-56 Å and, the earth's polar auroral zones emitting nascent oxygen 1304-56 Å and hydrogen Lyman-alpha 1216 Å.

Compare the small and large Magellanic Clouds and, check the S201 calibration, the far-UV colors and magnitudes of hot blue stars in the Milky Way.

The PI reported that 126 exposures were obtained of Comet Kohoutek and over 350 exposure's of other targets. To date, the PI has analyzed 30 Comet Kohoutek exposures which indicate the hydrogen halo on nine separate dates from 31.7 days preperihelion to 13.0 days postperihelion and 35 of the latter which indicate unexpected changes in camera sensitivity during the mission.

10. S228 Trans-Uranic Cosmic Rays. The PI for Experiment S228 is Dr. P. Buford Price, University of California, Berkeley, California.

The experiment was to provide a detailed knowledge of the relative abundances of nuclei with atomic number (Z) greater than 26 in the cosmic radiation, and specifically to observe and identify as many trans-uranic nuclei as possible. The data obtained will help determine upper limits on the super-heavy cosmic ray flux with Z greater than 110, and the cosmic ray energy spectrum (from about 150 to 1500 Mev/nucleon) with Z = 26, Z greater than 60, and Z greater than 83.

The experiment utilizes detector modules fabricated from Lexan plastic and deployed in the Orbital Workshop (OWS). Cosmic rays will penetrate the detector modules streaking the plastic sheets within. Subsequent to return, these plastic sheets are chemically etched and the cosmic rays tracks measured with an optical microscope to determine

the atomic number and energy of each observed particle. Thirty-six modules were launched on SL-1 and were deployed in two separate harnesses holding eighteen modules each. An additional module with bracket for mounting was launched and deployed externally on SL-4 to gather data on lower energy level nuclei; it was retrieved and returned on SL-4. Of the original thirty-six, one was returned on SL-3 to be used in setting up the data reduction program, thirty-four were returned on SL-4, and deployed in the MDA during deactivation for retrieval on a possible future revisit to Skylab.

Data analysis is progressing satisfactorily. The initial major phase, namely the location and preliminary identification of all the interesting ultraheavy events, has been completed. These results are summarized in table V.

TABLE V. ULTRAHEAVY COSMIC RAYS FOUND IN FIRST SCAN

Z	Number
93	0
90-92	1
84-89	4
80-83	14
76-79	9
72-75	20
68-71	7
64-67	9
60-63	3
56-59	0
Total	67

Additional preliminary analysis of cosmic ray tracks ($Z = 8$) is underway to gain additional insight into the source of recently discovered energetic charge particles. (This source, discovered last year, is neither solar nor galactic in origin.)

In addition to the investigations at Berkeley and in Ahmedabad, India, Dr. Don Brownlee, Astronomy Department, University of Washington, has found by stereomicroscope scanning and studied with an electron microprobe two micrometeorite craters in the aluminum tape wrapping the externally deployed module.

11. S230 Magnetospheric Particle Composition. The PI's for Experiment S230 are Dr. Donald Lind, JSC, Houston, Texas and Dr. Johannes Geiss, University of Bern, Bern, Switzerland.

The experiment utilized thin foils of aluminum and platinum to trap magnetospheric ions and particles. Using the techniques applied to the solar wind composition measurements in the Apollo Program, the foils are being analyzed. This will allow the determination of the fluxes and isotopic composition of the noble gas components of precipitating magnetospheric ions, to obtain an indication of their relative energies, and to determine the particle source. The foils were deployed as cuffs wrapped around two spools mounted on the AM deployment assembly.

Two inner and two outer cuffs were launched in position on SL-1. Two collectors were planned to be retrieved during SL-3 and SL-4. Due to the surface contamination deposited on the two outer cuffs during the SL-2 fly-arounds, one new collector was launched on SL-4. Thus three cuffs were returned from SL-3 and two (including the additional cuff) at the end of SL-4.

Preliminary results from the experiment were presented to the American Astronautical Society, August 20-22, 1974 in Los Angeles.

Thus far, selected sections of two foils have been analyzed. The noble gas components of the entrapped particles identified are: helium-4, helium-3, neon-20, and neon-22. Investigation of the average fluxes and their ratios have resulted in several interesting observations. The amount of $^2\text{He}^3$ relative to $^2\text{He}^4$ is a factor of 300 greater for the solar wind helium than for the terrestrial atmosphere helium. Therefore, by measuring this ratio, it is possible to determine the source and the ratio of an admixture of particles from these sources.

The $^2\text{He}^3$ fraction of terrestrial origin was found to be less than 15 percent. The $^2\text{He}^3$ is considered to be solar wind particles that have entered the magnetosphere and have been accelerated before precipitation. The terrestrial helium was noted, through stepwise heating during analysis, to be captured at energies much less than 1 kev/nucleon. In addition there was a strong suppression of the terrestrial helium on the foil located under the handrail. This leads to the conclusion that most of the terrestrial helium on the foil located under the handrail. This leads to the conclusion that most of the terrestrial $^2\text{He}^4$ is composed of helium atoms of the ambient neutral atmosphere that were rammed into the foil by the Skylab velocity.

For the first time isotopic fractionation in the upper atmosphere has been experimentally detected. A ratio of $^{20}\text{Ne}/^{22}\text{Ne}$ of 22 ± 3 was found in one case, the ratio that is predicted by atmospheric models for altitudes of approximately 350 km. The difference between this and the Skylab orbit of approximately 430 km could be due to a small degree of vertical mixing.

Analysis of the remaining foils will allow more detailed discussion.

12. S233 Kohoutek Photometric Photography. The PI for Experiment S233 is Dr. Charles Lundquist, Director of the Space Sciences Laboratory, MSFC, Huntsville, Alabama.

This experiment was added to the SL-4 mission to photograph the Comet Kohoutek. Some photographs were purposely taken out of focus to permit micro-densitometry studies to be performed on the film to obtain comet brightness measurements. About 99 frames of 35mm film were obtained with the comet in the field-of-view. Roughly 1/3 of these are focused and 2/3 defocused. Microdensitometry is being performed on both third generation film and the original film computer processing to reduce the microdensitometry data is in process.

13. Proton Spectrometer. The PIs for the Proton Spectrometer (an operation instrument) are Dr. Godehard Guenther, University of Alabama at Huntsville, Huntsville, Alabama and Dr. Thomas Parnell, Space Sciences Laboratory, MSFC, Huntsville, Alabama.

The instrument was to obtain a spatial and energy spectral flux distribution energetic protons and electrons outside the Skylab. The proton spectrometer was a high counting rate particle detector designed to measure protons (18.5 Mev to 400 Mev) and electrons (1.2 Mev to 10 Mev) trapped in the Van Allen Belts. The prime emphasis was to obtain data for protons above 100 Mev. There existed only limited data for energies above this level, and because they are capable of penetrating the spacecraft they contribute to the problem of radiation damage to sensitive materials such as photographic emulsions. This information could then be used in future spacecraft design, in material selection and design of protection through shielding. The lower energy levels were included because they were likely to exhibit time variations during the Skylab mission.

The instrument had a 45 degree acceptance cone and was mounted on the S194 experiment L-band truss to provide a clear view of the exterior environment. The instrument differentiated protons from electrons and place the electrons into one of three energy levels and protons into one of eight. After coordinating this data with vehicle pointing data, the flux could be described by the numbers of particles, their energies, and their direction of travel.

The instrument operation was initiated approximately 12 hours after the SL-1 launch, and data transmission through telemetry began. An error in the thermal analysis resulted in lower than predicted operating temperatures. This resulted in the loss of all the proton data channels and two of the electron data channels. What remained was one electron data channel and several housekeeping measurements. It is hoped that the data returned during the first few days of the Skylab mission, before the instrument experienced its low temperatures, will yield some proton information. In addition, it has been determined that the instrument, even in its degraded state, may provide information about transient cosmic gamma-ray events or gamma-ray bursts. These bursts were recently discovered by detectors aboard Vela satellites and are receiving attention by high-energy astrophysics scientists.

D. Materials Processing

Near-zero-g during orbital flight makes it possible to conduct materials processing operations that cannot be accomplished easily, if at all, on earth. Melting and mixing without the contaminating effects of containers, with suppression of convection and buoyancy in liquids and molten material, with control of voids and with the ability to use electrostatic and magnetic forces otherwise masked by gravitation, can lead to new knowledge of material properties and processes and possibly to valuable new products for use on earth. These potential products range from composite structural materials with highly specialized physical characteristics, to large (more perfect) crystals with valuable electrical and optical properties.

NASA is interested in the possibilities of welding in near-zero-g; such information is necessary for assembly in space. Several studies indicated that electron beam equipment offered the best potential for overall needs. As a result of these studies, the MSFC personnel began development work on compact electron beam welding apparatus in early 1963. Considerable interest was developing at that time in manufacturing products in space, for use on earth. The investigations described in this section probe the feasibility of several specific processes and should help select the most promising processes and products for use in providing sound design criteria for future space facilities.

The progress of Space Shuttle planning has raised the prospect that vehicle capabilities sufficient to support large-scale experiment programs and limited commercial manufacturing operations will probably become available soon. Practical experience gained while developing materials for use on Skylab, has already proved valuable in the conceptual planning of an improved and enlarged facility for the Space Shuttle program. Evaluation of Skylab experimentation results should assist engineers in finalizing the design of Space Shuttle equipment.

Table VI provides: the total number of planned FO's the number performed during each manned flight and the degree of success.

1. M512 Materials Processing Facility. The PI/Technical Manager for Experiment M512 is Mr. Gordon Parks, MSFC, Huntsville, Alabama.

The objective was to provide a basic apparatus and a common spacecraft interface for performance of a group of metallic and non-metallic materials processing experiments, utilizing the advantages of the near-zero-g and vacuum conditions afforded by the Skylab workshop.

TABLE VI. ACCOMPLISHMENT OF EXPERIMENT FUNCTIONAL OBJECTIVES

EXPERIMENT TITLE	FO'S PLANNED	FO'S PERFORMED			ACCOMPLISHMENT (Percent)
		SL-2	SL-3	SL-4	
Materials Processing [7, 8, 9]					
M512 Materials Processing Facility	N/A				
M479 Zero Gravity Flammability	5	0	0	5	100
M551 Metals Melting	3	3	0	0	100
M552 Exothermic Brazing	4	4	0	0	100
M553 Sphere Forming	2	1½	0	0	75
M555 GaAs Crystal Growth (Not Launched)	1	0	0	0	0
M518 Multipurpose Electric Furnace System	N/A				
M556 Vapor Growth of IV-VI Compounds	1	0	1	1	200
M557 Immiscible Alloy Composition	1	0	1	1	200
M558 Radioactive Tracer	1	0	1	0	100
M559 Microsegregation in Germanium	1	0	1	0	100
M560 Growth of Spherical Crystals	1	0	1	1	200
M561 Whisker-Reinforced Composites	1	0	1	1	200
M562 Indium Antimonide Crystal Growth	1	0	1	1	200
M563 Mixed III-V Crystal Growth	1	0	1	1	200
M564 Halide Eutectics	1	0	1	0	100
M565 Silver Grids Melted in Space	1	0	1	0	100
M566 Aluminum-Copper Eutectic	1	0	1	1	200

To fulfill this objective, a materials processing facility (MPF) was designed for the Skylab program. Obviously the near-zero-g conditions were readily available; however, experiments requiring vacuum conditions had previously been constrained to EVA operations. The M512 facility was designed to allow experiment performance under controlled vacuum conditions inside the Skylab spacecraft.

The facility concept provided the flexibility to perform a series of experiments, investigating various areas of materials processing, utilizing one common piece of hardware--the M512 facility.

The MPF provided a facility with supporting accessories for the performance of:

- M479 Zero Gravity Flammability,
- M551 Metals Melting,
- M552 Exothermic Brazing,
- M553 Sphere Forming,
- M555 GaAs Crystal Growth and,
- M518 Multipurpose Electric Furnace.

The MPF mounting capabilities were adapted by the Multipurpose Electric Furnace to permit the performance of an additional 11 experiments (see paragraph D7).

"The facility was mounted on a honeycomb panel which in turn was attached to the MDA structure by shock mounts. The panel also served as a radiator of heat." (See figure 12).

"The facility was made up of the following main parts:

- o Work chamber
- o Control panel
- o Electron beam gun and batteries
- o Storage boxes for experiment modules and ancillary equipment

The work chamber incorporated a mount to accommodate each experiment module in turn; the mount doubled as a heat sink with a predetermined and calibrated thermal impedance. Near the mount and inside the chamber was located an electrical connector through which power and signals were provided to all the experiment modules except the Multipurpose Furnace, which was a late addition and used only the heat sink/mount and the vacuum capability of the chamber.

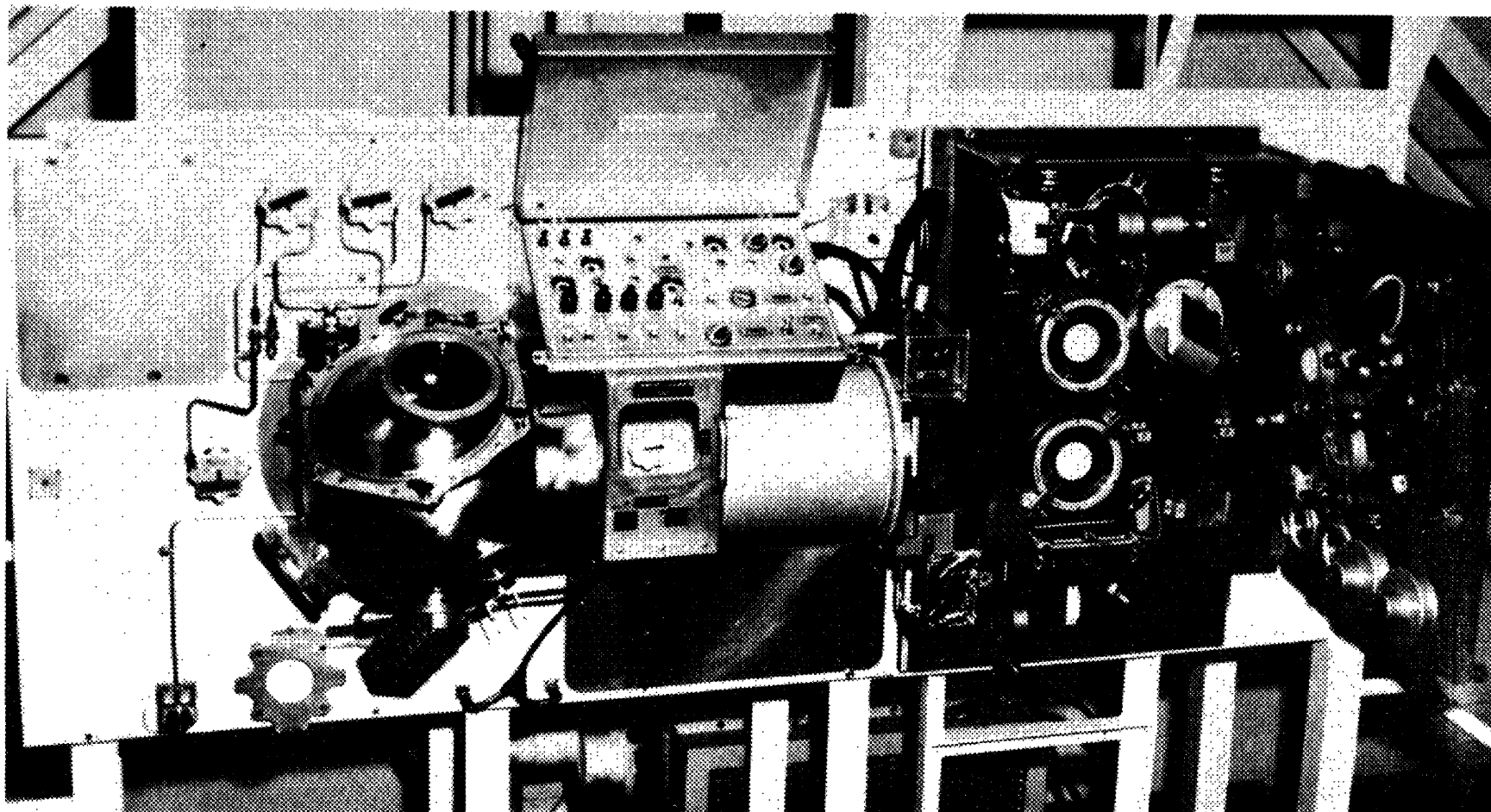


FIGURE 12. M512 MATERIALS PROCESSING FACILITY

The work chamber could be vented to space and thus provide an evacuated environment for the experiments when desired. Windows and illumination within the work chamber permitted viewing of the experiments in progress and also photography by a fixed camera. Gages on the control panel served to monitor the pressure in the chamber, certain temperatures and the beam current and voltage of the electron beam gun. In addition, switches and potentiometers served to operate and control the individual experiments.

The Metals Melting (M551) and Sphere Forming (M553) experiments used the electron beam gun to melt the specimens. It was a most compact gun for its 2 KW output (100mA at 20,000 V). The power supply package was contained in a canister pressurized with an insulating gas: perfluoropropane (C_3F_8). The filament and focusing devices were exposed to the vacuum of the work chamber. The gun was powered by batteries and thus was independent of the spacecraft power bus. Incidentally, the M552 Exothermic Heating experiment also derived its igniter power from these same batteries. All other experiments operated on spacecraft power.

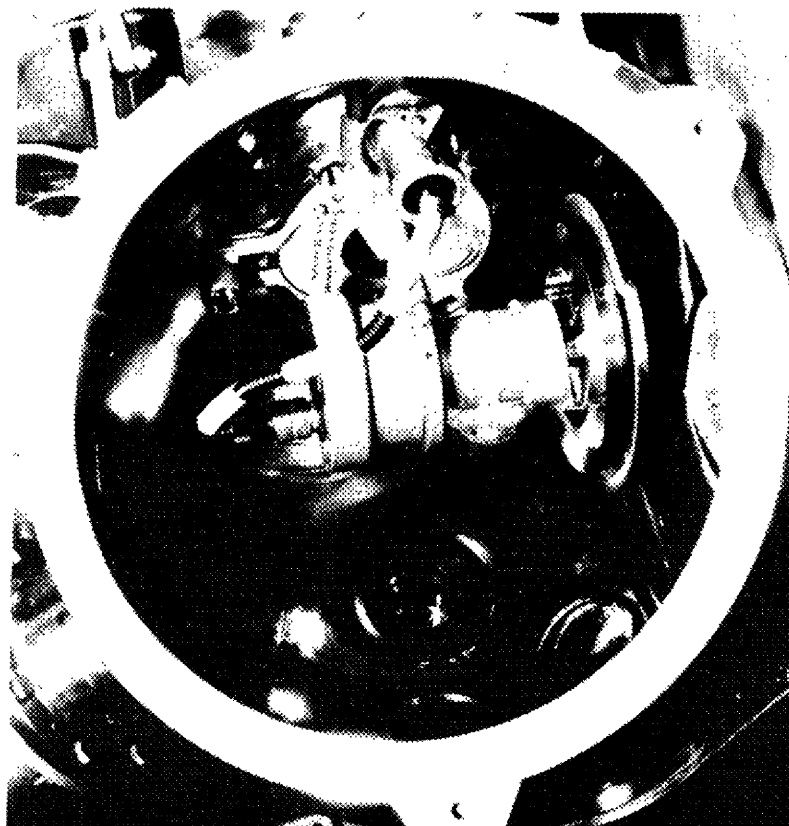
Most of the experiment modules and their accessories were stored in the storage container. To perform an experiment the appropriate module with its accessories was mounted in the chamber.

For the performance of the Metals Melting (M551) experiment the discs (figure 13) were driven by a motor. The electron beam was focused on a tungsten target incorporated in each disc; the disc was then rotated at constant speed to make a weld bead and finally was stopped to melt a puddle. Three discs of different materials were provided for this experiment. They were processed successively.

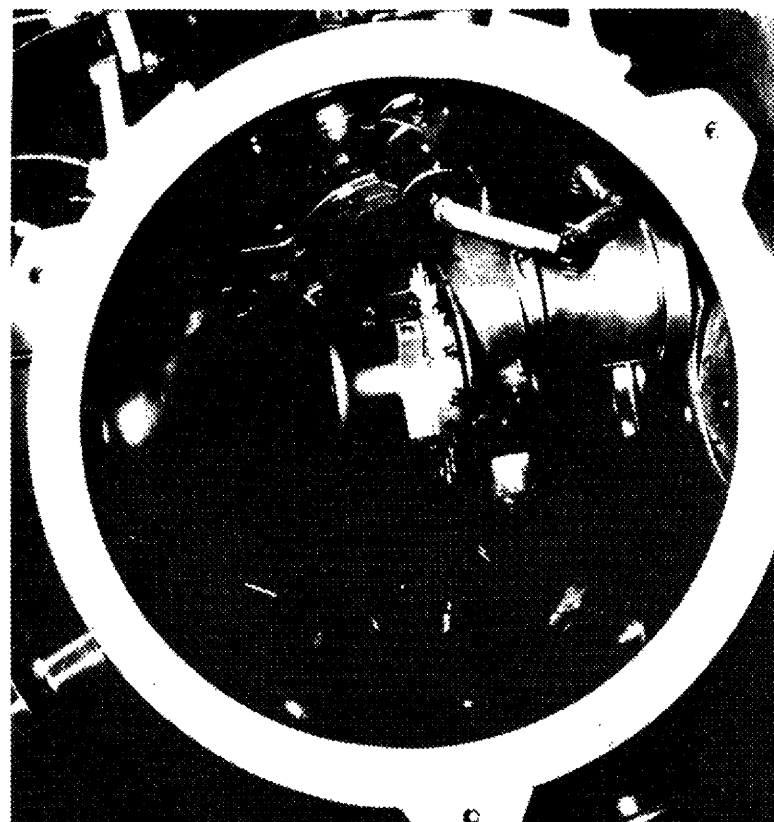
The sphere forming specimens (M553) were carried on two wheels which were successively mounted on an indexing motor, each wheel carried a tungsten focusing target and 14 specimens. After each specimen was melted by the electron beam, a new specimen was indexed into position.

The Exothermic Brazing experiment container (M552) (figure 14) held four exotherm packages. After the chamber was evacuated the exotherm packages were fired one at a time at about two hour intervals. The long intervals were necessary to allow for cooling between operations.

A set of experiments on Flammability (M479) was also performed in the chamber. To perform these experiments, an adapter was mounted in the chamber on the experiment connector; each specimen in turn was mounted in the adapter and ignited. The specimens could be burnt freely, or the combustion could be quenched by evacuating the chamber. Another quench system, by water spray, was also provided." [10]

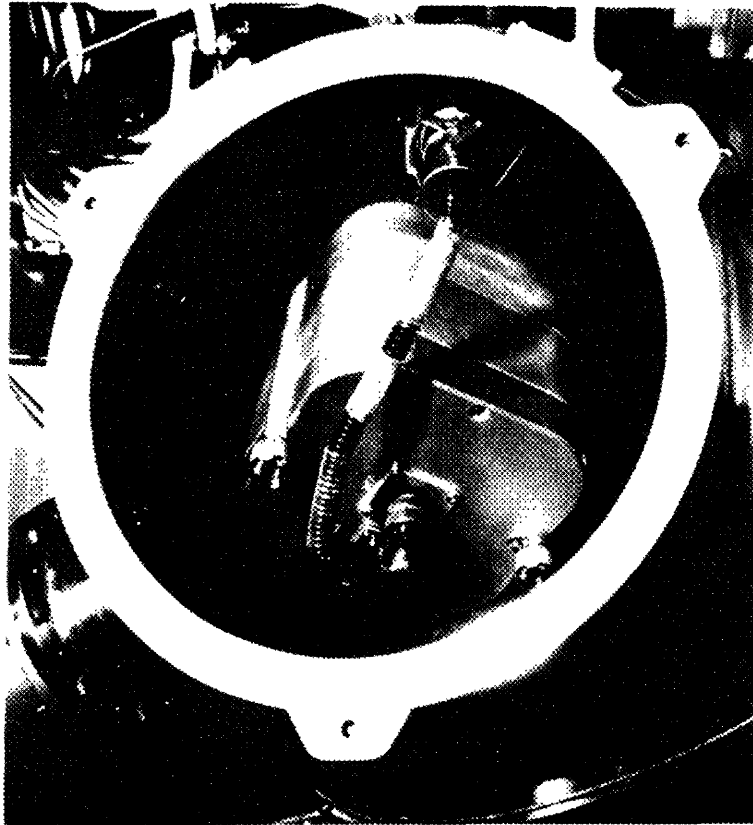


**M551 METALS MELTING
EXPERIMENT**



**M553 SPHERE FORMING
EXPERIMENT**

FIGURE 13. EXPERIMENT OPERATIONAL CONFIGURATION (M551, M553)



**M552 EXOTHERMIC HEATING
EXPERIMENT**



**M479 FLAMMABILITY
EXPERIMENT**

FIGURE 14. EXPERIMENT OPERATIONAL CONFIGURATION (M552, M479)

2. M479 Zero-Gravity Flammability. [11] The PI for Experiment M479 is Mr. J.H. Kimsey, NASA, JSC, Houston, Texas.

The objective was to ignite various materials (aluminized Mylar film, nylon, neoprene, coated nylon fabric, polyurethane foam, bleached cellulose paper, and Teflon fabric) in a 5-psia spacecraft atmosphere under zero-g. The following areas were investigated:

Extent of surface propagation flash over to adjacent materials.

Rates of surface and bulk flame propagation under zero convection and,

Extinguishment by vacuum or water spray and self extinguishment.

Each sample consisted of the test material, a Nichrome heater wire and an electrical socket all attached to a metallic frame. This configuration is shown in the photographs of the returned samples (figure 15). Thirty-seven tests were performed utilizing the Skylab atmosphere (65 percent oxygen at 5.2 psia). Figure 16 shows a sample installed in the chamber and ignited (sample 10 - polyurethane foam).

Motion pictures were taken of the test sequences, and detailed evaluation of this data is in progress. Preliminary results indicate that the process of ignition is essentially the same as under one-g conditions with no increase in the rate with time as is present under one-g.

The preliminary results in the area of extinguishment modes show that eddy currents formed during vacuum extinguishment causing increased burning. Water extinguishment is possible if the water application is controlled. Self extinguish occurs in non-melting materials (paper, carbon, etc.) and material requiring high heat for ignition (teflon), but did not occur in the other materials.

"In addition to video tape and motion pictures we have two still photographs which were taken. The first (figure 16) shows the burning of polyurethane foam in test number 10. Note the spherical shape of the flame and the diameter is estimated at more than 6 centimeters. This means that this material has a flame in zero-gravity (at this atmosphere) extending over 3 centimeters. Another picture immediately after the fire went out shows the smoke pattern. It reportedly persisted for a long period of time."

Four post-test specimens were returned (figure 15). These were numbers 2, 8, 11 and 26. Sample 11 is a remnant of a paper specimen (top right-hand corner of sample 8 container). The other three samples were nylon.

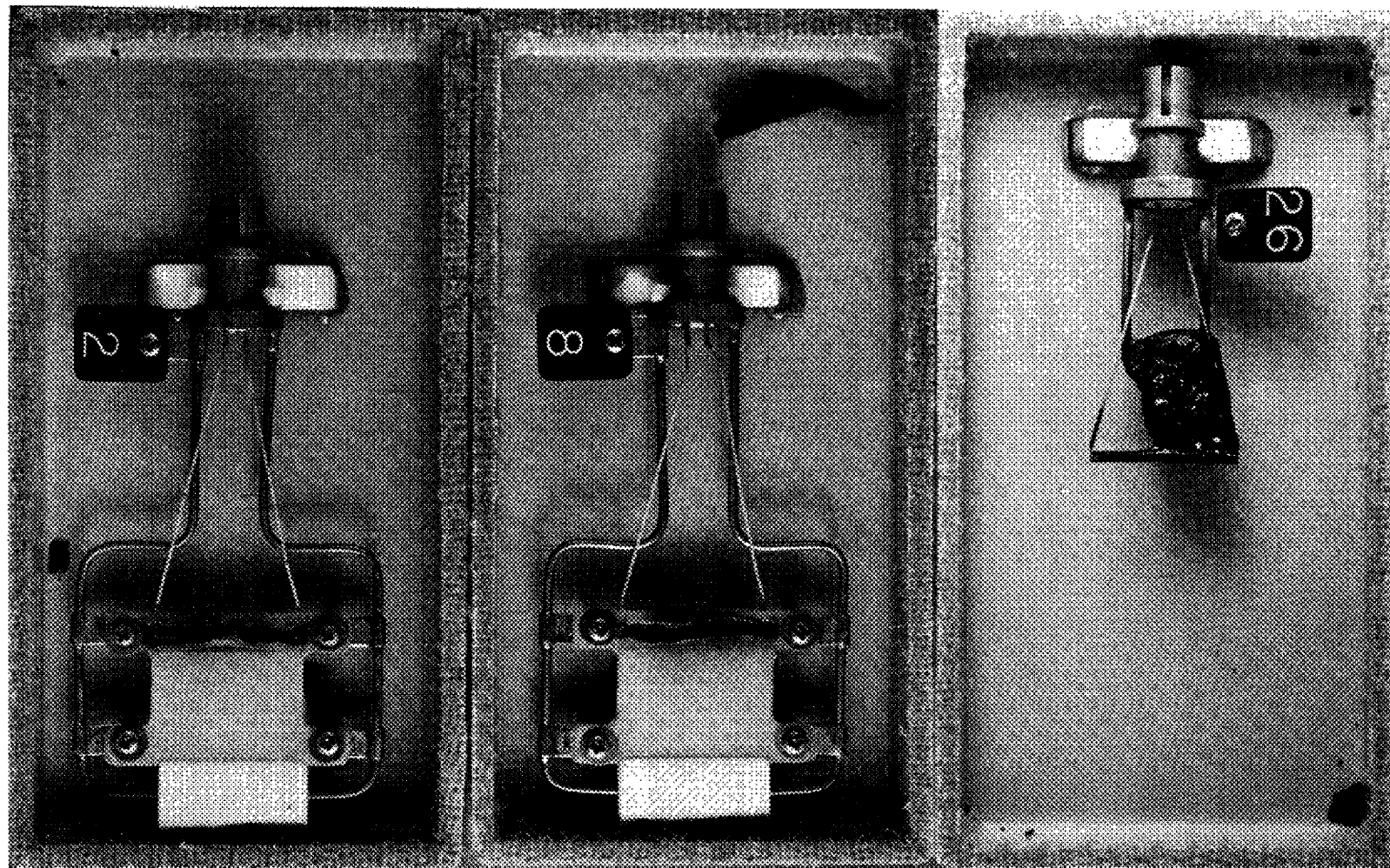


FIGURE 15. RETURNED M479 SAMPLES

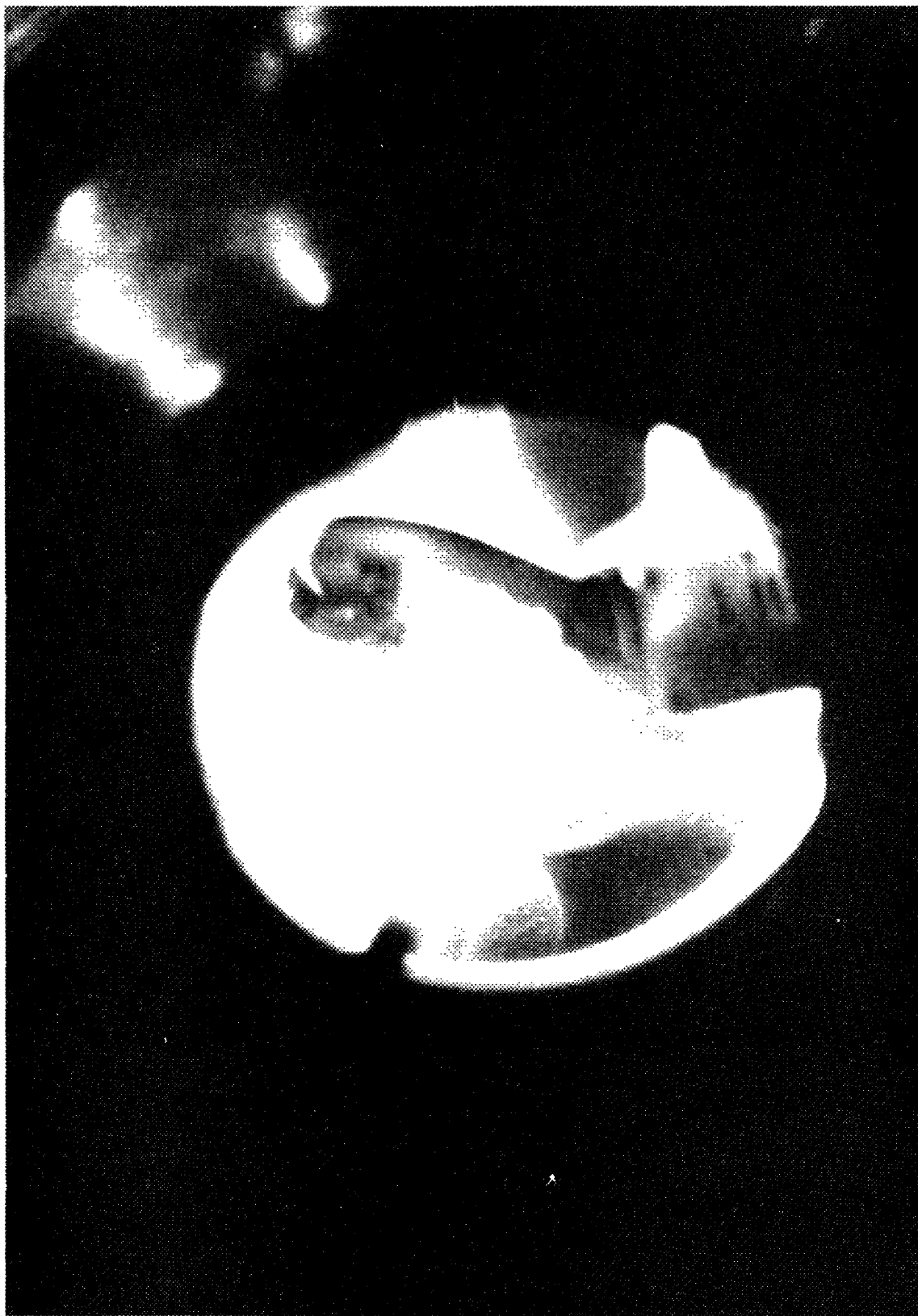


FIGURE 16. BURNING OF POLYURETHANE FOAM ON SL-4

3. M551 Metals Melting. [12] The PI for Experiment M551 is Mr. R.M. Poorman, MSFC, Huntsville, Alabama.

"The objectives of the M551 Metals Melting experiment are to (a) study behavior of molten metal, (b) characterize metals melted and solidified in the low gravity space environment compared to one-gravity of earth, and (c) determine feasibility of joining metals in space. The experiment used the electron beam (EB) and chamber of the M512 apparatus to make a dwell puddle and a melt in a rotating disc of varying thickness. Hence, the EB performed cut-through, full and partial penetration melts, in addition to a re-solidified button. The three disc materials were aluminum 2219-T87, 304 stainless steel and pure tantalum to provide a wide range of density and melting conditions.

The basic equipment used for the Metals Melting experiment is shown in figure 17; it consists of an electric motor drive mechanism which is attached to a three-legged mounting base and carries the disk-shaped experimental specimens as shown. The motor is a nominal 24 v, 1760 rpm D.C. motor, and the gear reduction in the drive mechanism is 300:1; in order to arrive at the output shaft speed of 2.6 rpm required for the experiment, the motor armature speed is reduced by running at an actual input voltage of only 12 v. Power for the motor is supplied through the cable connector shown on the end of the assembly." The specimen track traversed by the electron beam can be seen on the left photographs of the stainless steel flight sample (figure 18). The photograph shows the tungsten target (11 o'clock position), cut through (11 to 9 o'clock), full penetration melt (9 to 5 o'clock), partial penetration melt (5 to 1 o'clock) and resolidified button or device (12 o'clock).

"Observations to date include (a) the proof that EB welding, cutting and melting can be done successfully in low gravity. Earlier, some welding authorities had postulated that without gravity the EB would force the molten puddle out of contact. However, the experiment proved that surface tension forces predominate. (b) From the view-point of cast-solidification, small, equiaxed grains in Skylab specimens compared to large, elongated grains in ground-based specimens were observed. The former are thought to be associated with constitutional super-cooling and nucleation where the later are associated with dendritic solidification. In further support of the more equiaxed grain growth in Skylab, symmetric subgrain patterns were frequently observed where there was much less symmetry in ground-based specimens. Further work is being done to explain the differences in solidification.

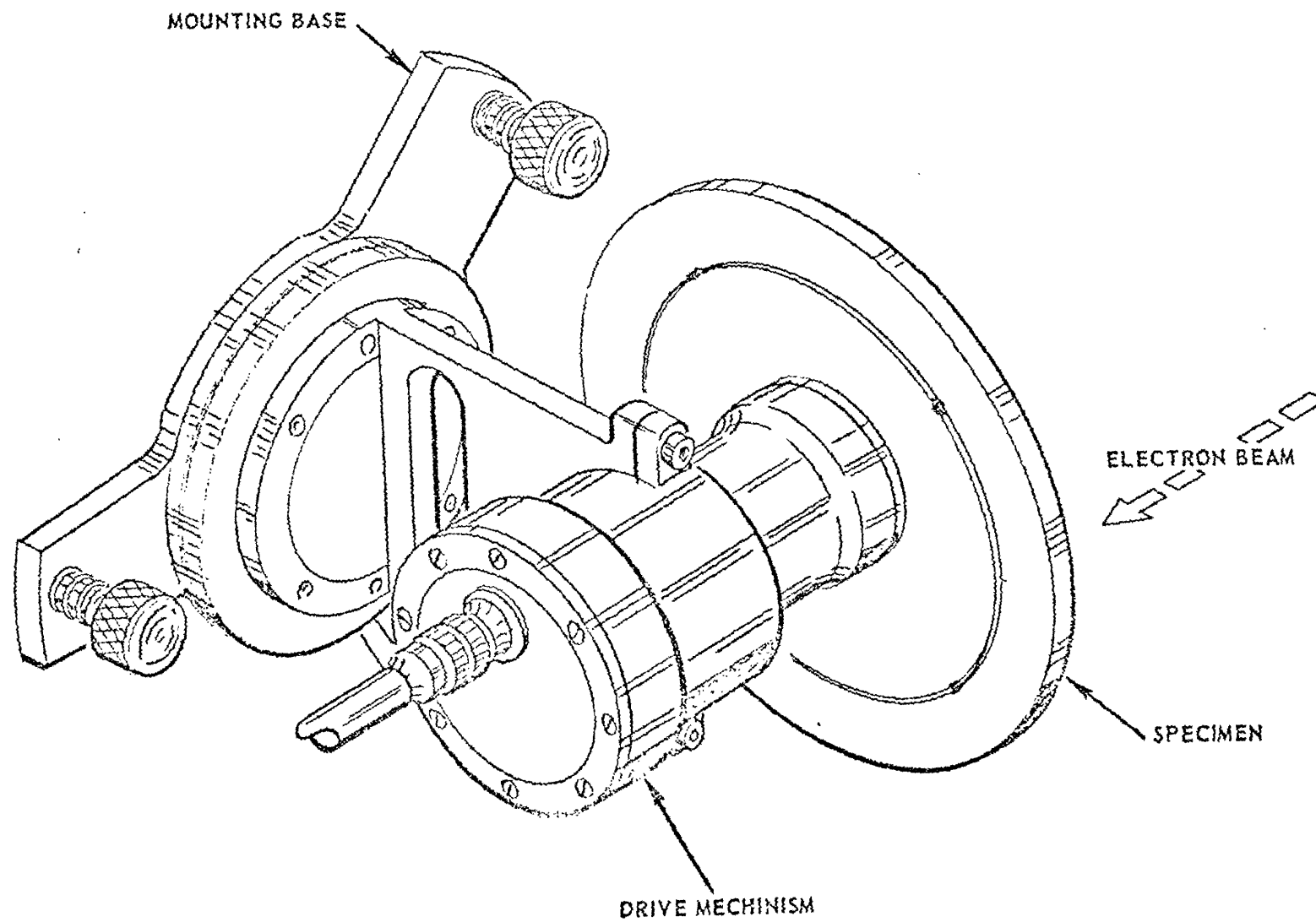


FIGURE 17. METALS MELTING ASSEMBLY

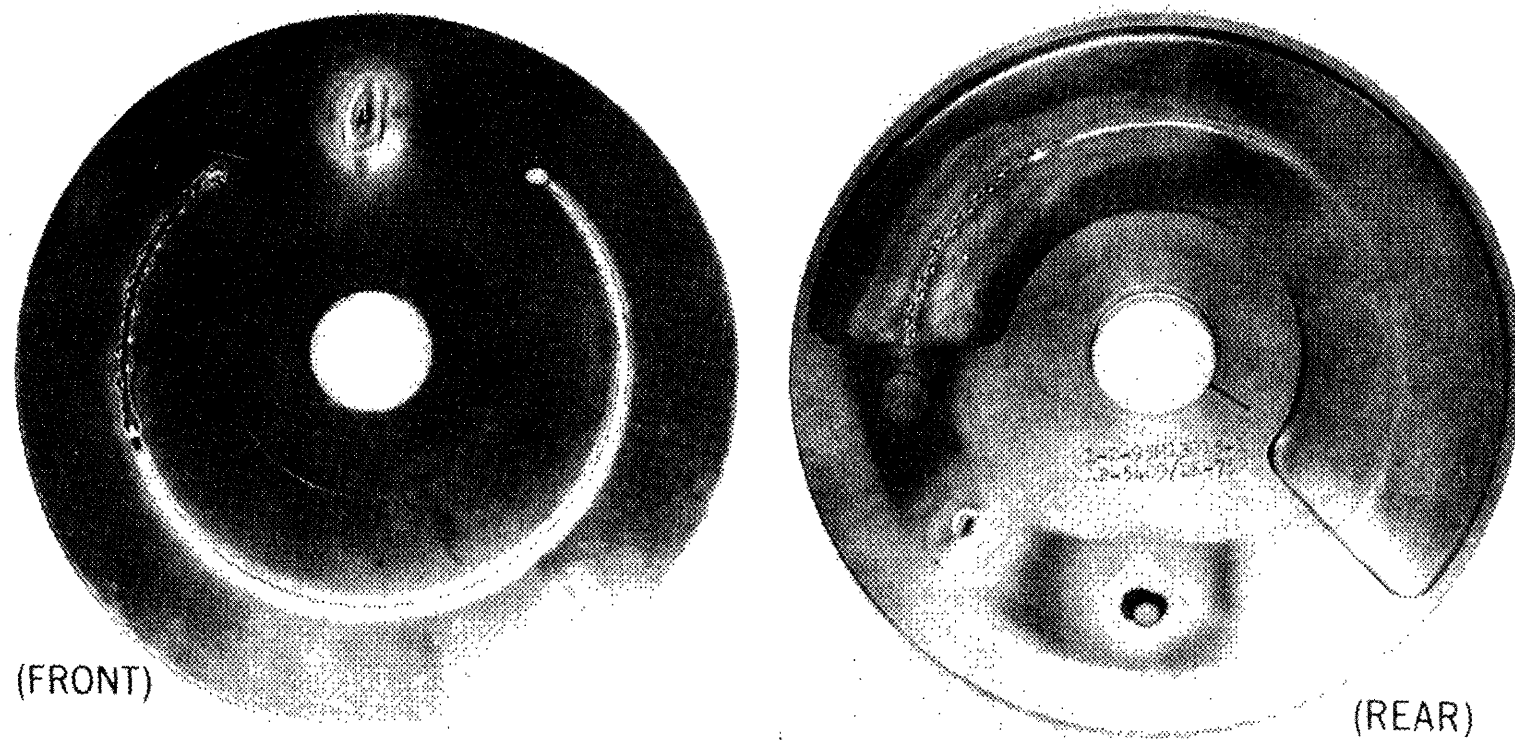


FIGURE 18. SKYLAB STAINLESS STEEL SAMPLE

Gravity effects appear to be small in the weld nugget configuration and puddle control of all three materials when related to typical welding problems. In all cases there was greater puddle sagging in the groundbase specimen with one gravity compared to the Skylab specimen with low gravity. This was particularly true for the weld dwell periods of 15 and 45 seconds. In the over, full, and partial penetration phases, puddle sag was very slight. Frequency of surface ripple, beading and weld spatter appeared to be somewhat related to gravity. All three were slightly reduced in the Skylab specimens which were melted in low gravity. These parameters are of more interest to a scientific study of solidification than to the practical aspects of welding. Basically, this experiment indicates that molten metal surface tension is the predominant force controlling the weld puddle. In low gravity the weld nugget is more symmetrical. All weld puddling and control techniques that are applicable on earth would be expected to be useful in welding in a space environment. Hence, this experiment has demonstrated the feasibility of welding in space.

This subject is developed in detail in a report by R.E. Monroe of Battelle Memorial Institute."

4. M552 Exothermic Brazing. [13] The PI for Experiment M552 is Mr. J.R. Williams, MSFC, Huntsville, Alabama.

"The objectives of this experiment were to evaluate brazing as a tube joining technique for the assembly and repair of hardware in space and to study the spreading, mixing and capillary action of molten braze material in near zero gravity."

An illustration of the complete M552 Exothermic Brazing Package with its electrical power cable is shown in figure 19.

"Each of the four braze specimens consisted of a tube, sleeve, inserts (spacers), and silver-copper-lithium braze rings. Each specimen, possessing a different clearance gap between the tube and sleeve, was positioned in a separate canister containing the exothermic material, ignitors and insulation. Two of the four specimens contained pure nickel tubes and sleeves. An isotope, 110-Silver with a half life of 253 days, was added to a section of one braze ring in the nickel specimens to enhance analysis of capillary flow. The other two tubes and sleeves were type 304L stainless steel with the tube partially slit through the center cross section but with some solid portions for support and to simulate a butt joint.

The aluminum housing which held the four exothermic brazing packages was made in two halves, and after installation of four exothermic packages, was bolted together. A thermocouple temperature

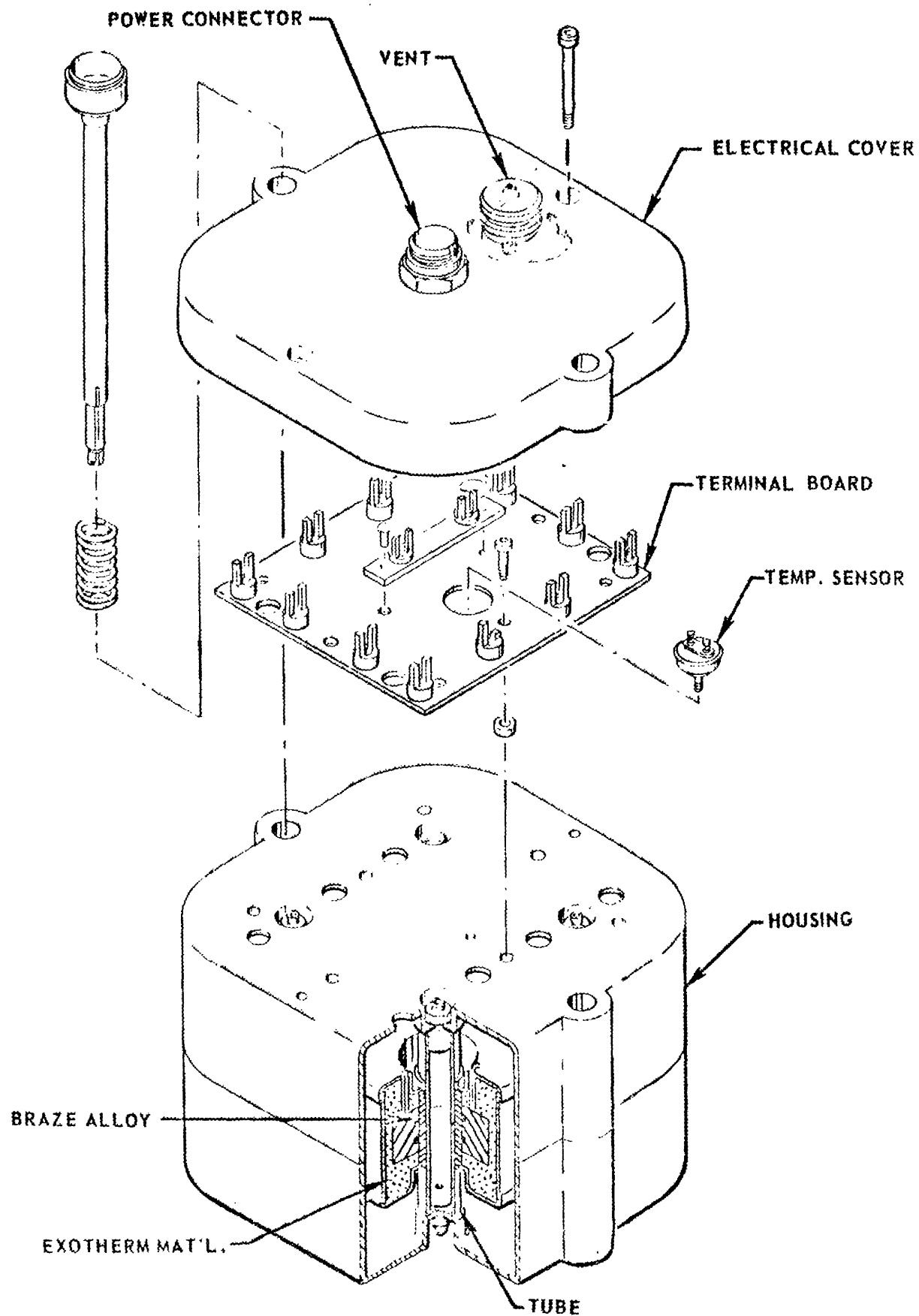


FIGURE 19. EXOTHERMIC BRAZING PACKAGE

sensor was bolted onto the top half portion of the housing, and electrical connections to this sensor and to the ignitor wires in the exothermic packages were soldered to an insulated terminal board attached to the top half of the housing. All electrical connections were led out of the case through the power connector on the cover.

Astronaut Weitz installed the M552 package in the M512 processing chamber in the Skylab MDA. The chamber door was sealed and the chamber atmosphere vented to space. After a 2 hour outgassing period, he initiated the ignition process. Approximately 2.75 hours was required for one exothermic package to be processed through its temperature profile. The other 3 units were processed similarly. All hardware and facility systems worked as designed; no anomalies were observed. The experiment package containing processed exothermic units was returned to earth on June 22 and to MSFC on June 26, 1973."

The following preliminary conclusions can be drawn from the sample evaluation to date:

"The absence of gravity greatly extends the scope of brazing and, thereby, the applicability of brazing to fabrication in space. In zero gravity environment, the surface tension forces driving capillary flow predominate, while on earth these forces must compete with gravity. Study of braze alloy distribution in Skylab specimens clearly indicates that dimensional tolerances, especially braze gap clearances, will be far less critical to joining operations in space than on earth. The .020" radial gap specimen was brazed; greater gaps could also be brazed. This, of course, could not happen in 1 g. The practical significance of this fact, which had been predicted but never tested, can hardly be overemphasized. In space fabrication, many joints, which on earth would be produced by welding, should probably be brazed to allow wider fit up tolerances.

The absence of gravity definitely and surprisingly changes the ways in which liquid and solid metals interact. For example, for the same time and temperature conditions of exposure (a) liquid silver-copper alloy dissolves nickel more rapidly in space than on earth, and (b) solid stainless steel dissolves copper from liquid silver-copper alloy more rapidly in space than on earth. The detailed mechanisms by which these reactions are hastened have not been positively identified, and this effect of space environment had not been predicted. The space environment appears to offer unique advantages for implementation of some liquid-solid reactions, and also the measurement of solubilities. For example, the Skylab experience clearly indicates a higher solubility of nickel in liquid silver-copper alloy than had been found in the earth-bound studies (in this reaction the silver is rejected and appears as almost pure metal); this is not

because nickel is more soluble in space, but rather because it dissolves more rapidly. This pattern of behavior suggests that saturated liquid metal solutions can be more easily produced, and true solubilities are more easily determined in space than on earth.

Liquid-vapor boundary surfaces (menisci), and the flow of liquid metal driven by surface tension are in close conformance with what had been predicted for zero gravity environment. There were no unexplained effects and in the Skylab specimens the surface tension of liquid silver-copper alloy appears to have been quite uniform.

The addition of a radioisotope tracer to the M552 brazing experiment provided a unique picture of the thermal history of braze melting within the annulus as well as useful representation of the braze alloy flow pattern during the melting solidification process. Silver isotope tended to settle (Ag is densest component) in ground samples; whereas complete circumferential mixing of the isotope was reported in Skylab samples. As predicted the ground base settling is due to gravity-induced sedimentation. The unexpected complete circumferential mixing which occurred on Skylab can be attributed to liquid-state diffusion and/or turbulence in the capillary flow.

The presence or absence of gravity has no observable effect on the mechanism of alloy solidification. Such microstructural details as dendritic configuration, and eutectic structure were the same in space as on earth.

The Skylab specimens exhibited fewer and smaller shrinkage defects than the comparative ground processed characterization samples indicating that gravity forces are significant during the capillary movement of the braze alloy.

The oxide build-up on both the M552 Skylab braze alloy and the substrate materials was less than on ground based specimens indicating the adequacy of utilizing the space vacuum and its infinite pumping capacity for brazing operations of this type configuration."

5. M553 Sphere Forming. [14] The PI for Experiment M553 is Mr. E.A. Hasemeyer, MSFC, Huntsville, Alabama.

"The M553 Sphere Forming Experiment conducted in the M512 Furnace Facility during Skylab II was designed to study the effects of a reduced gravity environment on the containerless solidification of face centered cubic metals. The metals studied were: pure Ni, Ni-1 wt % Ag, Ni-12 wt % Sn, and Ni-30 wt % Cu. The constant primary crystalline structure was selected because the solidification theory for face centered cubic materials is the most advanced and offered an attractive basis for planning the experimentation and evaluating the results."

The basic experiment equipment shown in figure 20 consisted on a drive motor and mounting base similar to experiment M551. The M553 motor positioned and indexed the samples through the EB for melting. Figure 20 is an illustration of the drive assembly with a sample wheel attached to the motor output shaft.

"The materials were electron beam melted and were either retained on stings of the same composition as the specimen or were to be released while molten, and solidified while floating free within the chamber. The latter operation was not entirely successful and some specimens intended to be released remained on their ceramic pedestals.

Careful analysis of the samples indicated that there was an outstanding record of both initial and terminal solute redistribution processes, and that this record may be substantially better than that obtained terrestrially for comparable experimental conditions. Further, the last regions to solidify evidence extensive solidification terracing; and for one alloy type, this terracing was found to be decorated with second phase precipitate particles. These particles were highly localized in systematic arrays which were frequently low index crystallographic systems.

Some of the samples underwent unanticipated solidification reactions rather than the anticipated solid/liquid processes. Subsequent consideration indicated that this phenomenon could have been anticipated and that it was a result of the reduced gravity environment - that is, the reduced gravity environment magnified a typically microscopic phenomenon terrestrially so that it became a macroscopic effect. Work is continuing on quantifying this effect.

It is felt that these and subsequent results will contribute to the detailed understanding of terrestrial solidification processes and have shown the importance of considering the gas phase during space processing. Whereas prior consideration of one-gravity solidification dealt with liquid/solid reactions, this work indicates that consideration of solid/liquid/gas reactions is important and potentially beneficial in a reduced gravity environment. It was anticipated that the reduced gravity environment would enhance the sphericity of the processed samples and this enhancement is shown in figures 21a and 21b for 1g and low g specimens, respectively. Typically, the 1g specimens had a sphericity value (R_{\max}/R_{\min}) of 1.28, whereas the flight samples were typically 1.01 to 1.04, a substantial enhancement due to the reduction in gravity."

6. M555 GaAs Crystal Growth. The PI for Experiment M555 is Mr. M.C. Davidson, NASA, MSFC, Huntsville, Alabama.

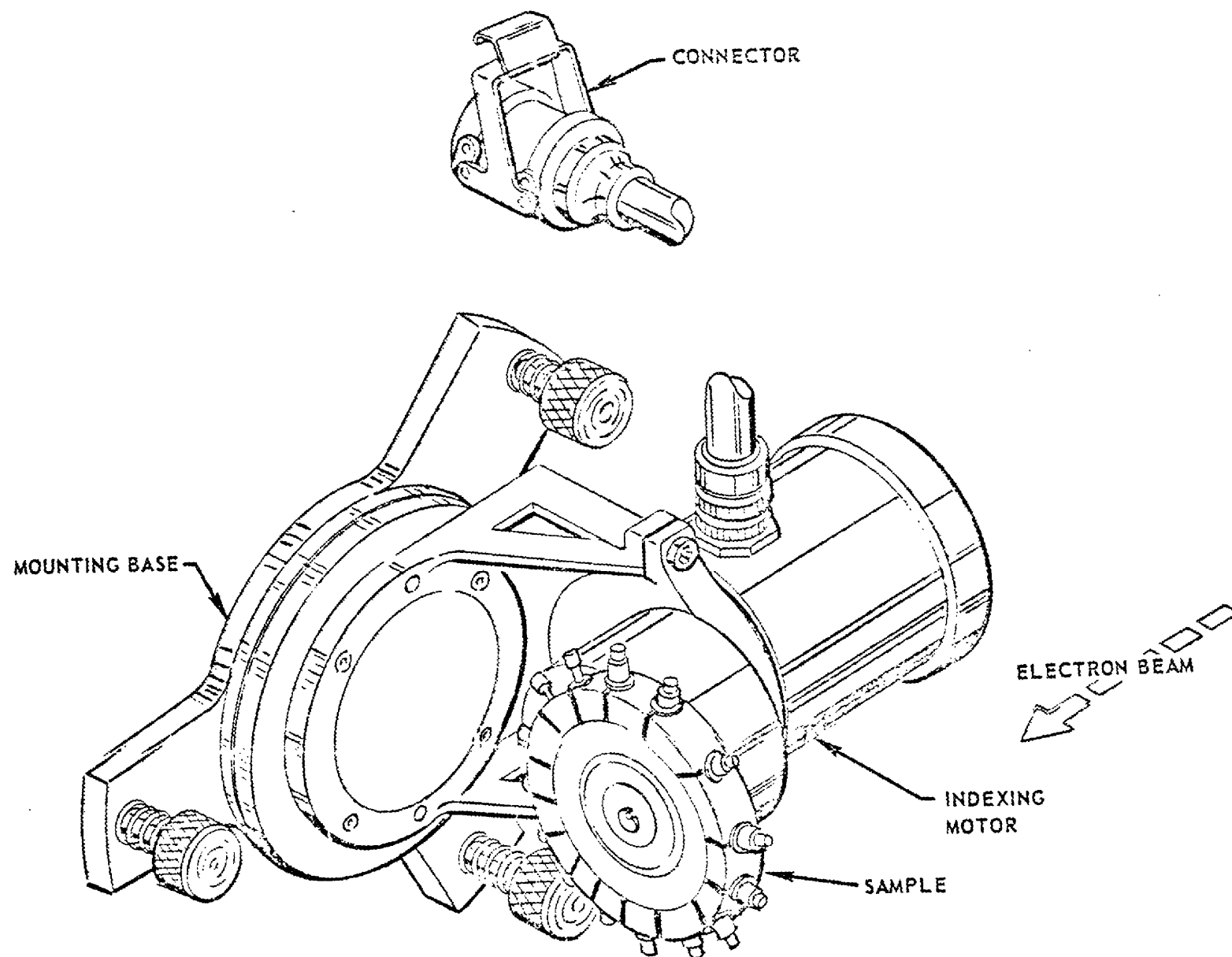
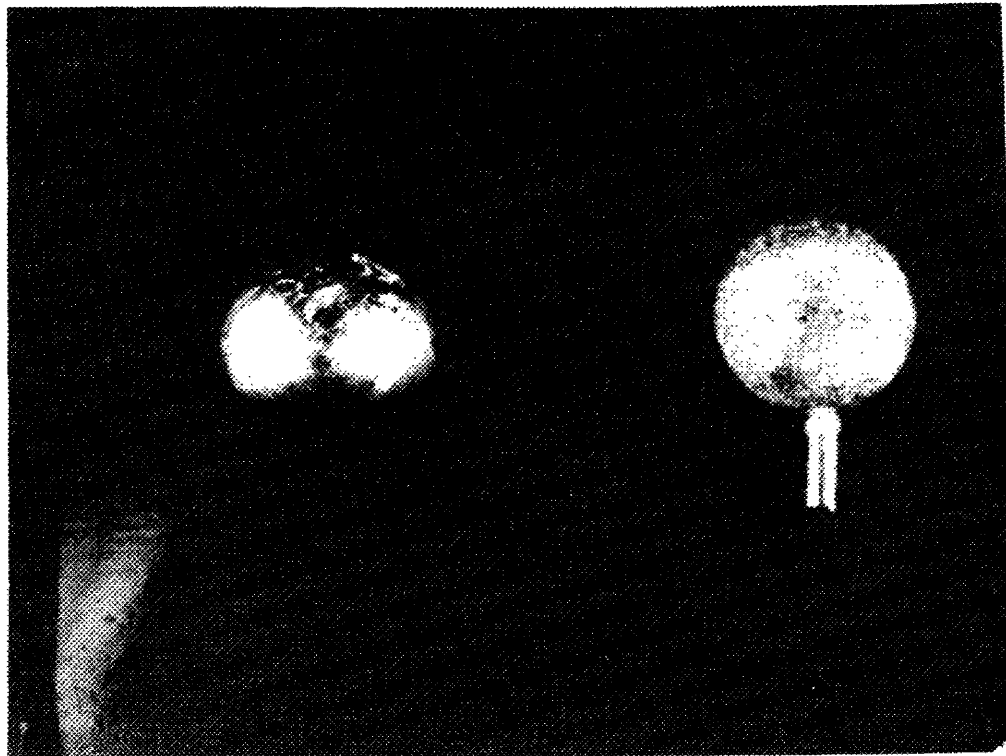


FIGURE 20. SPHERE FORMING ASSEMBLY



(a)
GROUND PROCESSED

(b)
SKYLAB PROCESSED

FIGURE 21. PHOTOGRAPHS OF M553 SAMPLES

This experiment was to grow single crystals of gallium arsenide from solution in near-zero-g, in anticipation of producing material of exceptionally-high chemical and crystalline perfection.

The hardware was scheduled to be launched in the SL-2 CM and performed in the M512 chamber during the first mission. However, the M555 launch container was removed from the SL-2 CM to provide additional launch space for contingency equipment.

Approval was obtained for launch and performance of M555 during the SL-3 mission, and the launch container was stowed in the CM. However, at the SL-3 Flight Readiness Review on July 24, 1973, NASA removed the container to allow stowage of the contingency rate gyro hardware.

The M555 hardware was included on a priority list for launch in the SL-4 CM. Due to several factors (weight, size, and priority number), the hardware was not launched on SL-4. The experiment hardware is currently stored at MSFC for a future program.

7. M518 Multipurpose Electric Furnace System. The PI/ Technical Manager is Mr. Arthur Boese, MSFC, Huntsville, Alabama.

The Multipurpose Electric Furnace System (MEFS) was intended to enhance the Skylab hardware capabilities by providing means to perform experiments on solidification, crystal growth and other processes involving phase changes in materials. The System was used to perform 11 experiments involving phase changes at elevated temperatures in systems comprising selected combinations of solid, liquid, and vapor phases. Because of the near-zero gravity aboard Skylab, the liquid and vapor phases were essentially quiescent and phases of different density had little or no tendency to separate.

The guiding design requirement for the MEFS was to produce apparatus that would apply prescribed heating and cooling programs and/or known temperature distributions to selected experimental samples of material. It would also provide the widest possible flexibility in applying the temperature distributions and temperature-versus-time sequences within the constraints imposed by existing interfaces to which the MEFS was to be designed.

The MEFS consisted of three main parts: the furnace, designed to interface with the M512 Materials Processing Facility; a programmable electronic temperature controller, used to control the temperature levels in the furnace; and experiment cartridges which contained the sample materials. The furnace (see figure 22) had three specimen cavities so that three material samples could be processed in a single run. The furnace was constructed to provide three different temperature zones along the length of each sample cavity as follows:

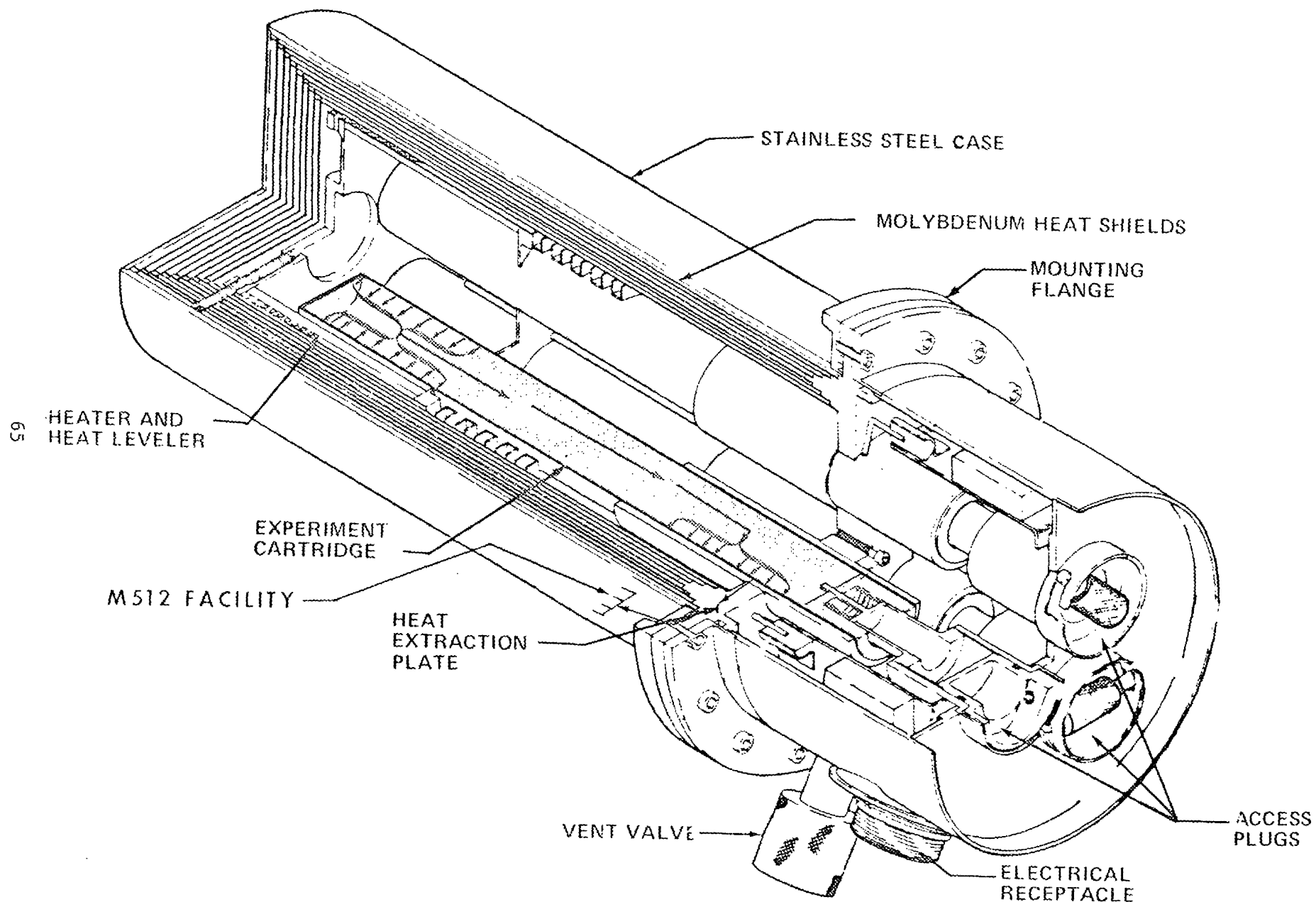


FIGURE 22. MULTIPURPOSE ELECTRIC FURNACE

A programmable constant temperature hot zone at the end of the sample cavity where temperatures up to 1050°C were launched.

A gradient zone next to the hot zone where temperature gradients ranging from 20°C to 200°C per centimeter were established in the samples.

A cool zone in which heat conducted along the samples was rejected by radiation to a conducting path that carried the heat out of the system.

The control package provided active furnace temperature control. It was adjustable to any specified temperature within the furnace capability. Two timing circuits in the controller permitted programming the soak time at the set temperature and the furnace cooling rate after the soak period. Active temperature control continued during programmed cooling.

The cartridge thermal design further controlled the actual temperature distribution applied to the sample.

The MEFS was used in conjunction with M512 MPF, for the performance of:

- M556 Vapor Growth of IV-VI Compounds
- M557 Immiscible Alloy Composition
- M558 Radioactive Tracer
- M559 Microsegregation in Germanium
- M560 Growth of Spherical Crystals
- M561 Whisker-Reinforced Composites
- M562 Indium Antimonide Crystal Growth
- M563 Mixed III-V Crystal Growth
- M564 Halide Eutectics
- M565 Silver Grids Melted in Space
- M566 Aluminum-Copper Eutectics

The M518 MEFS installed on the M512 MPF is shown in figure 23.

8. M556 Vapor Growth of IV-VI Compounds. [15] The PI for Experiment M556 is Dr. H. Wiedemeier, Reusselaer Polytechnic Institute, Troy, New York.

"The primary objective of our crystal growth experiments in space was to observe and to measure changes in the mass transport rate of a chemical system and in the morphology of crystals of IV-VI compounds. In the absence of gravity-driven convection and for given experimental conditions, the transport should be controlled by the

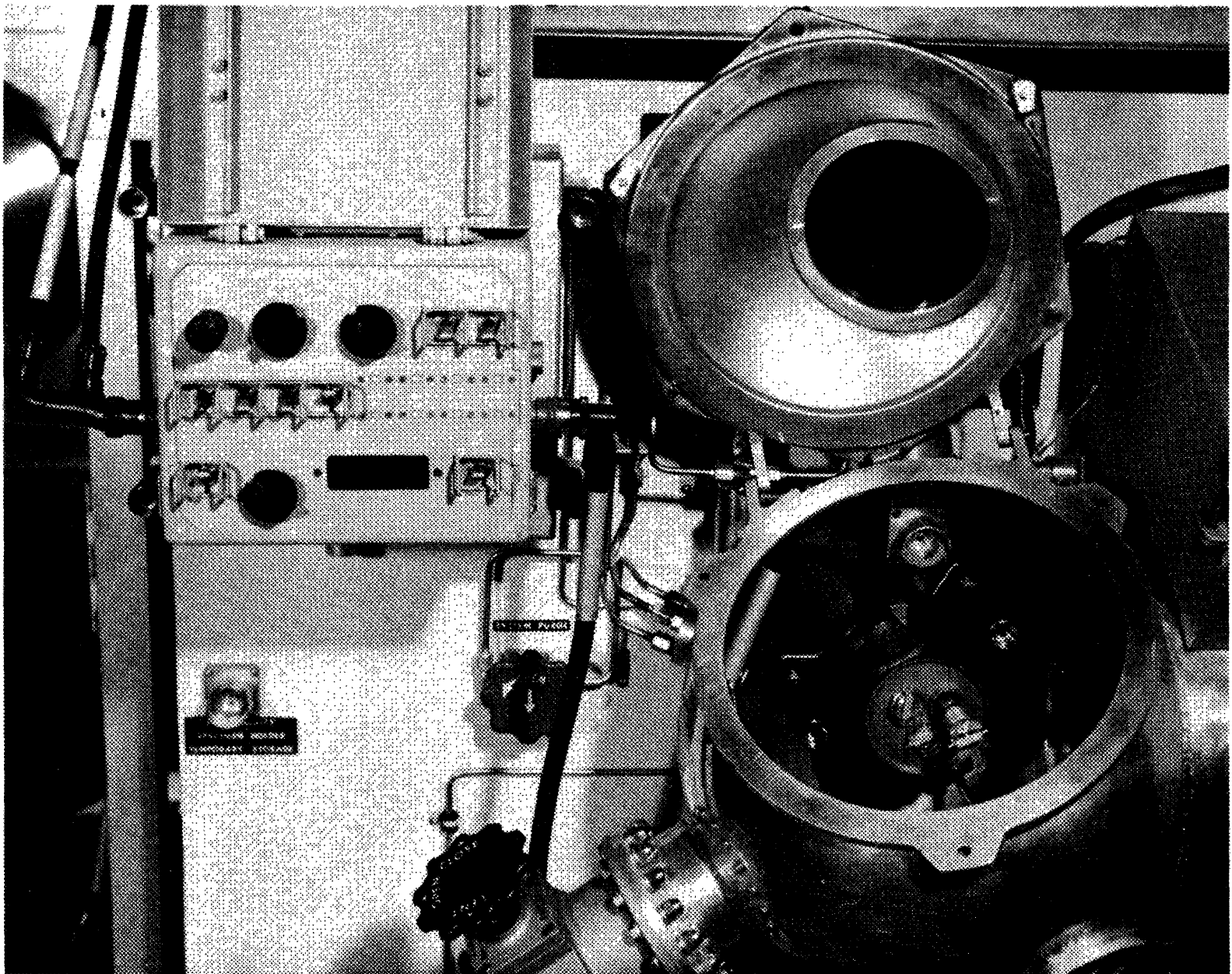


FIGURE 23. M518 MEFs INSTALLED ON M512 MPF

thermochemical parameters of the solid-gas phase reaction. The crystal habit and morphology should be primarily determined by the crystallographic properties of the respective crystal structures. In addition, information concerning the number and distribution of crystal defects is expected from these experiments."

"In a chemical transport reaction (...), a gaseous transport agent reacts at a given temperature with the solid source material to form exclusively gaseous products. The vapor species migrate from the source to the condensation zone of the reaction vessel where, at a different temperature, the reverse reaction occurs with formation of the solid. The necessary concentration gradient is established by means of a temperature gradient. Under optimal experimental conditions well defined single crystals are formed by the condensation reaction. The transport reaction is carried out in evacuated sealed ampules of fused silica which are subjected to the desired temperature gradient in a horizontal two-zone tubular resistance furnace."

"The transport ampules were made of fused silica tubing of 13.7 mm inner diameter and 150 mm in length. Close to one end the ampule contained three shallow indentations to hold the source material in place. The other ampule end was sealed after loading at a pressure of 10^{-6} torr or less. Prior to loading the cleaned ampules (...) were outgassed at a temperature of about 1000°C for 10 hours and a vacuum of 10^{-6} torr. The polycrystalline starting materials GeSe and GeTe were synthesized by annealing stoichiometric mixtures of high purity elements (99.999%) and subsequent sublimation of the product (...). The crystallographic identity of the materials was established by X-ray diffraction techniques. High purity GeI_4 (99.999%) was used as a transport agent. The ampule designated 3A in this experiment contained 2.0 gm of GeSe and 14.28 mg of GeI_4 per cm^3 tube volume. Ampule 3B was loaded with 1.0 gm GeSe and 1.28 mg/ cm^3 GeI_4 , and ampule 3C contained 1.0 gm GeTe and 7.14 mg/ cm^3 GeI_4 . After sealing the ampule, the starting material was quantitatively sublimed to the source end. For the temperature gradient $520 \rightarrow 420^\circ\text{C}$, these conditions corresponded to a high (GeSe, 3A), low (GeSe, 3B) and medium (GeTe, 3C) contribution of the convective component to the overall transport under ground-based conditions. This set of ampules was used for the SL-3 mission experiments."

"For the SL-4 mission experiments the back-up ampules 5A, 5B, and 5C were employed. The quantities of GeSe and GeTe and the initial amounts of transport agent GeI_4 used in these ampules was the same as in the corresponding SL-3 transport tubes. Due to the lower temperature gradient used for the SL-4 experiments ($412 \rightarrow 346^\circ\text{C}$), a partial precipitation of transport agent occurred in ampules 5A and 5C during transport. No precipitation of GeI_4 occurred in ampule 5B.

The resulting pressure conditions corresponded to a medium (GeSe, 5A and GeTe, 5C) and to a low (GeSe, 5B) convective contribution to the overall transport under ground-based conditions."

"The transport tubes were enclosed with the proper heat shields in evacuated metal cartridges (...). These cartridges were inserted into the multi-purpose furnace by the astronauts. The chemical transport reactions for the GeSe and GeTe systems and the experimental conditions employed for the studies in micro-gravity environment are summarized in Table VII. The GeI_4 pressures are calculated for the mean temperature of the gradient and ideal gas conditions.

TABLE VII. TRANSPORT REACTIONS AND EXPERIMENTAL CONDITIONS

$\text{GeSe(s)} + \text{GeI}_4(\text{g}) = 2 \text{ GeI}_2(\text{g}) + 1/2 \text{ Se}_2(\text{g})$	
$\text{GeTe(s)} + \text{GeI}_4(\text{g}) = 2 \text{ GeI}_2(\text{g}) + 1/2 \text{ Te}_2(\text{g})$	
T: 520 → 420°C (SL-3 Mission)	
GeSe (3A)	P $\text{GeI}_4(\text{g})$ = 1.50 atm
GeSe (3B)	P $\text{GeI}_4(\text{g})$ = 0.13 atm
GeTe (3C)	P $\text{GeI}_4(\text{g})$ = 0.75 atm
T: 412 → 346°C (SL-4 Mission)	
GeSe (5A)	P $\text{GeI}_4(\text{g})$ = 0.42 atm
GeSe (5B)	P $\text{GeI}_4(\text{g})$ = 0.12 atm
GeTe (5C)	P $\text{GeI}_4(\text{g})$ = 0.60 atm

After initiating the heating cycle aboard S/L-3, a temperature of 520°C at the source end and of 420°C at the condensation region of the ampule were achieved after 2.75 hours. These conditions were maintained ($\pm 3^\circ\text{C}$) for 33 hours, during which transport and crystal growth occurred. After termination of the experiment, cooling of the ampules to ambient temperature took place in the multi-purpose furnace over a period of about 12.5 hours. The heating cycle for the SL-4 experiments consisted of a heat-up period of 1.5 hours, a soak-time of 34 hours during which the temperature remained constant within $\pm 3^\circ\text{C}$, and a cool-down period of 7 hours."

"The combined experimental evidence from the analysis of space grown crystals confirms the predicted positive effects of micro-gravity on crystal quality." (See figures 24 and 25.) "This is based on a comparison of macroscopic crystal habits, deposition patterns, optical and scanning electron microscopy, and the results of thermal etching of cleaved crystals obtained under ground-based and microgravity conditions."

"In addition to improved crystal quality, a second major result of the Skylab experiment M556 is the observation of greater mass transport rates than expected in micro-gravity environment. This observation is of scientific and technological significance with respect to the theoretical extension of conventional transport models and the possibility of growing higher quality crystals at reasonable rates by the vapor transport technique in space. Continuing ground-based studies indicate that the interaction between gravity-driven and other convective components causes turbulence and the negative effects on crystal quality as observed on earth. The ultimate goal of these studies is to approximate the effects of micro-gravity on crystal quality under earth-bound conditions."

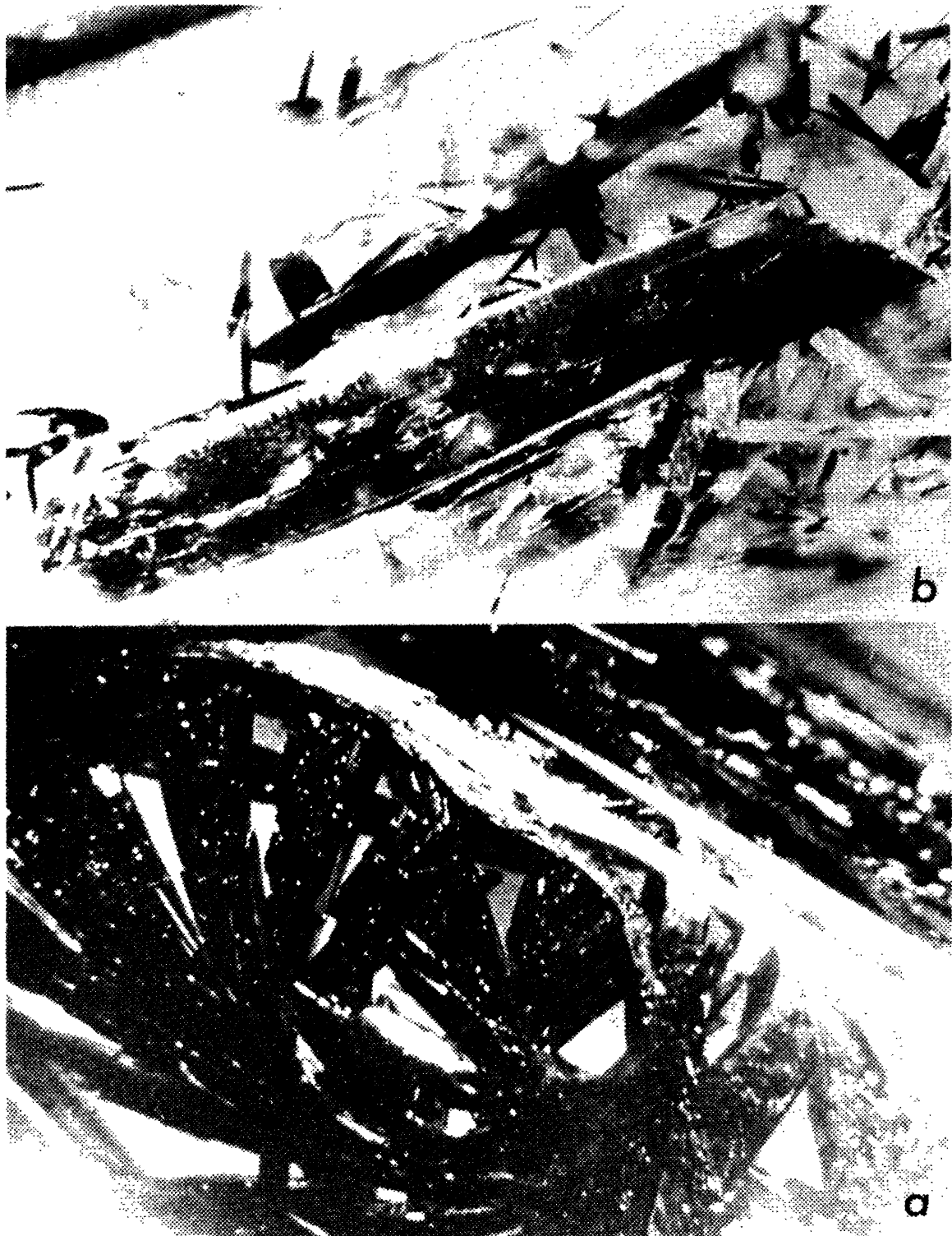
"The internal consistency of results obtained for two materials (GeSe and GeTe), two different temperature gradients and various pressures of transport agent strongly support the validity of the above conclusions."

9. M557 Immiscible Alloy Composition. [16] The PI for Experiment M557 is Mr. J. Reger, TRW, Systems Group, Redondo Beach, California.

The experiment was to determine the effects of near-zero-g on the processing of material compositions which normally segregate on earth.

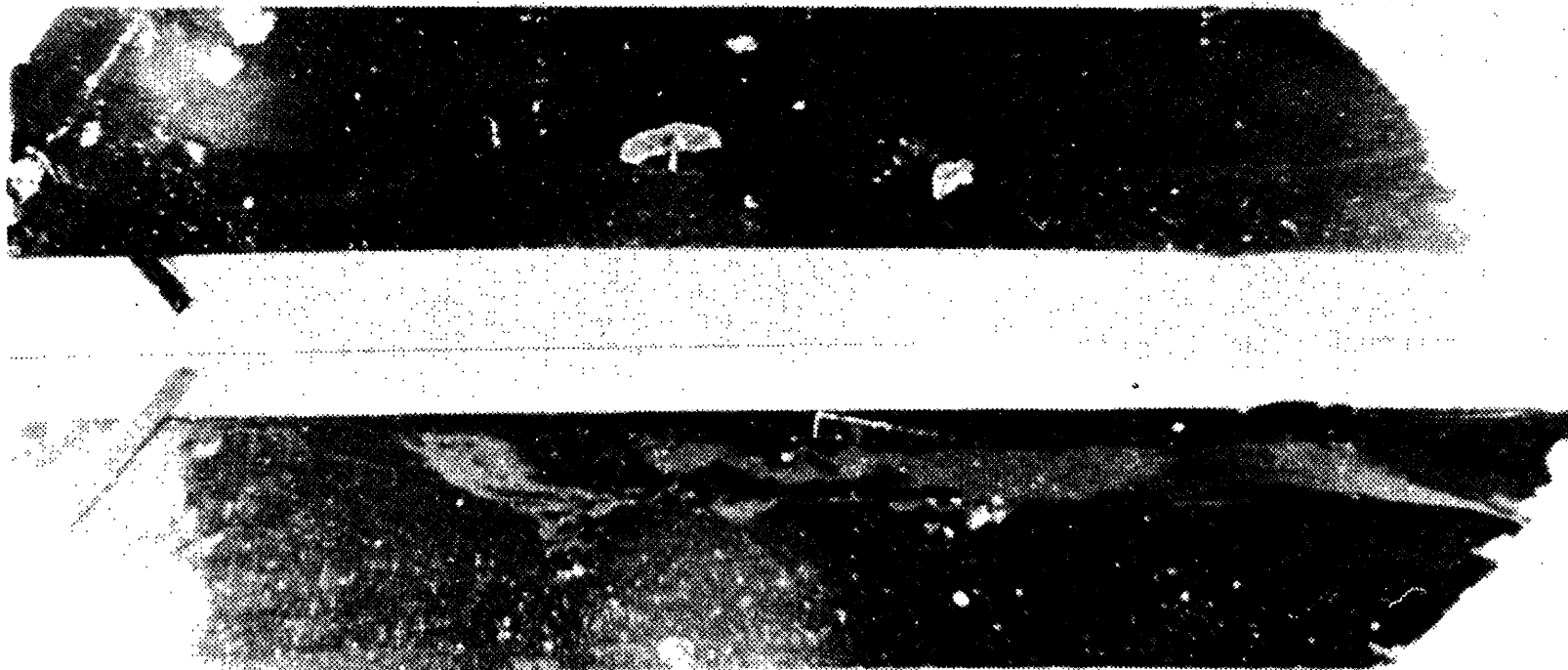
"Immiscible systems, with few exceptions, are one of the unique classes of materials which are non-producible in bulk form on earth. A number of these systems provided a potential class of new materials if they can be successfully produced in space. These potential applications include electronic, optical and other types of materials with unique physical characteristics.

Since segregation effects due to density differences and the relatively long time period necessary to solidify the materials from the liquid state are the primary reasons for inability to secure bulk samples, processing in a low gravity environment should circumvent the majority of the problems associated with the immiscible systems."



NOTE: View of the deposition region of GeSe (3A conditions) ground-based (a) and space (b) transport ampule. Edge lengths of space crystals (b) range from 0.2-18mm.

FIGURE 24. DEPOSITION OF GeSe CRYSTALS



Photographs of front and back side of the largest GeSe single crystal platelet grown under micro-gravity conditions (3A). Dimensions are 4x18mm, thickness is about 50 μ .

FIGURE 25. LARGEST GeSe CRYSTAL GROWTH

"Experiment M-557: "Immiscible Alloy Compositions", is comprised of three separate specimen ampoules per cartridge processed in the M-518 Multipurpose Electric Furnace; two in the isothermal portion and one in the gradient region of the furnace. The isothermal ampoules, designated A and B, contain 76.85 - 23.15 w/o gold-germanium and 45.05 - 45.06 - 9.89 w/o lead-zinc-antimony, respectively. Ampoule A, gold-germanium, exhibits almost complete solid state immiscibility and Ampoule B, lead-zinc-antimony, exhibits a liquid miscibility gap below a critical or consolute temperature. The gradient ampoule, designated C, contains 70.20 - 14.80 - 15.00 w/o lead-tin-indium, with tin as the precipitated second phase."

"Two sets of three cartridges each were processed under one gravity conditions as controls; three horizontally and three vertically in the furnace. Three cartridges were then subsequently processed in the M-512/M-518 facility on board Skylab during the SL-3 mission. Basically, the processing consists of heating the isothermal section of the cartridges to 720°C, holding the temperature for a soak period of 4 hours, then allowing the cartridges to passively cool to ambient temperature. This temperature was set to allow Ampoule B to be heated above the critical or consolute temperature where the liquid immiscibility gap is exceeded and the liquid elements become single phase. The soak period is sufficiently long for complete mixing and diffusion of the elements. The temperature at the cold end is clamped such that Ampoule C is not completely melted, thus a comparison of the solidification behavior between one gravity and low gravity processed specimens can be made." The experiment was repeated on the SL-4 mission using the same thermal conditions.

"From the metallurgical and electronic examinations, the low gravity processed specimens exhibited unique metallurgical features and enhanced electronic properties as contrasted to the one gravity processed controls."

"In all cases, the low gravity processed specimens exhibited better homogenization and microstructural appearances than the one gravity control specimens." (See figures 26 and 27.) "The electronic behavior of the low gravity specimens were equal or superior in every respect and the Ampoule B specimens exhibited an anomalous superconducting transition temperature approximately 2°K higher than either the elements or the one gravity control specimens. In addition, the low gravity processed A and B ampoules exhibited X-ray diffraction lines not identifiable with any referenced diffraction patterns.

Inasmuch as a low gravity environment suppresses thermal convection, high G/R ratios can be utilized to obtain directionally solidified structures having superior metallurgical and electronic features, exemplified by the C specimens, as contrasted to the one gravity processed specimens.



SPECIMEN 1A



SPECIMEN 5A

ONE GRAVITY PROCESSED SPECIMENS 1A AND 5A AND
LOW GRAVITY PROCESSED SPECIMEN 12A (10X)



SPECIMEN 12A

FIGURE 26. GOLD-GERMANIUM DISPERSION



SPECIMEN 3B



SPECIMEN 5B



SPECIMEN 12B

ONE GRAVITY PROCESSED SPECIMENS 3B and 5B AND
LOW GRAVITY PROCESSED SPECIMEN 12B (10X)

FIGURE 27. LEAD-ZINC-ANTIMONY DISPERSION

It must be emphasized that these materials represent only a fraction of the hundreds of systems possessing a miscibility gap which have been identified. However, the interesting electronic and metallurgical behavior of these processed materials has lead to cautious optimism regarding the potential use of this class of materials. Thus from this work, it is anticipated that future research into immiscible systems will benefit not only the basic understanding of materials behavior but ultimately enable materials to be produced which will have extremely useful applications."

10. M558 Radioactive Tracer. [17] The PI for Experiment M558 is Dr. A. O. Ukanwa, Howard University, Washington, DC.

"The objective of the M558 Radioactive Tracer Diffusion experiment was to measure self-diffusion effects in liquid metals in space flight and characterize the disturbing effects, if any, due to spacecraft acceleration. Because of the near-zero gravity aboard Skylab, the effects of convection on pure self-diffusion would be minimal.

Three cartridges were tested in Skylab. Each cartridge encapsulated a neutral zinc rod carrying a section of radioactive zinc-65. The radioactive sections were at the thermally cold end of one zinc-rod, at the thermally hot end of another zinc-rod and at the central section of the third zinc rod. The diffusion time involved 2 hours of heat-up, 1 hour of soak under a temperature gradient and 13 hours of passive cool down in the M518 Multipurpose Electric Furnace. Three cartridges, configured similar to the Skylab cartridges, had also been tested on earth to provide ground-base data under normal gravity for comparison.

Data from the Skylab samples have been markedly different from the ground-base data obtained on earth. On earth, radioactive zinc-65, propelled by gravity-induced convection, rapidly diffused through the neutral zinc samples in less than 1 hour of soak time, to yield an almost uniform distribution of zinc-65 throughout the sample." (See figures 28, 29 and 30.) "On the other hand, in the near-zero gravity environment of Skylab, the slow distribution of zinc-65 revealed the pattern attributable mostly to pure volume diffusion in the absence of appreciable convective currents." (See figures 31, 32 and 33.)

"The distribution of zinc-65 tracer, after melting, maintaining at soak temperature for 1 hour of soak time and then resolidifying, was obtained by sample sectioning. The concentration of activity of each section (microcurie/gram) was plotted against positions along the sample axial and radial position. Experimental data and theoretical results from solution of Fick's law of diffusion in one dimension

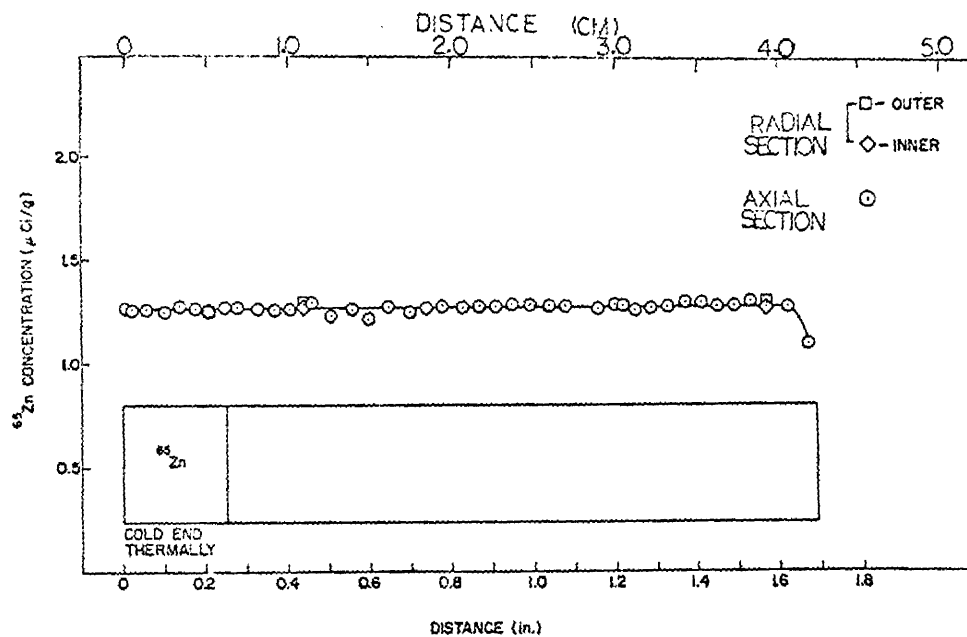


FIGURE 28. M558 GROUND BASED SAMPLE A-13

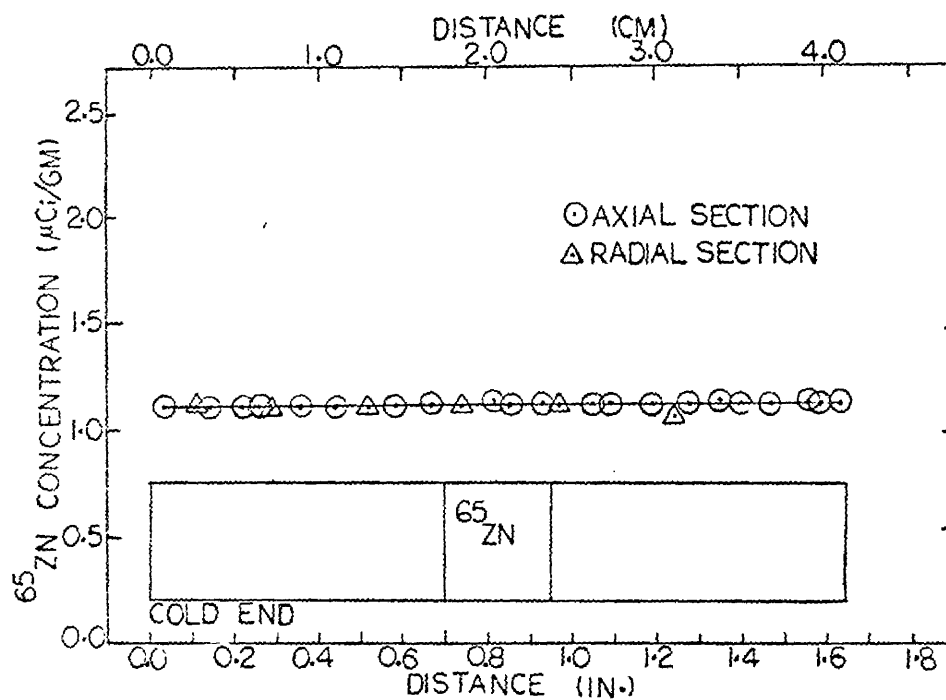


FIGURE 29. M558 GROUND BASED SAMPLE B-13

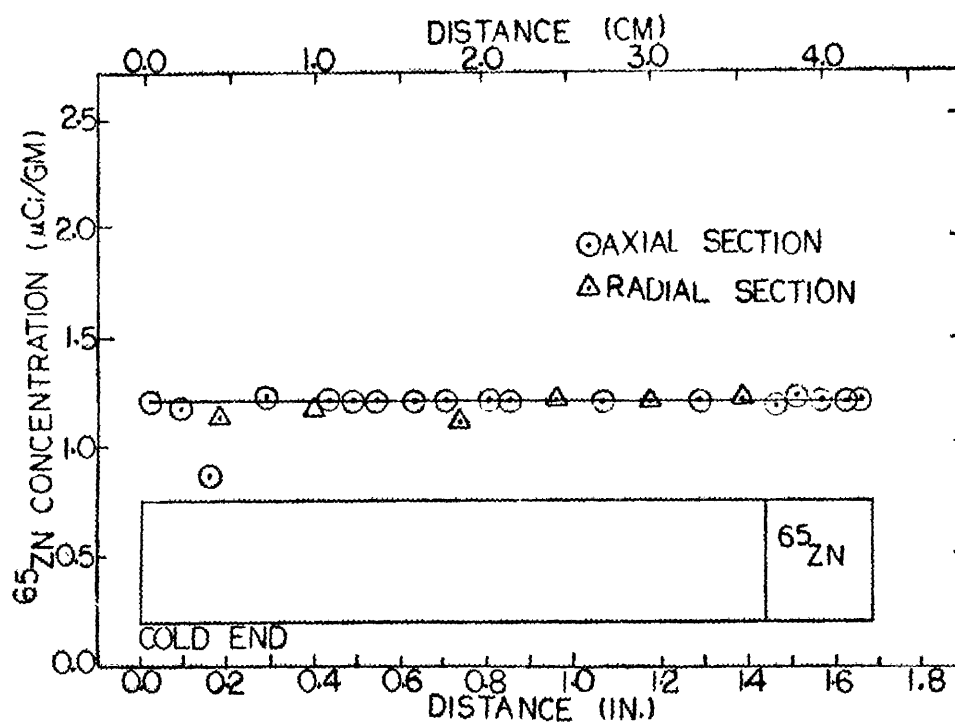


FIGURE 30. M558 GROUND BASED SAMPLE A-1

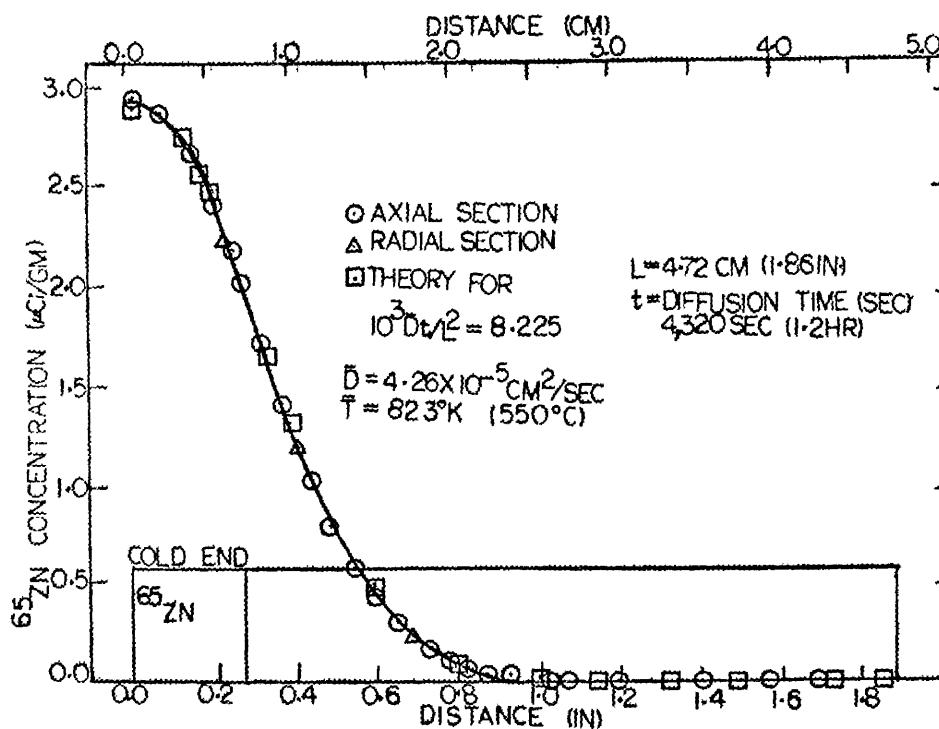


FIGURE 31. M558 FLIGHT SAMPLE A-6

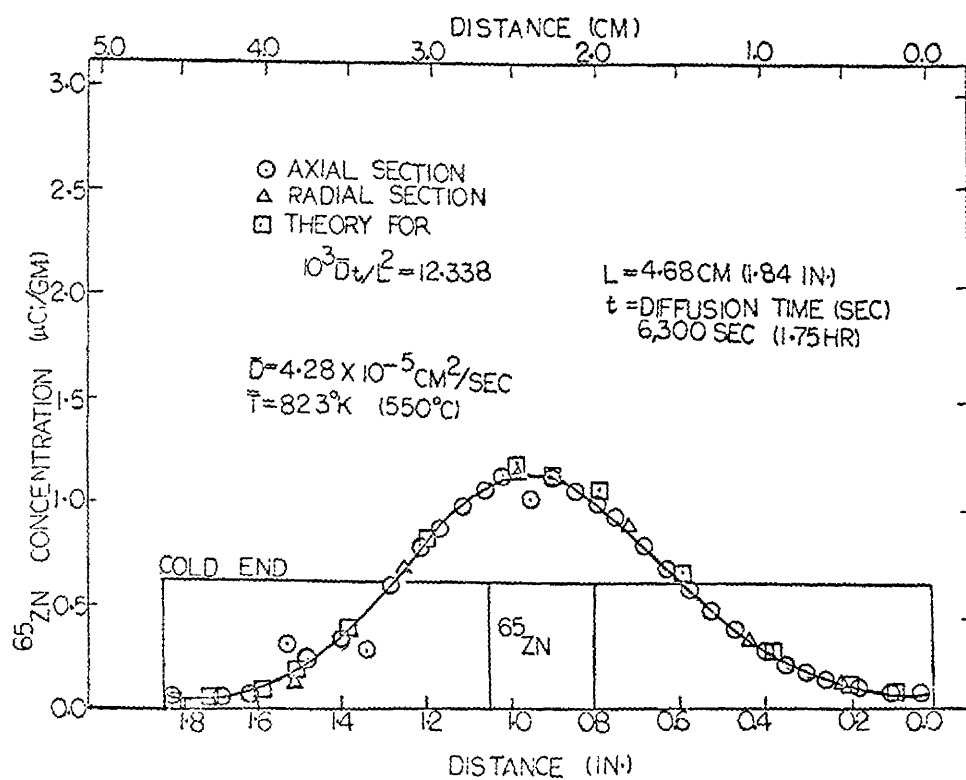


FIGURE 32. M558 FLIGHT SAMPLE B-5

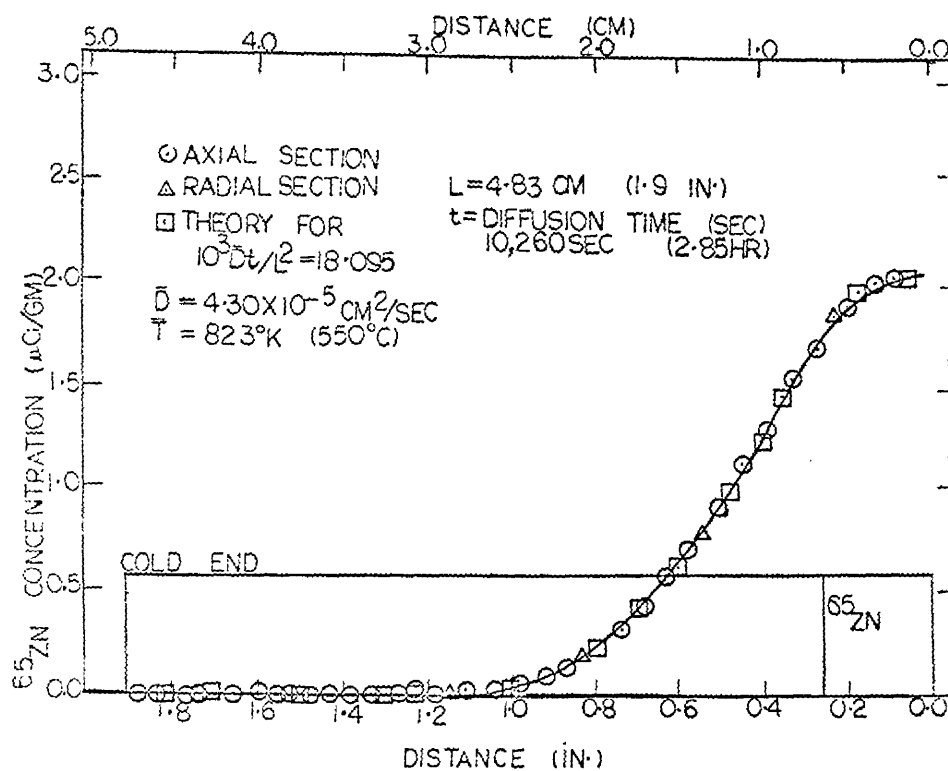


FIGURE 33. M558 FLIGHT SAMPLE A-7

were compared. Samples tested on earth showed very rapid diffusion. Diffusion coefficient in unit gravity was 50 times the zero-gravity diffusion coefficient of Skylab. This order of difference was attributable to unit gravity convective velocity of only 4.16×10^{-4} cm/sec in magnitude. The convection-free diffusion coefficient of Skylab was found to be $D = 9.17 \times 10^{-4} \exp(-5,160/RT)$ cm²/sec for the temperature range from 693°K (420°C) to 973°K (700°C). The diffusion coefficient at 550°C was found to be 4.28×10^{-5} cm²/sec."

11. M559 Microsegregation in Germanium. [18] The PIs for Experiment M559 are Dr. F.W. Voltmer and Dr. J.T. Yue, Texas Instruments Inc., Dallas, Texas.

"The objective of the experiment is to investigate whether or not an improvement can be obtained in solute microsegregation for crystal growth of a semiconductor material in a gravity-free environment, and if improvement can be obtained whether or not it can be quantified.

Solute microsegregation is defined as micro-inhomogeneities of the solute species which occurs during solidification in crystal growth. (...) Solute microsegregation, which leads to resistivity variations in the semiconductor material both in parallel and perpendicular directions of crystal growth, can have adverse effects on semiconductor device performance. (...) The present interest in the semiconductor industry is to grow semiconductor materials with homogeneous dopant distributions.

A major contribution to segregation behavior is the always-present convection current (...) in the melt during crystal growth. Presently, the magnitude of gravity-induced convective mixing on segregation and particularly microsegregation is not known. For terrestrial crystal growth, contributions to convective mixing associated with gravity are intrinsically coupled with contributions arising from temperature gradient differences and fluctuations and it is therefore, nearly impossible to isolate the influence of gravity. By comparing crystals grown in a space environment, with identical crystals grown in a terrestrial environment, the effects of gravity can be isolated for the first time.

(...) In order to define the influence of gravity on terrestrial crystal growth, both horizontal and vertical directions of solidification were used. The vertical crystals were grown in temperature stabilizing positions. (...) The process chosen for crystal growth was the gradient freeze method (...) because of the simplicity involved: 1) no movement was required of the melt during crystal growth and 2) a constant rate of solidification could be controlled by lowering the furnace temperature by a uniform power reduction.

Three identical sets of germanium crystals were prepared. Each set contained three differently doped crystals: gallium, antimony, and boron. Two sets were used as ground control samples with one set grown in the temperature stabilizing position and the other in the horizontal position. The third set of germanium crystals was grown in space. The experiment consisted of remelting a portion of the germanium crystal and then resolidifying the remelted portion under controlled conditions."

"Both the terrestrially grown and space grown germanium crystals underwent similar remelt temperature cycles. For any one set, all three crystals were exposed to the same furnace conditions as each multipurpose electric furnace was able to contain three cartridges simultaneously. At the start of the remelt cycle, the furnace temperature was increased to the soaking temperature of 1000°C within 3 hours. (...) At this temperature, an appreciable portion of the original germanium crystal would be remelted (the melting point of germanium is 938°C). The soak temperature was held for about 2 hours at a steady level in order to allow the system to reach steady state conditions. The cool-down cycle was then initiated by reducing the temperature at the hot end of the cartridge at a rate of 0.6°C per minute, which enabled the crystal to re-solidify. As the cool-down cycle proceeded, rapid freezing would suddenly occur in the crystal when the heat leveler temperature fell below 938°C . Microsegregation characterization only in the region of slow solidification was examined."

"The results of this first experiment on solidification in space has indicated that quantitative data on the influence of gravity on solidification can be obtained. Germanium crystals have been grown for the first time in space. It has been shown that solidification in space can provide six-fold improvement in macrosegregation and nearly two-fold improvement in microsegregation for crystal growth by the gradient freeze method. The influence of gravity on convective mixing has been quantified for solute redistribution in nearly unidirectional solidification and its role in macro and microsegregation is now better understood. A theoretical model based on the implications of the BPS theory has been found to be consistent with the results obtained from the spreading resistance measurements. Additional detailed analysis and SR measurements are still in progress in order to further define the influence of gravity on microsegregation."

12. M560 Growth of Spherical Crystals. [19] The PI for Experiment M560 is Dr. H.U. Walter, University of Alabama in Huntsville, Alabama.

"The present study on "Seeded, Containerless Solidification of InSb" (Skylab Experiment M-560) deals with some of the basic aspects of containerless crystal growth. The objectives of the investigation were defined as follows:

Investigate the feasibility of containerless processing of single crystals in space environment.

Obtain information on the structural perfection of space-grown crystals as compared to samples grown on earth.

Demonstrate the potential of space for producing homogeneously-doped semiconductor material."

"The basic experimental approach can be described as follows: An oriented, cylindrical single crystal of InSb is mounted into a graphite base that is located at the cold end of the gradient furnace. From this support, the sample extends through the gradient section of the furnace into a hemispherical heating cavity that is located in the hot zone of the furnace. As the graphite cavity is heated, a temperature gradient is established along the crystal, and the sample slowly melts back starting at the bottom of the graphite cavity. The melt adheres to the end of the seed crystal and detaches from the graphite. A spherical melt that is suspended at the end of the seed crystal is formed in the gradient region. During soak, the melt will homogenize; inclusions will partly be accumulated at the surface of the melt and static conditions will be established. During cool down, the seed crystal will grow according to temperature gradients into the containerless melt, and a single crystal will eventually be formed."

"Two sets of cartridges were processed during Skylab missions SL-3 and SL-4. All cartridges were returned undamaged. With both sets of experiments, recommended soak temperature ($653^{\circ}\text{C} \pm 8^{\circ}\text{C}$), soak time (1 hr.), and cool-down rate ($0.6^{\circ}\text{C}/\text{min}$) were met. X-ray shadowgraphs of SL-3 samples taken prior to opening are shown in figure 34. For comparison, a shadowgraph of a sample that was processed on the ground is shown in figure 35. Samples processed during SL-4 mission have similar silhouettes" to the SL-3 samples.

"Overall views of two representative samples processed during SL-3 and SL-4 missions are given in Fig. 36 and Fig. 37. Prior to more sophisticated analysis of structural perfection of the samples, single crystallinity could be assessed due to the following reasons: (1) As determined by optical reflection goniometry, well-developed growth facets agree with the crystallographic symmetry of the samples, (2) Single crystal Laue diffraction patterns were obtained, (3) With the exception of two samples (E1 and E3), no grain boundary grooving could be observed. Grooving in the two samples could later be related

1A101E

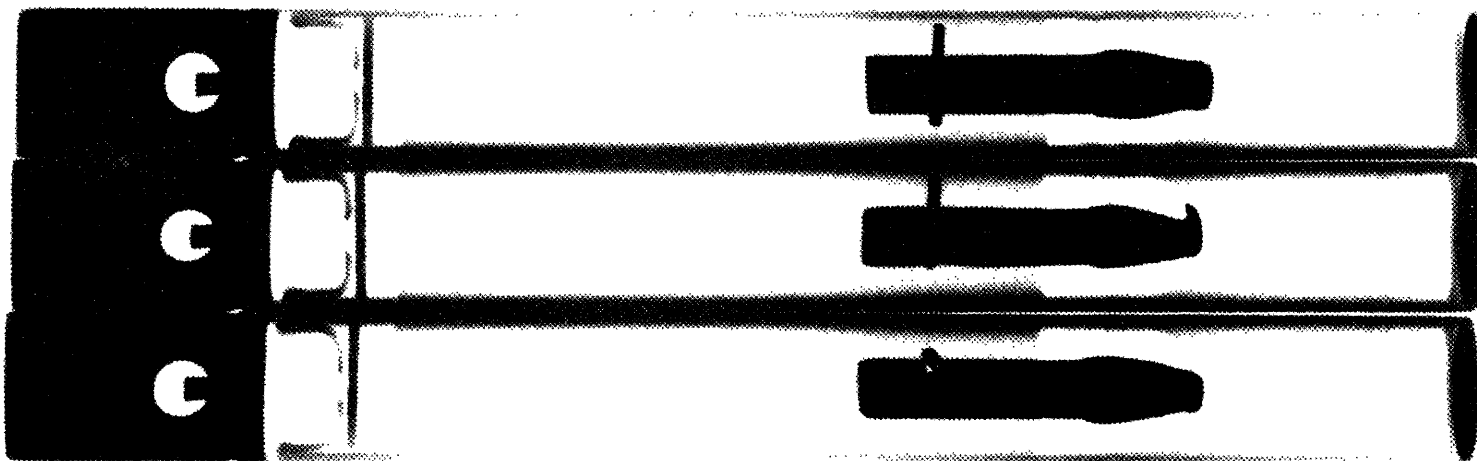


FIGURE 34. X-RAY SHADOWGRAPHS OF SL-3 CARTRIDGES

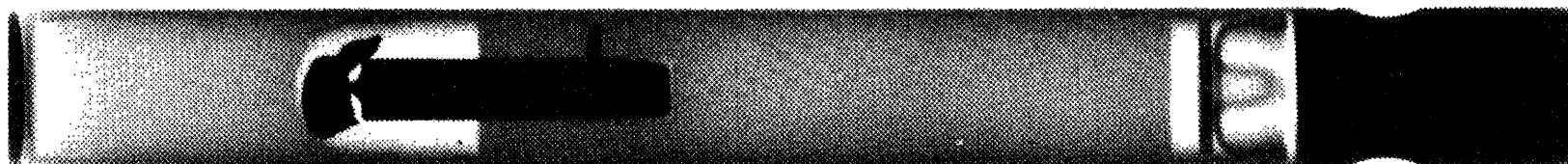


FIGURE 35. X-RAY SHADOWGRAPHS OF GROUND TEST SAMPLE AFTER THERMAL TESTING

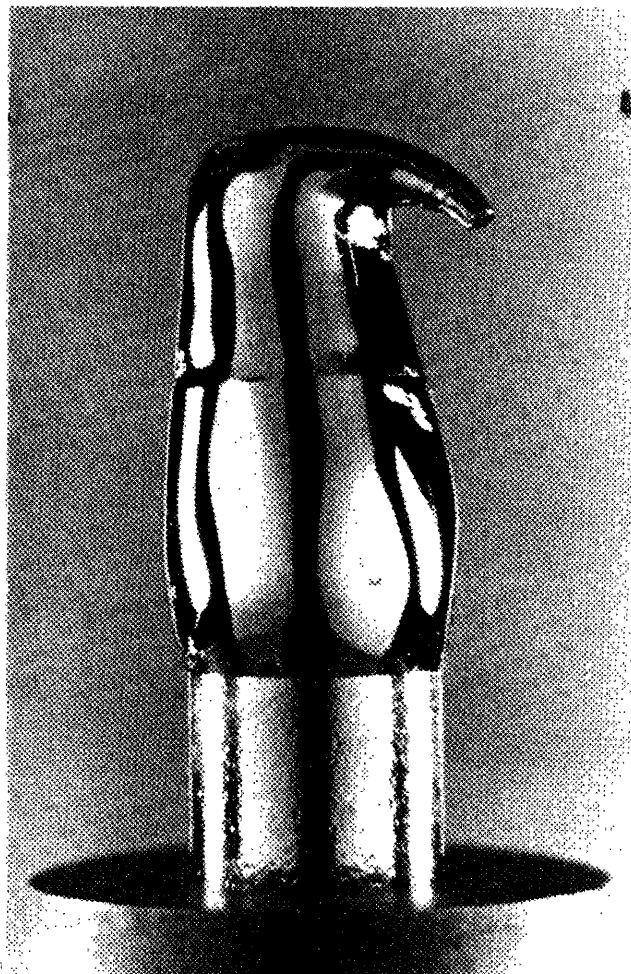


FIGURE 36. SAMPLE PROCESSED DURING SL-3

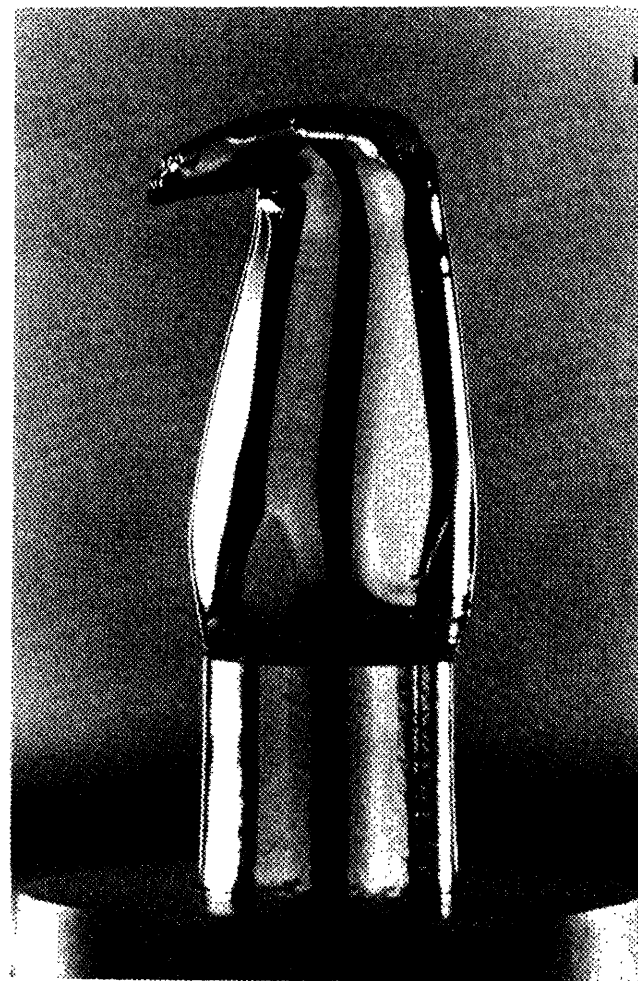


FIGURE 37. SAMPLE PROCESSED DURING SL-4

to a twin-boundary parallel to III which could be traced into the seed; the second twin boundary, apparently (211) , was initiated at the periphery of the sample. The generation of this boundary appears to be related to oxide specks that were accumulated at the surface in this area.

An EREP maneuver that was conducted during solidification of SL3 samples (...) apparently caused a disturbance of growth that left a distinct ring-shaped mark on all of the SL3 samples (see Fig. 36). This time mark in conjunction with the time where cool-down was initiated allows determination of an average growth rate as follows: D1: 10.4 mm/hour, D2: 12.8 mm/hour, E1: 13mm/hour. Since identical furnace settings were used on SL4, an average growth rate of 12 mm/hour can realistically be assumed for SL4 samples.

The general shape of the crystal implies that the melt did adhere to the graphite of the heating cavity instead of being freely suspended at the end of the seed crystal. A teardrop-shaped melt was, therefore, formed that was supported at one end of the seed and that was attached to the bottom of the heating cavity at the other end. The small protrusion at the end of the crystal can be explained by the fact that InSb expands by approximately 11% upon solidification; directional solidification would consequently result in a small amount of melt having to escape when the solidifying crystal meets the bottom of the heating cavity."

Directional solidification of a containerless melt that was suspended at the end of a seed crystal was employed to produce single crystals of InSb during Skylab missions. Extremely well developed growth facets (110) and (111) are observed. With undoped crystals, facets and subfacets are flat within a few hundred Å. Material produced under steady state growth conditions shows continuous improvement of structural perfection; typically dislocation densities, as revealed by etching, are reduced by a factor of 5 to 10 over a distance of 1 cm to 20 - 30 dislocations per cm^2 . Incorporation of dopant (selenium) is homogeneous during steady state growth.

"Based on this investigation, the following conclusions concerning containerless processing of single crystals from the melt in low gravity environment can be reached:

- (1) Highly perfect single crystals can be prepared by seeded, containerless solidification. For processing of highly reactive materials and high melting temperature materials, the technique described should be especially valuable; large crystals could be prepared by this technique as well.

(2) Even though dopant inhomogeneities are observed, all indication points to essentially no-fluid-flow conditions. Consequently, production of homogeneously doped single crystals by containerless techniques appears to be feasible."

13. M561 Whisker-Reinforced Composites. [20] The PI for Experiment M561 is Dr. T. Kawada, National Research Institute for Metal, Tokyo, Japan.

"The object of the experiment was to get Ag and SiC whisker composites with high density and uniform distribution of whiskers by heating and pressurizing sintered products above the melting point of Ag in a weightless environment."

"Composite materials of metallic matrix reinforced by high-strength whiskers such as SiC and Al₂O₃ have been attracting much attention as promising candidates for high-strength materials. At present, however, their practical application has not been realized. The greatest trouble in processing such whisker composite materials is that it is difficult to obtain sufficiently high-density material by applying the usual powder metallurgical techniques of mixing, compacting and sintering.

As for a method to cope with this difficulty, it may be expected that a process of melting and pressurizing the metal matrix is effective for raising the density of the product in processing such materials. Unfortunately, there is a possibility that the mixture might separate into two components, i.e., metal and whiskers, as soon as the metal matrix is melted down, and lose its unity as a composite material, because the specific gravity of the whisker is generally lower than that of the metal matrix.

If in a weightless environment such as on Skylab a metal-whisker composite which is prepared by the conventional powder metallurgical technique is kept in a molten state, it would be possible to obtain a homogeneous composite material, because there is no influence of buoyance and thermal convection in a weightless environment. But by the melting process only, it will be impossible to raise the density of the composite by removing voids further than that of the sintered state. Therefore, one of the points" of this experiment "was laid in a procedure to positively remove voids by pressurizing the sample during melting."

"After the screening of some materials, silver of m.p. 961°C and specific gravity 9.4 at molten state was selected as the matrix and silicon carbide (SiC) whiskers of specific gravity 3.1 as the reinforcing material. The particle size of fine powder of silver used was under 0.5μm in diameter. The SiC whiskers used were about 0.1μm in diameter on average and 10μm in length on average."

"SiC whiskers of 2, 5, and 10 volume % were mixed in Ag powder. Before mixing they were coated with Ag. Cylindrical green samples of 8mm in diameter and about 35mm in length were prepared by well mixing the whiskers and Ag powder, compacting the mixture in a press, sintering it at about 900°C in a hydrogen gas atmosphere and finally hot-pressing it lightly."

"The ampoule assembly consisted of a silica tube, a graphite sheath, a piston rod of graphite and silica and a coiled spring for pressurizing the sample from one end. The spring was made of special heat-resistant alloy. The applied force by the spring was adjusted to about 30kg in the initial condition before melting. The pressurizing mechanism was designed so as to crush voids in the material in molten state by hydrostatic pressure applied to the sample."

"The sample ampoule was loaded and sealed into the cartridge made of stainless steel. Three sample ampoules were set together in the multipurpose electric furnace and heat treatment was performed under a prescribed condition."

a. SL-3 Experiment. "The samples were heated at the maximum heat leveler temperature of 1010°C for about 4 hrs and then cooled in the switched-off furnace. It was estimated from the results of the ground-based tests that the measured temperature was about 20°C higher than that at the center of the sample. Accordingly, the temperature of the samples is thought to have been kept above the melting point of Ag for about 5 hrs."

b. SL-4 Experiment. The samples were heated at a heat leveler temperature of 991°C for one hour and then cooled at a rate of 0.6°C per hour.

c. Ground-based experiment. "In the ground-based experiment the samples were heated and cooled in a furnace that was quite similar to the multipurpose electric furnace on Skylab. The sample axes were held in the vertical position and their spring ends were kept downward." The heat leveler temperature was held at 990°C for 2.5 hours and the samples passively cooled in the switched-off furnace.

"The products processed on Skylab and on the ground were subjected to comparative evaluation and the following conclusions were obtained:

1) An increase in the density ratio was obtained by melting and pressurizing. The degree of increase was approximately the same for the Skylab and the GBT samples.

2) Floating and coagulation of whiskers were observed at the upside end of the GBT samples. The GBT samples showed a decreasing tendency in the distribution density of whiskers towards the upside end. No such phenomena were observed for Skylab samples.

3) The microhardness was generally smaller for the GBT samples than for the Skylab samples and showed large fluctuations along the axial direction as compared with the Skylab samples.

4) The above results are considered to indicate clearly the influence of buoyancy and thermal convection in the melted GBT samples, while the Skylab samples were devoid of such influence since they were processed in a weightless environment." (See figures 38 and 39).

14. M562 Indium Antimonide Crystal Growth. [21] The PIs for Experiment M562 are Dr. H.C. Gatos and Dr. A.F. Witt, Massachusetts Institute of Technology, Cambridge, Massachusetts.

"The objectives of growing Te-doped InSb in Skylab were to confirm the advantages of zero-gravity environment, to obtain basic data on solidification, and to explore the feasibility of electronic materials processing in outer space. Thus, the experiment was designed to achieve diffusion-controlled, steady-state solidification and to investigate the associated growth segregation behavior on a micro- and macro-scale. Direct comparison of growth and segregation on earth and in space was to be achieved by melting and resolidifying in space a portion of each crystal grown on earth."

"Structural and compositional control during solidification of materials is impeded by gravity-induced effects in the melt. Thermal gradients necessary for crystal growth lead, in the presence of gravitational forces, to thermal convection which in general causes uncontrolled variations in the solidification rate and in diffusion boundary layer thickness; such variations lead directly to periodic and/or random microscopic and macroscopic segregation inhomogeneities. Furthermore, in the presence of gravity, establishing steep thermal gradients, often required to prevent constitutional supercooling, is impossible and consequently interface breakdown is unavoidable."

Gravity effects are, thus, primarily responsible for the present lack of reliable solidification data and the existing gap between theory and experiment. Consequently, crystal growth and associated segregation phenomena are still based on empiricism, and the properties and performance of solids are not at their theoretical limits."

"The experiments performed during the Skylab-III and -IV missions included the growth of undoped, tellurium-doped," ($\sim 10^{18}/\text{cm}^3$) "and tin-doped" ($\sim 10^{20}/\text{cm}^3$) "indium antimonide. The present report is concerned primarily with results obtained on tellurium-doped InSb."

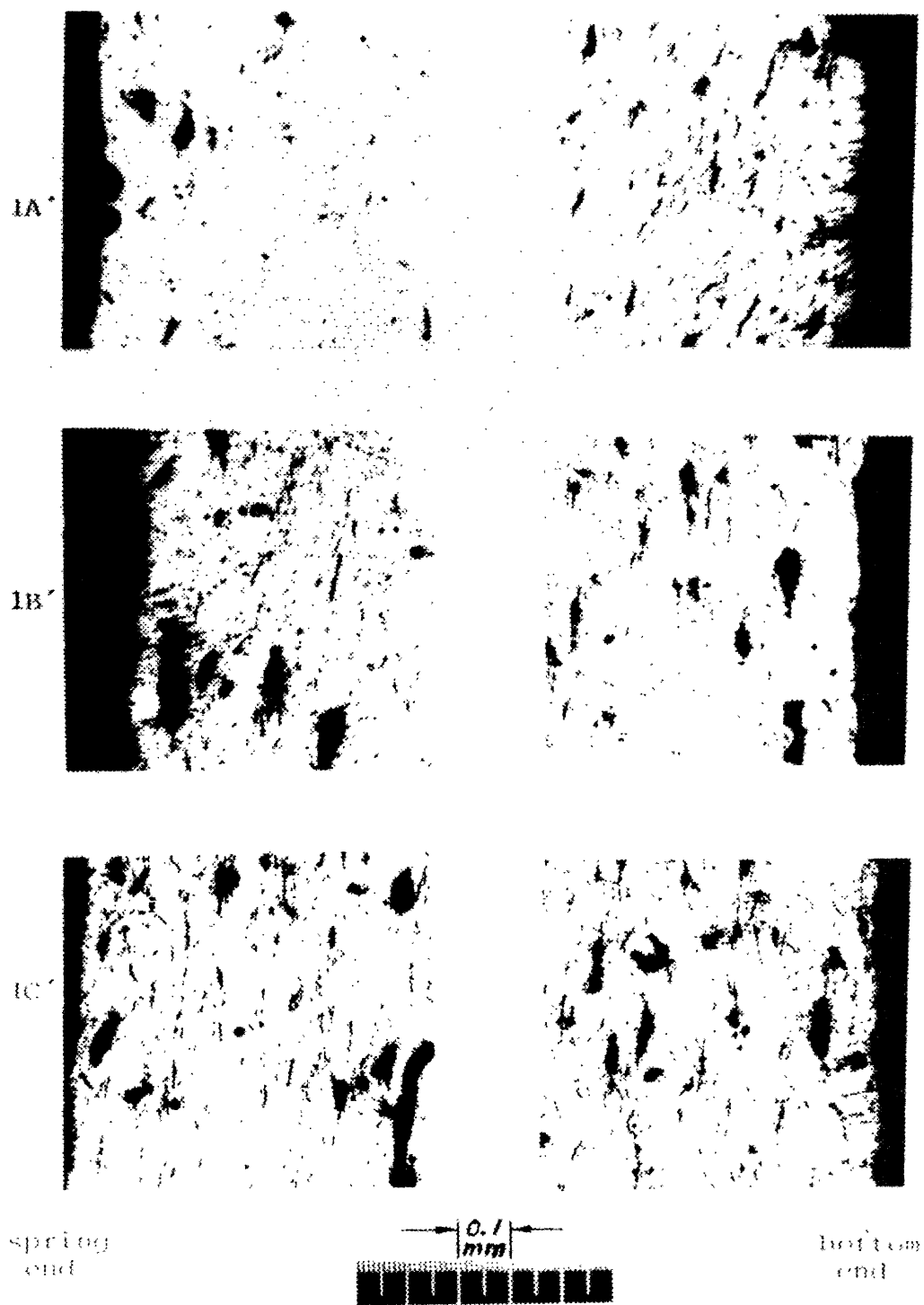


FIGURE 38. MICROSTRUCTURE OF SL-3 SAMPLES

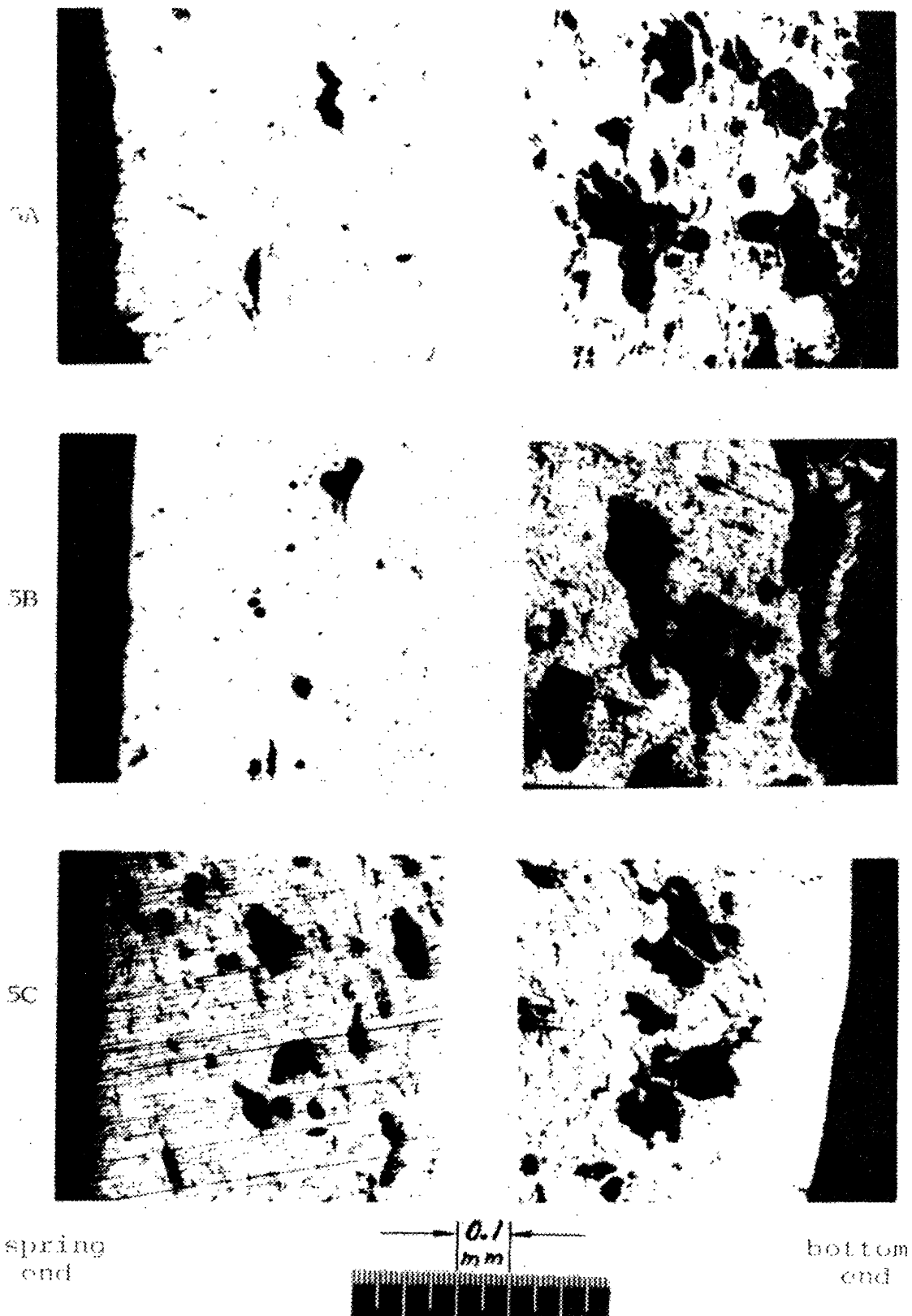


FIGURE 39. MICROSTRUCTURE OF SL-4 SAMPLES

"Skylab-III Mission Experiment: The samples were inserted into the multipurpose furnace and back-melting was initiated by turning on the power. The desired back-melting was achieved in 120 minutes. Then the system was kept at temperature for a period of 60 minutes (soaking period), to achieve thermal equilibrium in the system and homogenization of the melts. Subsequently, a cooling rate of $1.17^{\circ}\text{C}/\text{min}$ was established by controlled power reduction at intervals of 14.4 sec. Four hours after initiation of regrowth the power was turned off and passive cooling to the ambient temperature took place."

"Skylab-IV Mission Experiment: The remelting and thermal soaking procedure was identical with that of the Skylab-III experiment. However, in this (...) experiment the growth system was subjected to a mechanical shock by striking the furnace assembly at a predetermined time; furthermore, the constant cooling rate of $1.17^{\circ}\text{C}/\text{min}$ was interrupted 140 minutes after initiation of regrowth and a second thermal soaking period of 60 minutes was introduced by maintaining the furnace power at a constant level. The power was subsequently turned off and the system was allowed to reach ambient temperature. (...) These changes in the growth procedure were intended to provide time reference markings in the crystal and to obtain data on the dependence of transient segregation on growth rate."

"The present InSb experiment proves unambiguously the uniqueness of zero-gravity conditions for obtaining directly fundamental data on crystal growth and segregation associated with solidification. Furthermore they demonstrate the striking advantages of processing materials in space.

Specifically the following results and conclusions were obtained for the first time:

Ideal steady state growth and segregation (exclusively diffusion controlled) were achieved leading to three-dimensional chemical homogeneity on a microscale over macro-scale dimensions (several centimeters in the present case)" (See figure 40); "the transient segregation profile preceeding steady state solidification was determined; limitations in the experimental arrangement and in the presently available microanalytical techniques do not permit, at this time, the extraction of fundamental data pertinent to solidification.

Surface tension effects led to phenomena previously never observed and theoretically not predicted: the Te-doped melt, not wetting the quartz wall, solidified with a free surface (unconfined) configuration" (See figures 41 and 42). "Under forced contact conditions, intimate contact between the melt and the confining walls was prevented and the growth system was essentially isolated from its container by the formation of narrow surface ridges. It was also shown that surface tension effects in space remained localized on the surface and did not effect growth and segregation in the bulk.

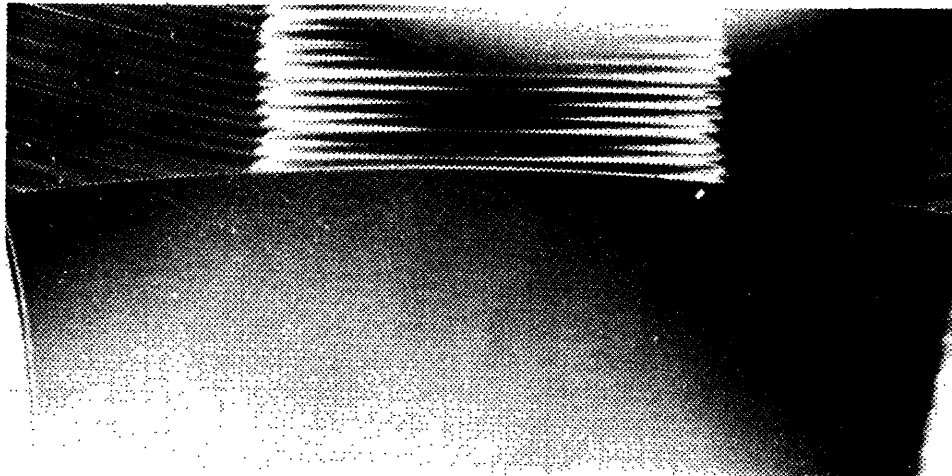


FIGURE 40. CRYSTALLINE HOMOGENEITY IMPROVEMENT---ETCHED CROSS-SECTION (UNDER DARK-FIELD ILLUMINATION) OF CRYSTAL GROWN DURING SKYLAB-IV MISSION; SPACE GROWN REGION (BOTTOM), IN CONTRAST TO EARTH GROWN REGION (TOP), EXHIBITS NO COMPOSITIONAL INHOMOGENEITIES; 12x.



FIGURE 41. SL-3 FREE SURFACE CONFIGURATION---PART OF THE Te-DOPED CRYSTAL, GROWN DURING SKYLAB-III MISSION, 3.7 TO 5.9 cm FROM THE INITIAL REGROWTH INTERFACE. SURFACE RIDGES BROADEN AND BRANCH-OUT AT THE LATE STAGES OF GROWTH (RIGHT-HAND SIDE); 6.8x.

In the absence of convective interference it was possible to identify segregation discontinuities associated with facet growth and to explain their origin on the basis of spurious nucleation. The absence of convective interference permitted, further, the determination of the mode of nucleation (formation of misoriented nuclei at the three phase boundary line) and propagation of rotational twinning.

A mechanical-shock perturbation intentionally introduced during growth was identified in the crystal and found to cause a localized increase in dopant segregation; this dopant discontinuity was used as a time reference for the determination of the average macroscopic growth rate" (See figure 43).

"On the basis of the present results it is no longer a matter of speculation that fundamental data necessary for bridging the gap between theory and experiment can be reliably obtained in the absence of gravity and that outer space presents one of the greatest opportunities ever afforded science and technology."

15. M563 Mixed III-V Crystal Growth. [22] The PI for Experiment M563 is Dr. W. Wilcox of USC. The objective of this experiment was to determine how weightlessness affects directional solidification of binary semiconductor alloys and, if single crystals are obtained, to determine how their semiconducting properties depend on alloy composition.

"Although a wide variety of semiconductor compounds are available, the selection of electronic and other physical property combinations is limited. The range of available property combinations becomes much larger if one considers solid solution alloys. For example, the electronic properties of InSb-GaSb alloys are such that Gunn microwave oscillation can be observed with some compositions, but not in pure InSb or GaSb (2). Unfortunately, large homogeneous single crystals of concentrated alloys are not produced. Films of many alloys can be produced by chemical vapor deposition or by liquid phase epitaxy, but many applications require bulk single crystals.

Directional solidification of concentrated alloy semiconductors produces a polycrystalline material. Homogeneous polycrystalline ingots may be produced by very slow zone leveling either with or without a solvent added, under conditions such that interface breakdown due to constitutional supercooling is avoided. One may speculate that grains are generated by the compositional variations arising from hydrodynamic fluctuations in the melt. In order to test this suggestion, directional solidification experiments were performed on InSb-GaSb alloys. These were carried out on the earth in vertical and horizontal positions, with and without a magnetic field, and in Skylab." "Mixtures initially containing 10%, 30% and 50% InSb were employed."

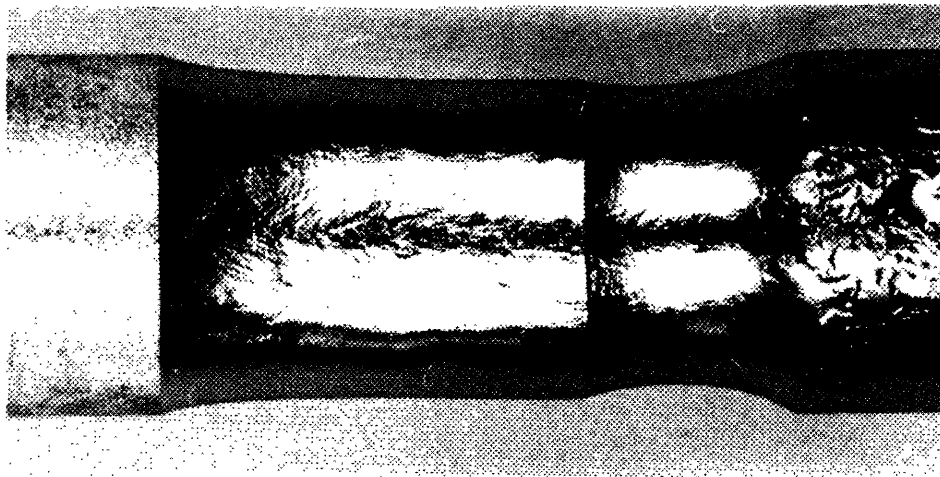
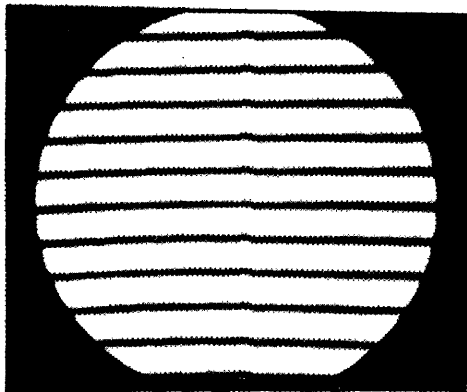
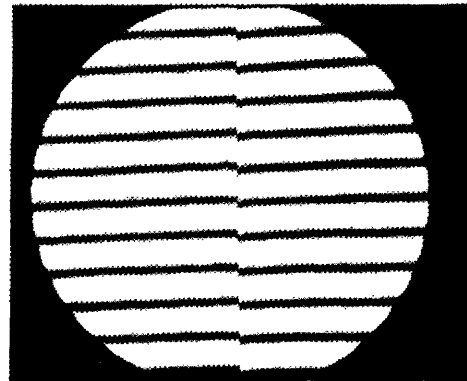


FIGURE 42. SL-4 FREE SURFACE CONFIGURATION---
Te-DOPED CRYSTAL GROWN DURING THE SKYLAB-IV
MISSION; NOTE DECREASE IN CRYSTAL DIAMETER
UPON INITIATION OF GROWTH; SURFACE RIDGES
APPEAR ON RIGHT-HAND SIDE AFTER CRYSTAL
DIAMETER REACHES ITS MAXIMUM CONSTANT VALUE;
4.8x.



(a)



(b)

FIGURE 43. INTENTIONAL CRYSTAL GROWTH DISCONTINUITY---
DOUBLE BEAM INTERFEROGRAMS OF SEGREGATION
DISCONTINUITIES AS REVEALED BY ETCHING (a)
CAUSED BY MECHANICAL SHOCK AND (b) CAUSED
BY REGROWTH AFTER THERMAL SOAKING.

Cast ingots of the mixtures were prepared (See figures 44 and 45) and installed into carbon-coated 8mm I.D. silicon ampoules. The ampoules were evacuated and lockfilled with 10 torr of helium prior to sealing, and were then sealed in stainless steel cartridges under a vacuum of $\leq 10^{-4}$ torr.

"Three cartridges were processed simultaneously in each run. As shown in Table VIII, three samples were processed vertically with the heater on top, three horizontally, three on the second Skylab mission, and three on the last Skylab mission. Power was applied so that the heater was at 960°C or 1020°C. This resulted in melting of somewhat over half of each ingot. After soaking for 16 hours to allow homogenization to occur, directional solidification was accomplished by programming down the heater temperature at 0.6°C per minute. This resulted in a steadily increasing freezing rate since the temperature gradient decreased as solidification proceeded. When the solid-liquid interface moved within the heater, the freezing rate increased rapidly because of the low temperature gradient there."

"Several interesting effects of gravity were revealed by these experiments. The concentration profiles and the compositional homogeneity were both strongly influenced by the magnitude and direction of g, as expected from free convection effects. The lack of convective stirring in space-processing leads to a significant initial compositional transient which cannot be entirely avoided, although it can be greatly reduced by lowering the freezing rate. A lower freezing rate would also avoid compositional inhomogeneities due to constitutional supercooling. Production of a homogeneous ingot would probably eliminate cracking.

The most exciting development was the great reduction in twinning brought about by space processing" (See figures 46 and 47). "Since the cause of growth twinning is not really known, we can only speculate that foreign particles are responsible and that these interact more frequently with the growing interface when convection is present.

The ingots processed in SL-3 had a smaller diameter than the tube. Apparently the melt did not wet the carbon coating. Surface tension decreases with increasing temperature, and the temperature increased with distance from the interface down the melt. This would have forced the melt to contract near the interface and to expand at the hot end. Those processed in SL-4 had the same diameter as the tube. The only difference between these two runs was that the heater temperature was higher in SL-4. Since the compositions were the same, the interface temperatures were the same, although the portion of the melt in the heater would have been hotter in SL-4. We can only speculate that this higher temperature caused the melt to first wet the tube wall and then to spread down to the interface.

TABLE VIII. SUMMARY OF NASA EXPERIMENTS

No.	Starting Composition	m.p. (°C)	Heater (°C)	Deviation from <111>	Length in Heater/Cooler ¹	Meltback (cm)
Vertically Processed						
1A	In _{0.1} Ga _{0.9} Sb	700	960		8.5/27.5 = 0.31	3.5
3B	In _{0.3} Ga _{0.7} Sb	678	960	18°	10.0/26.0 = 0.38	4.2
2C	In _{0.1} Ga _{0.9} Db	700	960	16°	12.0/24.0 = 0.50	3.7
Horizontally Processed						
3A	In _{0.5} Ga _{0.5} Sb	646	960		9.5/26.5 = 0.36	4.6
4B	In _{0.3} Ga _{0.7} Sb	678	960	17°	14.0/22.0 = 0.64	4.6
4C	In _{0.1} Ga _{0.9} Sb	700	960	6°	8.5/27.5 = 0.31	4.0
Skylab (SL-3) Processed						
2A	In _{0.5} Ga _{0.5} Sb	646	960		16.7/19.3 = 0.87	4.4
1B	In _{0.3} Ga _{0.7} Sb	678	960	9°	19.1/16.9 = 1.13	4.0
1C	In _{0.1} Ga _{0.9} Sb	700	960	9°	17.4/18.6 = 0.94	3.7
Skylab (SL-4) Processed						
5A	In _{0.5} Ga _{0.5} Sb	646	1020		10.1/25.9 = 0.39	4.7
2B	In _{0.3} Ga _{0.7} Sb	678	1020		15.0/21.0 = 0.71	4.5
3C	In _{0.1} Ga _{0.9} Sb	700	1020		11.3/24.7 = 0.46	4.2
¹ In min.						

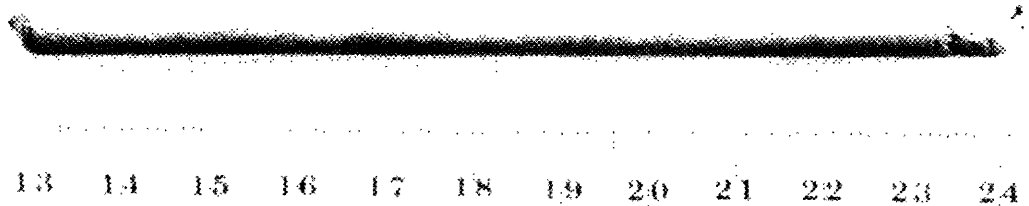


FIGURE 44. PHOTOGRAPH OF CASTING

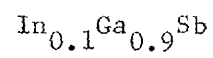
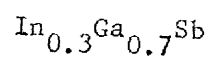
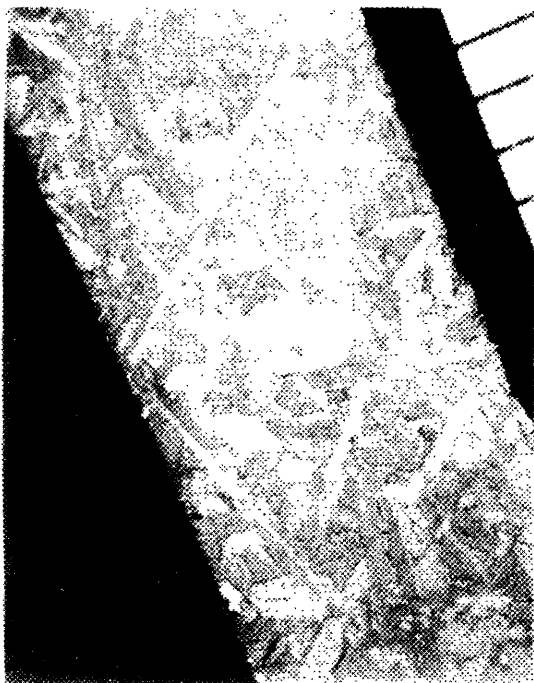


FIGURE 45. PHOTOGRAPHS OF CAST INGOTS

Sandblasted longitudinal slice of
SL-3 ingots, with portion which
was in heater on top.

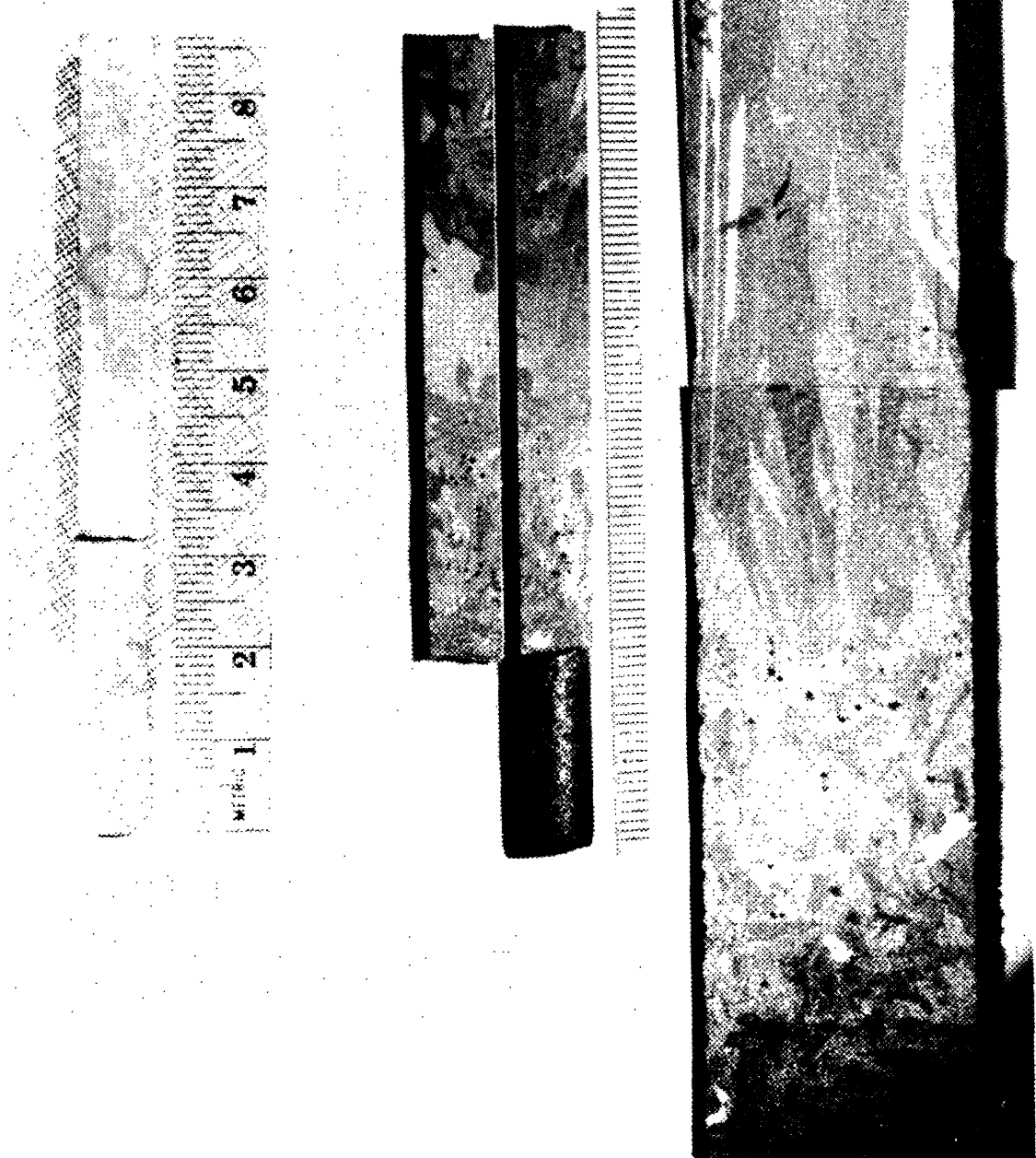
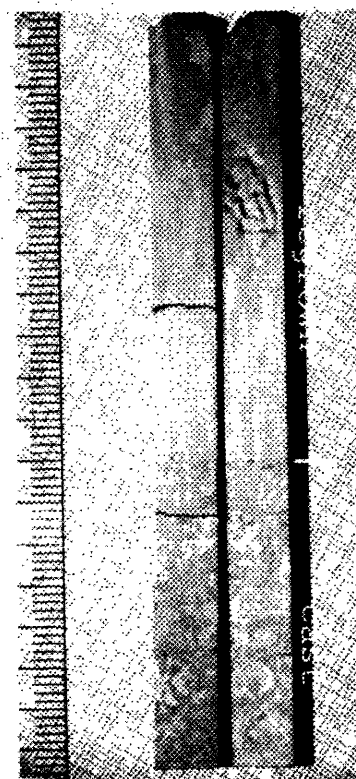


FIGURE 46. SL-3 INGOTS



Sandblasted
longitudinal section of
3C processed in SL-4.

FIGURE 47. SL-4 INGOTS

A wide variety of grain sizes was observed, but with no trend yet observed. Sadly, there appears to be no large advantage to space processing of alloys from this standpoint.

The preferred grain orientation was (111) in all cases.

We have no explanation for the great difficulty in distinguishing grains in the space-processed ingots.

Gas bubbles were more uniformly distributed in the space-processed ingots, but this is not significant since they can be avoided entirely by solidification in a reasonable vacuum (3)."

16. M564 Halide Eutectics. [23] The PI for Experiment M564 is Dr. A.S. Yeu, University of California, Los Angeles, California.

"When certain binary eutectic mixtures solidify, one of the two phases can form fibers or platelets in a matrix of the second phase. For example, when a eutectic liquid of NaCl and NaF solidifies, fibers of NaF form in a matrix of NaCl.

Fiberlike and platelike eutectics produced on earth are limited in perfection by the presence of a banded structure, (...) discontinuity, (...) and faults (...) due, at least in part, to vibration and convection currents in the melt during solidification. The presence of these defects renders the solid-state eutectic devices inefficient and useless (...).

If the solidification process is performed in a space environment, where there is no vibration and convection current in the melt, there is reason to believe that continuous fiberlike eutectic microstructures can be produced. The electric, thermomagnetic, optical, and superconducting characteristics of such fibers will be strongly anisotropic, and this will make possible various exciting device applications."

The purposes of this experiment are to prepare, in a space environment, fiberlike NaCl-NaF eutectic with continuous NaF fibers embedded in a NaCl matrix and to examine the eutectic microstructure, and to measure the relevant optical properties of the space-grown and earth-grown eutectics.

"Experimental studies have been carried out at UCLA to acquire all possible knowledge of the solidification process of the eutectic mixture involved, short of doing the space experiments themselves. Calculations and design of equipment have been followed by a program of solidifications at various rates and with various temperature gradients at the interface.

The objective of the earth-based studies is to maximize the likelihood of success of the space experiments.

Ingots of NaCl-NaF eutectics, 0.31 inch in diameter and 2.5 inches long have been grown unidirectionally on earth and in the Skylab in a multipurpose furnace at one freezing rate and a steep temperature gradient." "It was found that continuous and discontinuous NaF fibers were embedded in a NaCl matrix from ingots grown in space and on earth, respectively. The production of continuous fibers in a eutectic mixture was attributed to the absence of convection current in the liquid during solidification." (See figure 48)

"Macroscopic and microscopic examination on longitudinal and transverse sections of space-grown and earth-grown ingots were made. It was found that during the major portion of the space solidification process, the NaF fibers were aligned with the ingot axis. However, they were normal to it during the very beginning of the solidification process. This indicated that the direction of heat flow was perpendicular to the ingot axis. The best microstructures were obtained from ingots grown in space." (See figure 49) "These microstructures were compared with those produced on earth with and without convection current in the liquid during growth.

Optical transmittance measurements of transverse and longitudinal sections of the space-grown and earth-grown ingots were carried out with a polarizer in a Perkin Elmer Spectrometer. It was found that for a given sample thickness, the highest percentage of transmittance was obtained from ingots grown in space. The effect of sample thickness on transmittance was investigated. It was found that the thinner the sample, the higher the transmittance over a range of wavelengths, in agreement with the general optical property of transparent materials exposed to electromagnetic waves."

17. M565 Silver Grids Melted in Space. [24] The PI for Experiment M565 is Dr. A. Deruyttere, Katholieke Universiteit of Leuven, Leuven, Belgium.

"Some products made by powder and fibre metallurgy are intentionally porous, e.g., self-lubricating bearings, filters and damping devices. When a high porosity is desired, the necessary cohesion of the material can only be obtained through solid phase sintering, as any substantial melting would cause a rapid collapse of the porous structure. However, this may no longer happen when the melting is done in weightless condition. The melting of a porous material in space may produce a porous part in which size, shape and distribution of the pores are different from those obtainable on earth by classical powder metallurgy. Hence, some properties of the material, such as strength or filtering characteristics, may also be different from

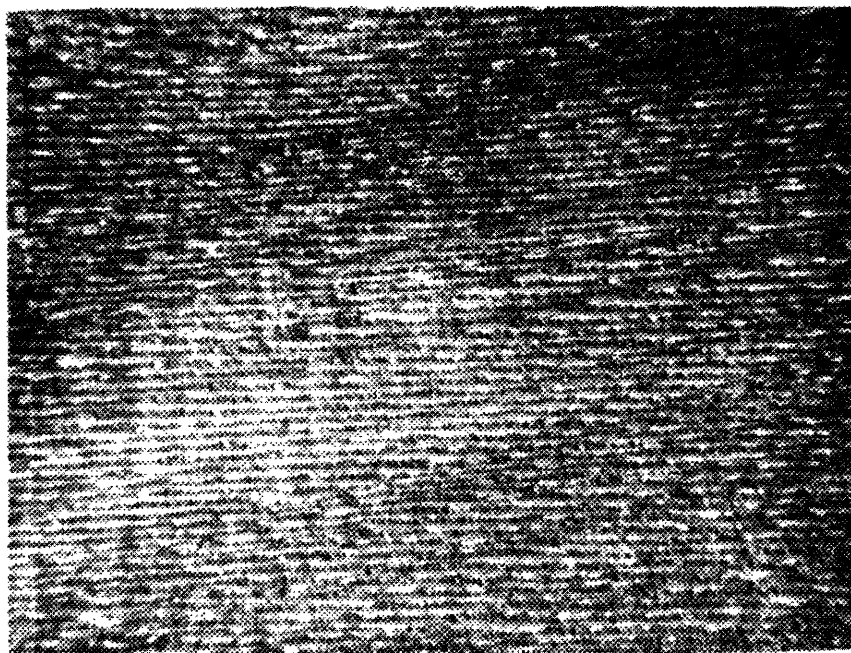


FIGURE 48. CONTINUOUS SODIUM FLUORIDE FIBERS

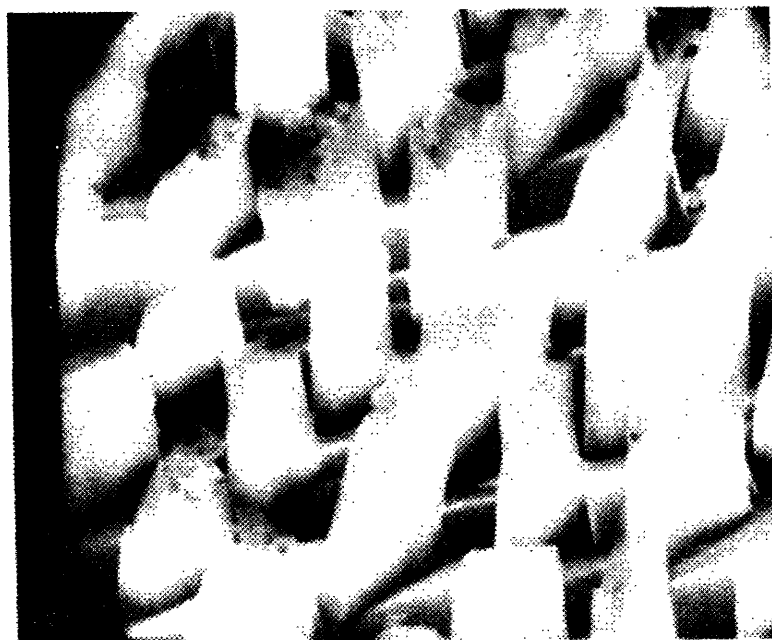


FIGURE 49. SODIUM FLUORIDE FIBERS

those that have been obtained so far. Knowledge gained through melting and resolidifying experiments on porous material in space, may therefore promote the development of new materials or the development of space techniques, e.g., repairing porous spacecraft parts by welding in space."

"Silver was chosen as the experimental material because it is a typical metal, readily available with high purity, fairly unexpensive, easy to roll and draw, and melting at a temperature (961.9°C) below the maximum available temperature of 1000°C . The silver was of 99.999% grade (electrolytic silver melted under hydrogen in graphite crucible).

The ampoules were loaded as follows:

Ampoule A (...) contained 8 silver discs of 14 mm diameter and 0.1 mm thickness in which one or more holes had been spark cut or drilled as follows, when counting from the hot end of the ampoule:

P8: 1 central hexagonal hole of 3.5 mm side
P7: 1 central hexagonal hole of 3.5 mm side
P6: 1 central square hole of 1 mm side
P5: 4 square holes of 1 mm side and 6.4 mm apart
P4: 9 round holes of 1 mm diameter and 3.2 mm apart
P3: 21 round holes of 1 mm diameter and 1.6 mm apart
P2: 14 round holes of 2 mm diameter and 0.8 mm apart
P1: 21 round holes of 2 mm diameter and 0.4 mm apart

The silver discs were held apart by silica ring spacers and, in order to avoid mixing of the melting products from different discs, the silica ampoule was divided in compartments by stainless steel grids. The silica ampoules were sealed under a vacuum of about 10^{-5} mm Hg. Before sealing they were heated for one hour at 350°C in the same vacuum in order to decompose any Ag_2O present.

Ampoule B had exactly the same load as ampoule A, except that the discs had a thickness of 0.5 mm.

Ampoule C (...) contained a single sample made of silver fibres of 0.4 mm diameter and 10-15 mm length. The fibres had been poured as randomly as possible into a cylindrical die, compressed into a disc of about 4 mm high and 50 mm diameter (maximum pressure about 10 kg/mm^2). The disc was sintered in hydrogen for two hours at 900°C . From this disc a prism was cut to dimensions $40 \times 14 \times 4\text{ mm}$. The porosity was 30% for the Skylab sample and 33% for the ground based test sample."

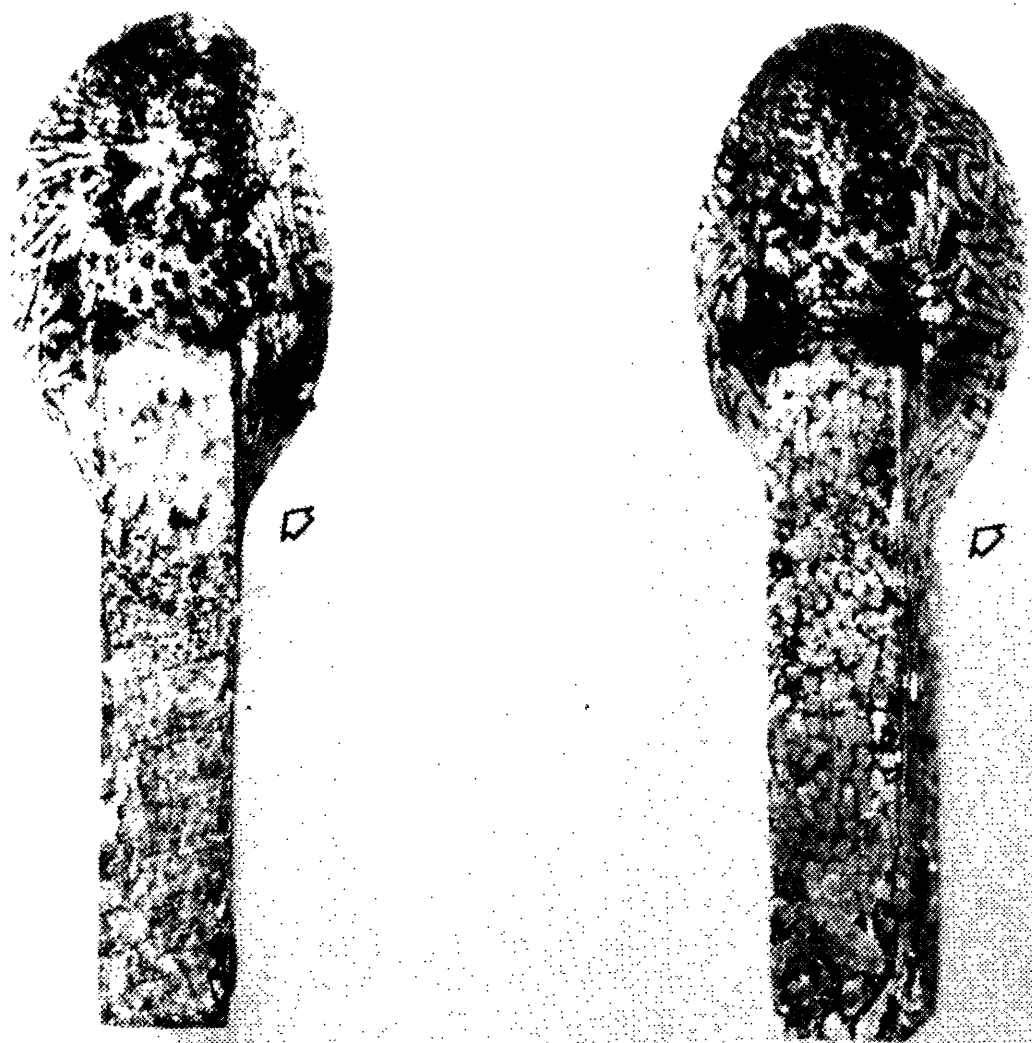
The cartridges which contained the ampoules were designed "such as to provide a small temperature gradient in the hot zone. The purpose was that a part of the samples would not melt. This appeared to be the only way to be sure that the temperature had not exceeded too much the melting temperature, as the actual temperature of the samples could not be measured. Moreover, a varying temperature might yield additional information." The M518 Furnace was heated to 1035°C in 3½ hours and remained for 1 hour at the maximum temperature at which time the power was turned off. The initial passive cooling rate was 38°C for the first five minutes.

"The examination and study of the experimental results is not yet finished. Some samples, such as the A series (thin plates), have still to be examined in detail. The presence and distribution of impurities in all specimens has to be checked. An attempt is being made to calculate theoretically the shape of the various specimens after melting and solidification. Moreover, other experiments should be performed. Therefore, the following conclusions are only provisional:

Most of the original porosity in the samples has disappeared during the melting stage." (See figures 50, 51 and 52) This has been favoured by the fact that the pores were of the open type, by the presence of a temperature gradient and by the low pressure. It should be possible to obtain a more porous product when starting from a material with gas filled closed pores, and if the stay above the melting point is not long enough to allow the pores to coalesce and to migrate to the free surface by diffusion and surface tension induced convection. Even with samples with open pores such as those used in the present investigation, the obtention of a porous product might be possible if the heat input was the same on all sides of the specimen so that a molten surface layer would enclose the still unmelted material. As regards the way in which the geometry of a porous specimen (e.g., a grid) changes with time on melting in weightless condition, one should perform experiments using levitation melting and high speed image recording.

The experiment has shown that the shape" (See figure 53) "and surface condition of a sample melted and solidified in space is not only determined by surface tension: shrinkage may cause the formation of a pipe" (See figure 54) "and constitutional supercooling, caused by impurities, may result in a cellular substructure" (See figure 55) "leading to a network of grooves on the surface. These disturbing factors might be reduced by modifying the thermal conditions and by increasing the purity of the metal or avoiding any contamination.

The leveling out of concentration gradients, as may be caused by pickup of the impurities at the surface, appears to be slow in the molten metal when gravity induced convection is absent. Therefore the action of diffusion and of convection due to variations in surface tension, appears to be slow.



◊ = shoulders

FIGURE 50. SIDE VIEWS OF SKYLAB-TESTED FIBRE SPECIMENS

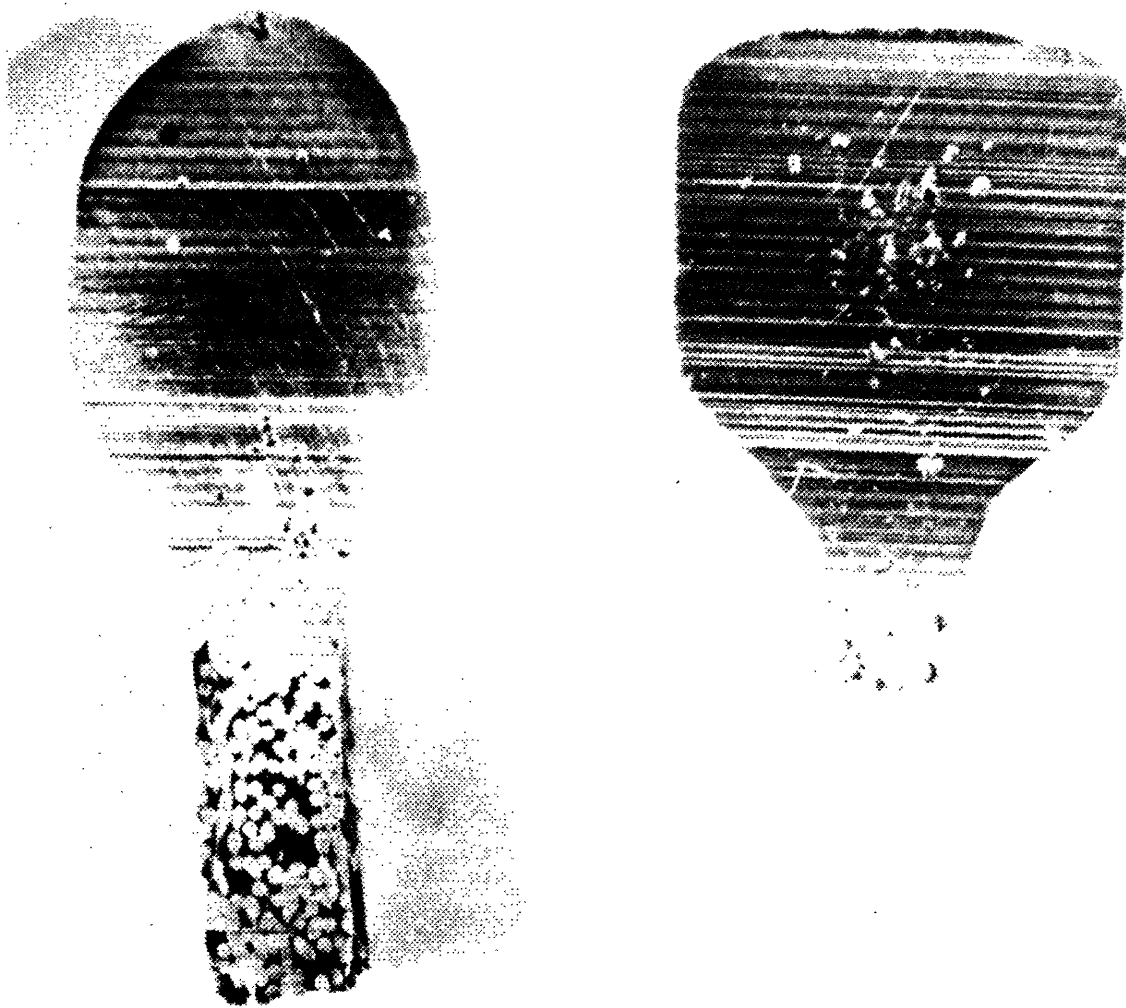


FIGURE 51. SECTIONED SAMPLES



FIGURE 52. POLISHED SECTION THROUGH SKYLAB SAMPLE X6

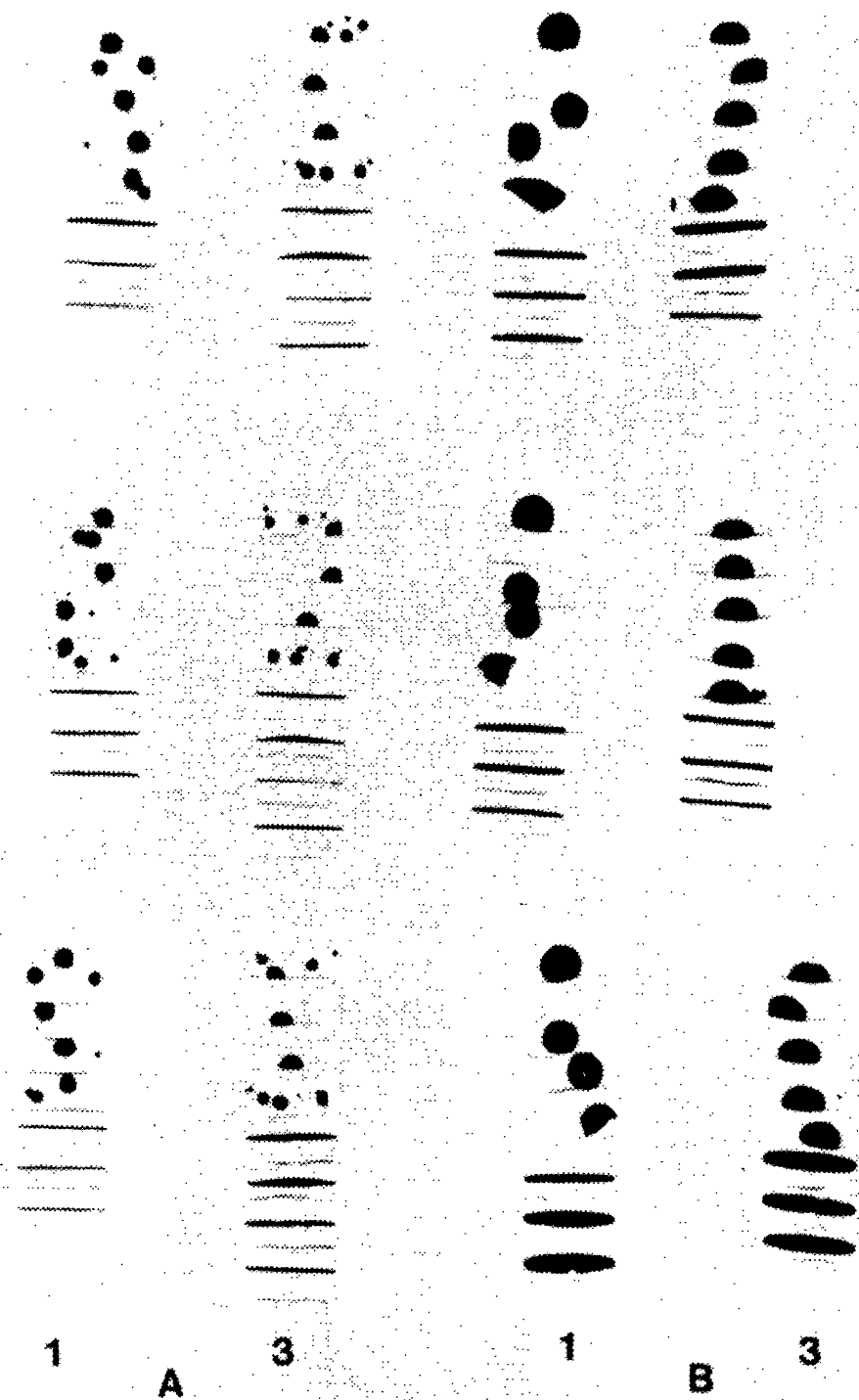


FIGURE 53. AMPOULE X-RAYS---
 RADIOGRAPHIES OF THE SKYLAB (1A and 1B) AND
 GROUND (3A and 3B) TESTED SAMPLES IN THEIR
 UNOPENED AMPOULES. THREE RADIOGRAPHIES AT
 120° OF EACH AMPOULE.



FIGURE 54. SKYLAB SAMPLE 1BP6 SHOWING PIPING AND SUBSTRUCTURE X92

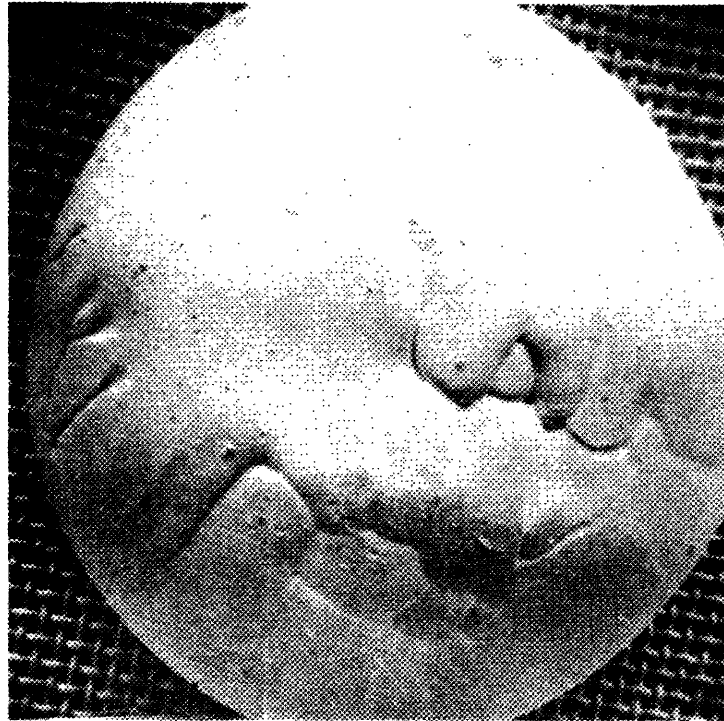


FIGURE 55. SKYLAB SAMPLE 1BP7-8 SHOWING CELLULAR SOLIDIFICATION
SUBSTRUCTURE X20

When only a part of a solid is melted in zero gravity, the tendency of the molten part to become spherical can be much restricted. This would be important for applications such as zone melting in space and welding of porous or massive material in space."

18. M566 Aluminum-Copper Eutectics. [25] The PI for Experiment M566 is Mr. E.A. Hasemeyer, MSFC, Huntsville, Alabama.

The experiment was to determine the effects of weightlessness on the solidification of lamellar structure in a eutectic alloy when directionally solidified.

"Directionally solidified eutectics as prepared in a one-g environment, almost always exhibit termination faults, mismatch surfaces and other defects. These growth imperfections limit their strength when used as structural composites and prevent their use for non-structural applications such as Micro Capacitors. The formation of a mismatch surface in an aligned eutectic involves an increase in net surface area. (...) The appearance of terminations allows lamellae to maintain their parallel growth but there is no compensation for the excess surface and increased energy at the mismatch surfaces. Because of the incomplete explanation for occurrence of all such defects in lamellar eutectics, it appeared reasonable (...) that an experiment in the orbiting Skylab would show that an improved structure could be grown in the absence of gravity induced thermal convection. The growth of a eutectic composite of aligned lamellae in low gravity should also provide new insights into the parameters affecting their solidification. The CuAl_2 eutectic (67% Wgt Aluminum-33% Wgt Copper) was selected as a model system on the basis of its moderate eutectic temperature and the extensive background of solidification information available with which zero-g results may be compared."

"Single-grained specimens for this experiment were prepared by directional solidification. The initial castings were made from master heats of zone-refined aluminum and spectrographic copper. (...)

The design of the M566 cartridge is similar to others used in the M518 Multipurpose Electric Furnace. (...) The copper-aluminum eutectic specimen is 6.25 mm in diameter and 12.7 mm in length.

The cartridge assembly for each specimen was designed so that the molten eutectic alloy would contact graphite only. The following heating and cooling parameters were selected for ground-based tests and the Skylab experiment:

E. Engineering Operations

These experiments were designed to study the Skylab interior and exterior environments. They further evaluated the crew impact on the spacecraft and the spacecraft design effect on crew well-being. Assessments were made of mobility aids and the crew's proficiency to perform repetitive tasks over long periods.

The exterior environment was studied in two distinct operational phases. In one phase, various material samples were exposed to the transient launch and staging environments. In the other, the samples experienced the long-term effects of space vacuum, radiation, and particle bombardment.

The spacecraft habitability aspects were analyzed in detail during the three missions. This included monitoring the physical conditions such as: daily aerosol and dust particle counts throughout the spacecraft; local air flow and temperature measurements and sound level and frequency determinations. But more important, it included the psychological evaluation of habitability provisions such as: the utility and convenience of living facilities, the workload demands and the recreational aid effectiveness. As part of this overall evaluation, repetitive tasks of operational significance, such as manual navigation sightings, were performed to assess the crew's ability to maintain or improve proficiency during long periods in zero-g.

Different types of maneuvering aids were compared for use by crews during future missions, both for inside and EVA activities. The spacecraft capability to serve as a highly stable platform in space for making extremely accurate stellar measurements was correlated to crew motions of all types.

Table IX provides: the total number of planned FO's, the numbers performed during each manned flight and the degree of success.

1. D024 Thermal Control Coatings. The PI for Experiment D024 is Dr. William L. Lehn, Air Force Materials Laboratory, Air Force Systems Command, Wright-Patterson Air Force Base (W-PAFB), Ohio. This experiment complemented M415 which investigated the launch phase external environmental effects on thermal control coatings, while D024 investigated orbital phase effects.

This was a passive experiment installed and operated on SL-1/SL-2, SL-3, and resupplied and operated on SL-4 to determine the space environmental effects on selected thermal control coatings and polymeric film strip samples. These samples were returned in a sealed container to avoid changes to these effects caused by atmospheric recombination. This was the first opportunity to test returned samples in a vacuum. Planned objectives were calibration of earth-based laboratory tests

TABLE IX. ACCOMPLISHMENT OF EXPERIMENT FUNCTIONAL OBJECTIVES

EXPERIMENT TITLE	FO's PLANNED	FO's PERFORMED			ACCOMPLISHMENT (PERCENT)
		SL-2	SL-3	SL-4	
<u>ENGINEERING/OPERATIONS</u> [7, 8, 9]					
D024 THERMAL CONTROL COATINGS	3	1	1	1	100
M415 THERMAL CONTROL COATINGS	4	4	0	0	100
M487 HABITABILITY/CREW QUARTERS	59	19	18	21	98
M509 ASTRONAUT MANEUVERING EQUIPMENT	12	0	6	5	92
T002 MANUAL NAVIGATION SIGHTINGS	68	0	32	25	84
T003 INFLIGHT AEROSOL ANALYSIS	56	10	20	26	100
T013 CREW/VEHICLE DISTURBANCE	1	0	1	0	100
T020 FOOT-CONTROLLED MANEUVERING UNIT	6	0	2½	1	58

and definition of degradation mechanisms. Experiment hardware for each mission was a tray with 36 coated discs, another tray with 32 polymeric film strips, and a material return container. Materials that were flown are listed in table X and XI. Two hardware sets were launched on SL-1 mounted on the ATM deployment assembly truss, under the payload shroud. They were exposed when the shroud was jettisoned. The first set was recovered after 36 days (on DOY 170) and the second set after 131 days (on DOY 265). The third hardware set was launched and recovered during SL-4 to avoid contamination from the CM control rockets during docking, undocking and fly-around. Deployment occurred on DOY 326 and retrieval on DOY 034 for a 73 day exposure.

All returned hardware was significantly contaminated, apparently by the cloud of effluents and venting gases related to a manned spacecraft. The contamination was visually evident by a golden, yellow-brown discoloration in sun lit areas with negligible discoloration in shaded areas. See figure 56 [26]. Variations between missions of discoloration, reflectivity of thermal control coatings, bulk properties of polymeric film strips and contamination thickness are shown in table XII.

The contamination compounds and specific sources have yet to be completely identified. Contaminated surface laboratory analysis and hypothesized condition simulation are in progress.

The SL-4 container had atmospheric pressure when received in the laboratory. The cause is undetermined but will not be further investigated because contamination masked atmospheric effects. Spectral reflectance, solar absorptance, and total normal reflectance measurements are in progress. Contamination measurements are using Auger electron spectroscopy. The presence of silicon, oxygen, carbon, and phosphorous has been detected, but compounds are still being investigated. Optical transmission, frustrated multiple interval reflections spectra, and electrical and physical properties have been measured on polymeric film strip samples. Results on these strips approximate the expected changes from solar radiation with little effect from contamination. Contamination is mainly a surface effect and strip measurements were of bulk properties.

2. M415 Thermal Control Coatings. The PI for Experiment M415 is Mr. E. C. McKannan, NASA MSFC, Huntsville, Alabama. The purpose was to determine the effects of prelaunch, launch, and space environments on degrading the absorptivity/emissivity and stability characteristics of three material coatings commonly utilized for passive thermal control.

NOTE: SL-1/SL-2 FLIGHT
PART NUMBER: 71NE2403-12 SN1
LAUNCHED 14 MAY 1973
RETRIEVED 19 JUNE 1973
RECOVERED 22 JUNE 1973

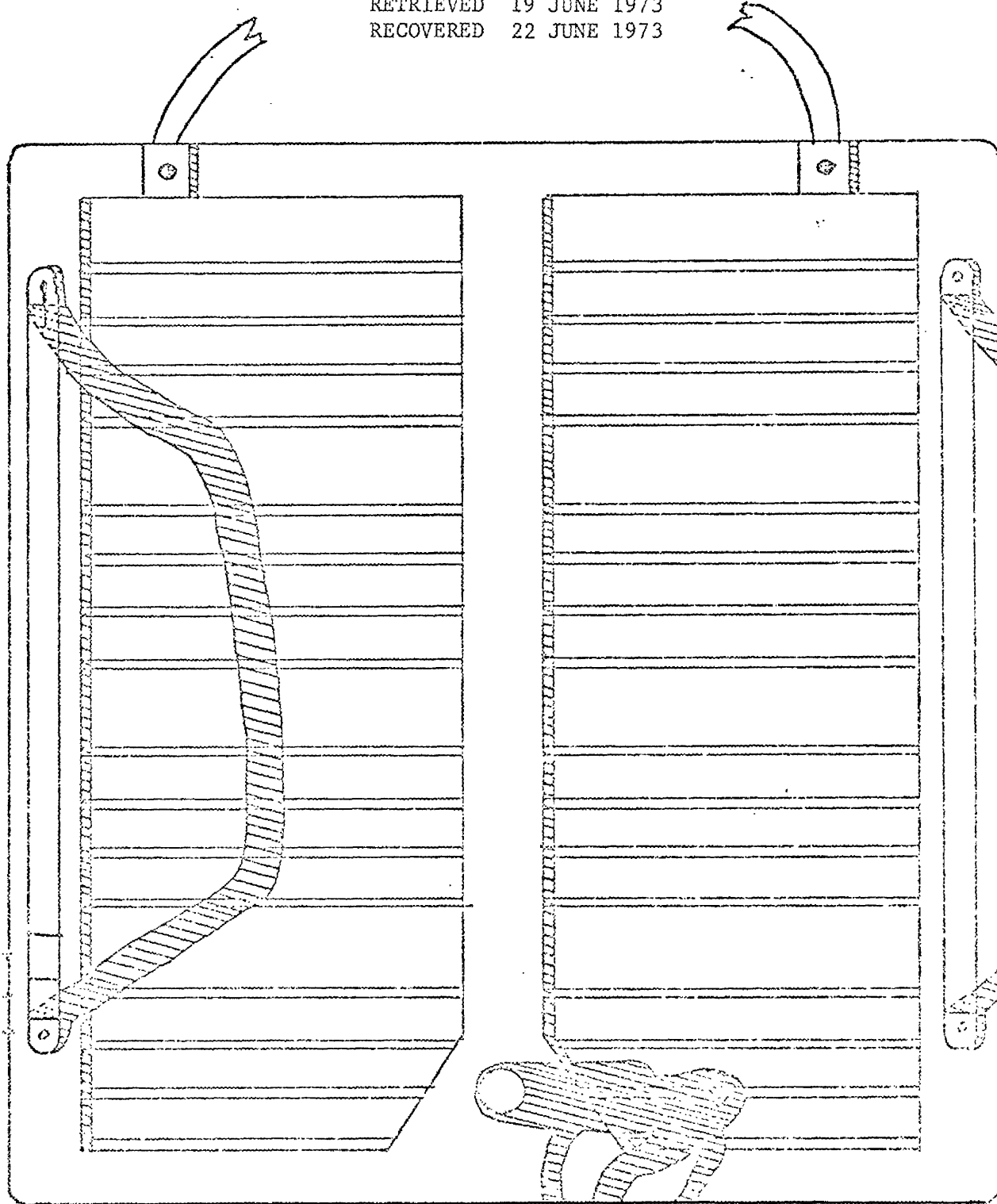


FIGURE 56. EXPERIMENT D024 POLYMER FILM STRIP

TABLE X. D024 THERMAL CONTROL MATERIALS LISTING

<u>Item</u>	<u>Material</u>	<u>No. of Samples/Tray</u>	<u>Description-Comments</u>
1.	aAl ₂ O ₃ /K-Silicate	1	Linde C calcined pigment (1.0u) in PS-7
2.	Eu ₂ O ₃ /M-Silicone	1	AFML silicate coated pigment in RTV 602
3.	aAl ₂ O ₃ /M-Silicone	1	Controlled dehydrated pigment in RTV 602
4.	CaTiSiO ₅ /M-Silicone	1	Hydrothermally prepared pigment in RTV 602
5.	TiO ₂ /M-Silicone	1	Commercial pigment in RTV 602
6.	Leafing Al/Silicone-Acrylic	1	Commercial pigment in SR82 and B-72 blended resins
7.	(No. 1) Processed 5u Astroquartz, 8H	1	
8.	(No. 2) 10u Astroquartz, 8H	1	
9.	(No. 3) 3D-QFY-Al 150 1/0	1	
10.	(No. 4) SiO ₂ /Al interweave	1	Fabric composites bonded to Skylab coupons with either SR 585 or RTV 102 adhesives
11.	(No. 5) Control 5u Astroquartz, 8H, (Not processed)	1	
12.	(No. 6) 3D-QFY 150 1/0 no VDA	1	
13.	FEP/Ag	2	Second surface mirror bonded onto Skylab coupons with transfer tape

TABLE X. D024 THERMAL CONTROL MATERIALS LISTING (Continued)

<u>Item</u>	<u>Material</u>	<u>No. of Samples/Tray</u>	<u>Description-Comments</u>
14.	FEP/Al	2	Second surface mirror bonded onto Skylab coupons with transfer tape
15.	Fused Quartz/Al	1	Second surface mirror bonded onto Skylab coupons with RTV 566/A/B
16.	Microsheet/Ag	1	Second surface mirror bonded onto Skylab coupons with RTV 566/A/B
17.	Anodized Aluminum (0.2 mil)	1	Processed Al disc bonded onto Skylab coupon with Eccobond Epoxy Type 57C
18.	Anodized Aluminum (0.5 mil)	1	Processed Al disc bonded onto Skylab coupon with Eccobond Epoxy Type 57C
19.	Alzak Anodized Aluminum	1	Alcoa processed Al disc bonded to Skylab coupon Eccobond Epoxy Type 7C
20.	S-13G	2	Silicate treated ZnO pigment in RTV 602. One sample is coated disc bonded to Skylab coupon, other sample is a coated coupon
21.	Z-93	2	ZnO pigment in potassium silicate (PS-7). One sample is coated disc bonded to Skylab coupon, other sample is a coated coupon.

TABLE X. D024 THERMAL CONTROL MATERIALS LISTING (Concluded)

<u>Item</u>	<u>Material</u>	<u>No. of Samples/Tray</u>	<u>Description-Comments</u>
22.	Zn ₂ TiO ₄ /M-Silicone	2	IITRI prepared pigment in Owens Illinois 650 resin. Both samples are coated discs bonded to Skylab coupons.
23.	Black Velvet Paint	3	Two samples in "Thumb" area; other sample receives "normal" exposure and handling
24.	PV-100	1	TiO ₂ pigmented silicone alkyd
25.	S-13	1	ZnO (as received) pigment in RTV 602
26.	ZrO ₂ /M-Silicone	1	Silica coated ZrO ₂ pigment in a single package silicone
27.	Au/Quartz Crystal	1	Passive quartz oscillator mechanically attached to Skylab coupon
28.	Ag/Quartz Crystal	1	Passive quartz oscillator mechanically attached to Skylab coupon
29.	SiO ₂ /M-Silicone	1	Hydrothermally prepared pigment in RTV 602

TABLE XI. POLYMERIC FILM STRIP MATERIALS

Material	Material
1. Nylon 6/6	5. Polycarbonate
2. Polyphenylquinoxaline	6. Mylar
3. Polyimide	7. FEP (Type XC20)
4. FEP (Type A)	8. Teflon

TABLE XII. SAMPLE CHARACTERISTICS

Mission	Duration (days)	Degree of Discoloration	Change in Reflectivity	Bulk Property Change	Contamination Thickness
SL1/SL2	36	intermediate	intermediate	least	thickest
SL-3	131	deepest	greatest	most	intermediate
SL-4	76	lightest	least	intermediate	thinnest

Three different types of coatings used on spacecraft exteriors were exposed sequentially to prelaunch, liftoff, stage separation and in-orbit environments during the SL-2 launch. The degree to which the samples became contaminated (less white) during each phase determined the equilibrium temperature reached by each sample upon achieving orbit in the proper sunlit orientation. This temperature data was telemetered to earth.

The experiment performed properly. Indications are that all control coatings darkened somewhat from the launch pad high humidity and salt spray atmosphere. From that time on through launch and insertion into orbit an additional amount of degradation took place. This information will be very useful in designing thermal control systems for future spacecraft in choosing the optimum coatings for the anticipated launch environments.

Data analysis is still in progress

3. M487 Habitability/Crew Quarters. The PI for Experiment M487 is Mr. Caldwell C. Johnson, Chief of the Spacecraft Design Division, JSC, Houston, Texas.

Periodically throughout the three manned visits to Skylab, flight crews evaluated the Orbital Assembly habitability features during their daily, routine activities including housekeeping tasks and self-sustaining chores such as sleeping, eating, personal hygiene, etc. The nine habitability features encompass:

Environment,
Architecture,
Mobility and restraints,
Housekeeping,
Communications,
Personal hygiene,
Food and water,
Garments and personal accouterments, and
Off-duty activities.

Habitability evaluations, obtained from tape-recorded comments, TV and video tapes, 16mm film clips, and supplemental environmental measurements (temperature, air flow, sound levels, etc.) provided data useful for future manned spacecraft design.

Habitability evaluation data was obtained from three sources: crew subjective and debriefing comments; photography; and instrument measurements.

a. Crew Subjective and Debriefing Comments. Both subjective and debriefing comments were solicited at scheduled times and at opportune moments from each crewman relative to their habitability assessment of compartments and equipment. Representative comments recorded during the missions indicate the following general assessments:

General arrangement and orientation of the workshop was adequate. The wardroom proved to be the central point of crew congregation. The wardroom table was extensively used for paper work sessions and as a work bench for trouble-shooting or repairing small items. The need for magnetic or spring-type hold down devices on documents were identified.

Bagging and disposition of trash through the trash airlock proved more time-consuming than originally estimated. The need for more portable trash receptacles was identified.

Loose or misplaced items (food particles, screws, etc.) tended to drift toward the air mixing chamber screen where they became entrapped. The screen served as an excellent collection point.

The light-duty foot restraints in the waste management and wardroom compartments were unfavorable.

Lighting levels throughout the workshop were generally too low for close work. Pen lights were extensively used while performing maintenance-repair activities.

b. Photography. The Skylab crews obtained motion picture film clips of certain daily tasks which demonstrated their adaptability to the zero-g environment and also presented documentaries of task performances. Tasks photographed during the missions included the following:

- Eating meals,
- Donning/doffing clothing and ingressing/egressing sleep restraints,
- Cleaning air mixing chamber screens,
- Using the trash airlock, and
- Using the waste management and personal hygiene facilities.

c. Instrument Measurements. Portable measuring instruments, supplied by Experiment M487, were used during the missions to obtain measurements of ambient air temperatures, surface temperatures, air velocities, sound pressure levels and frequency distributions, reflective illumination levels, locational dimensions, and push/pull forces.

In addition to the experiment objectives, the measuring instruments were extensively used to obtain ambient and surface temperature measurements of operational hardware, such as the rate gyro six pack, experiment film canisters (S020 and T025), air diffusers, etc.

All Experiment M487 hardware performed satisfactorily and within procurement specifications.

4. M509 Astronaut Maneuvering Equipment. The PI for Experiment M509 is Major C. E. Whitsett, USAF, JSC, Houston, Texas.

The purpose was to evaluate the utility of several astronaut maneuvering techniques by performing in-orbit maneuvering tests. The test data will be used to evaluate ground based simulation techniques and, more significantly, to establish the design requirements for future operational maneuvering units for EVA tasks.

The maneuvering unit was a backpack type with multiple fixed position nitrogen gas thrusters which provided translation and rotation capabilities. The nitrogen pressure bottle, telemetry system, battery and two types of gyro-controlled automatic stabilization systems were contained within the unit. Desired flight paths were flown by operating aircraft-type hand controllers on arms extending from the backpack. A hand-held thruster unit, similar to that used in Gemini EVA, was provided and supplied from the backpack nitrogen system.

The experiment was operated six times on SL-3 and five times on SL-4. Three runs were performed with the operator wearing his pressure suit. The equipment performed extremely well through the

entire Skylab mission and all test objectives were met. The SL-3 test program was expanded to include a test run by the Science Pilot who was untrained for this experiment, but easily mastered the technique of flying the prescribed maneuvers.

The equipment's/operator's flying capabilities proved to be very good in all modes except the hand-held maneuvering unit mode. Actual equipment operation proved to be very comparable to the six-degree-of-freedom ground simulator used in the preflight training program. The manually stabilized direct mode, which represents the less complex lighter weight system, was easy to fly and could conceivably be chosen as the mode to be used in future operational units. The automatically stabilized modes, rate-gyro and CMG, worked very well and would certainly be advantageous for an operational unit, particularly in the performance of an EVA task in areas where restraint/docking capabilities are limited or non-existent.

The desirability for equipment of this type in future space missions was vividly demonstrated by the numerous external repairs, inspections, etc., performed by the three Skylab crews. Such tasks would have been greatly simplified and much less time consuming if an operational astronaut maneuvering unit had been available.

5. T002 Manual Navigation Sightings. The PIs for Experiment T002 are Mr. Robert J. Randle, NASA Ames Research Center, Moffett Field, California, who was concerned with the mid-course navigational aspects, and Lt. Col. Stanley W. Powers, U.S. Air Force Academy, Colorado, who was concerned with orbital navigation.

The dual objectives were the measurement of the crewman's ability to make reliable and accurate celestial observations during extended periods of weightlessness and to test an orbital navigation method. Data can be extrapolated to estimate crewman's general ability to perform tasks that require dexterity and judgement during long weightless periods.

A series of 34 celestial observations were planned on each SL-3 and SL-4 missions to accomplish these objectives. Each observation performance was to consist of 10 to 15 sightings. The mid course observations measured three types of angles: between stars, between a star and the moon, and between opposite moon edges using a sextant. These last two measurements would provide navigational information because the angles are dependent upon spacecraft position. Orbital observations included two types: one using a stadimeter to measure the curvature of the earth's horizon as an indication of spacecraft altitude, and the other using a sextant to measure the angle between a star and the earth's horizon. These orbital observations were to be combined into an operational sequence.

The two optical instruments used during the experiment were a sextant and a stadimeter.

The sextant was similar to a common marine sextant, and was the same type as used in the Gemini program, with minor modifications. It provided a superimposed image display and a measure of angles between celestial bodies with readout markings every thousandth of a degree.

The stadimeter was used to observe a segment of the earth's horizon curvature and measure the angle between the lines of sight from the observer to the arc center and the chord center. A split optical display was provided enabling reference points to be located on the observed horizon and optically aligned by a manual control. The readout markings were every thousandth of a degree. The spacecraft altitude could then be determined from the angle and the planet's diameter.

Three additional components assisted in experiment performance. These were: a collapsible hood for arrangement over the wardroom window preventing internal lighting reflections, a stowage locker cushion protected the instruments from launch loads and provided in-orbit storage; and a battery transfer case facilitated resupply of the instrument illumination batteries.

T002 was planned for operation at the crew's convenience on a non-interference basis. As a result, it was performed 32 times on SL-3 and 25 times on SL-4 by the PLT.

A measure of data reliability (precision) is one standard deviation (1σ). In a normal distribution resulting from randomly obtained data, 1σ includes 68.26 percent of the data points. The SL-3 PLT achieved a $1\sigma = 10.0$ arc-seconds during preflight training. On the 46th day, he again achieved a $1\sigma = 10.0$ arc-seconds showing no degradation caused by his time in orbit. Table XIII shows the result obtained for each type of observation. [27] The angular sightings across the moon showed a strong positive bias (an average +22.5 arc-seconds larger than the computed angle) and a very small 1σ indicating almost faultless precision. The bias is presumably due to irradiance (a tendency of a bright, extended surface against a dark background to appear larger than it actually is), but no systematic change occurred when various filter combinations were used. Actually, the sighted angles were larger using various filters than with no filter. No ready explanation exists for this as yet.

The three earth horizon sightings, during SL-3, marked the first stadimeter operation in space. The planned daylight earth horizon, and the night airglow horizon were used. Table XIII indicates greater than anticipated variability attributable to a non-uniform, diffuse earth horizon. [28] The top of the night airglow horizon provides best results, and observations made near orbital noon produce almost as good results.

TABLE XIII. T002 SL-3 MISSION RESULTS

TARGETS	OBSERVATIONS		MEAN ERROR (BIAS)	STANDARD DEVIATION
	PLANNED	COMPLETED		
<u>Mid-Course Sightings</u>				
Star to Star	6	6	0	11.5 arc-sec
Star to Moon	12	10	0	11.4 arc-sec
Across Moon	6	6	+22.5 arc-sec	3.8 arc-sec
<u>Orbital Sightings</u>				
Earth Horizon	2	3	6.77 nm	2.3 to 6.5 nm
Star to Horizon	3	3	.266 to 2.4 deg.	0.5 to 3.5 nm
Combined Operational Sightings	5	4	Not Available	Not Available

Further investigation is required to study the various options for navigational solutions. A safe re-entry could be accomplished using Skylab data.

All SL-4 mid-course observations (except the last two observations) produced unusable data because of the wardroom window transparent protective shield was not removed prior to performing T002. [29] Sightings through this shield resulted in large biases and large standard deviations, demonstrating the need for a high-quality optical window. The last two mid-course observations, performed with the protective shield removed, did show that nominal biases and nominal standard deviations could be achieved. The mean standard deviation achieved during pre-flight training was 12.0 arc-seconds. During the last two observations the mean bias was 14.9 arc-seconds and the mean standard deviation was 12.8 arc-seconds. Thus no significant change in proficiency occurred even though the PLT had been in orbit for 69 days when the last T002 performance was made.

Reduction and analysis of orbital navigation data is in progress. Four of the planned five stadimeter observations were performed using a nominally uniform horizon. These observations resulted in a range of 1σ from 2 to 4.6 nm. Most of the wardroom window protective shield effects are less than the range of stadimeter 1σ 's. The SL-3 and SL-4 stadimeter results were comparable, so it may be concluded that the shield had negligible effect upon stadimeter results.

No planned star-earth horizon sightings were taken during SL-4. Consequently, no orbital navigational computation will be possible.

6. T003 Inflight Aerosol Analysis. The PI for Experiment T003 is Dr. William Z. Leavitt, U.S. Department of Transportation, Transportation Systems Center, Cambridge, Massachusetts.

This experiment was to measure the aerosol particulate matter concentration and distribution in the spacecraft during each Skylab mission, as a function of time and location.

The data cards and the filter-impactor system from Skylab missions 2, 3 and 4 are undergoing analysis. The real-time measurements recorded on the cards indicate a very clean spacecraft. The environmental control system is efficiently removing the particles. From analysis, there appears to be no major source of particles from equipment operating in the spacecraft. Particle distribution is constant throughout the spacecraft, again indicating the efficiency of the environmental control system. Particle loading in the 3 to 100 micron size range averages approximately 200 particles per cubic foot of air; particle loading in the 1 to 3 micron range averages about 3,000 particles per cubic foot of air.

Analysis of the impactor pads by scanning electron microscope showed that the major particle contribution is from skin squamae, most likely produced by the astronaut operating the aerosol analyzer. There are very few fibers and particles which are not skin. The micrographs confirm the optical counting results.

NASA initiated a request to determine whether the aerosol analyzer was capable of detecting cooling fluid (Coolanol-15) leaks and answers to the following questions were sought:

If coolant droplets were produced by a leak, would they be stable and could they be counted by the instrument?

If they were collected on the impactor pads, could they be identified on a micrograph?

Did the actual impactor pads from Skylab 2 show any Coolanol-15 droplets?

To establish the feasibility of coolant detection, several experiments were performed in the laboratory. First, Coolanol-15 was nebulized; using the T003 aerosol analyzer, the aerosol produced was detected and found to be stable up to at least four feet from the nebulizing source. Second, Coolanol-15 liquid was flowed onto an impactor pad and a strong infrared reflection spectrum was obtained with a scanning infrared interferometer system, indicating the presence of the material on the pad. After four days, the measurement was repeated with the identical impactor pad and no indication was obtained. Third, Coolanol-15 was nebulized and collected on an impactor pad. Attempts to detect the coolant both with an electron microscope and by infrared techniques proved negative. Following these laboratory tests, the impactor pads from SL-2 were examined for indications of Coolanol-15, and, as expected, the results were negative. The study demonstrated that leaks of Coolanol-15 which produced aerosols in the spacecraft could be detected by the aerosol analyzer in real-time but would not register for postflight analysis.

Data analysis is continuing. The used filters from Skylab 3 and 4 missions are presently being evaluated. The results will permit further identification of the spacecraft particulate contaminants by material, shape and quantity.

7. T013 Crew/Vehicle Disturbance. The PI for Experiment T013 is Dr. Bruce Conway, NASA Langley Research Center, Langley, Virginia.

This experiment was to measure the various crew motion effects on the dynamics of manned spacecraft; specifically, the torques, forces, and vehicle motions produced by the astronaut's body motions. Attitude and pointing control systems of future manned spacecraft with high pointing accuracy requirements must be designed to consider these motions. The data will also be used to verify the ground simulation techniques.

The experiment hardware consisted of the: limb motion sensing system (LIMS), force measuring system (FMS), and experiment data system (EDS). The LIMS consisted of an exoskeleton incorporated into a flight-type suit with instrumentation for monitoring motion at the major body joints. The FMS consisted of two force measuring units (FMUs) attached to the OWS for measuring the actual forces and moments applied to the spacecraft. The EDS conditioned the data output of the LIMS and FMS into the desired format for recording and telemetry. This data is time correlated for comparison with applicable ATM pointing control system data. Two DACs were used to obtain 16mm motion picture data for additional monitoring of the test subject motions.

The prescribed tasks included basic activities such as gross body motions, simulated console operations, and worst case control system inputs. Preliminary analysis of the obtained data has shown several significant deviations from the predictions. The maximum input forces during soaring was measured to be slightly in excess of

70 lbs., which was greater than expected and may have contributed to the anomaly that occurred in one of the FMUs during the performance of the worst case operations. The DAC film data has shown soaring velocities of 6-9 ft/sec were achieved compared to predictions of 2.5-3.5 ft/sec. These findings will be further analyzed and used to up-date the ground simulation techniques and predictions.

The experiment results will logically lead to additional ground-based investigations and simulations which are expected to result in publishing a catalog of expected crew motion disturbance predictions. The catalog would be of significant benefit for the design of future spacecraft attitude control systems and applicable structural design and analysis.

8. T020 Foot-Controlled Maneuvering Unit. The PI for Experiment T020 is Mr. D. E. Hewes, NASA Langley Research Center, Langley, Virginia.

The experiment was to provide information pertaining to the design and use of astronaut maneuvering systems by conducting in-flight and ground based evaluations of a relatively simple unstabilized foot controlled maneuvering device.

The Foot Controlled Maneuvering Unit (FCMU) was mounted between the operator's legs and contained the control pedals and two four-nozzle thruster sets just outboard of the feet for attitude and translation movements. The propulsion gas tank and battery were contained within a backpack strapped to the operator's back.

The experiment was operated three times on SL-3 and two times on SL-4. The third SL-3 run was made in the pressure suited mode, all others were made in the shirtsleeve mode. A modification kit, containing additional restraint straps and brackets for rigidizing the backpack to the FCMU, was launched on SL-4. The kit was installed prior to the SL-4 runs and resulted in improved handling characteristics and alleviated the harness loosening and inadequacy experienced during the first run. A temporary fix using on-board restraint straps were used for the latter SL-3 runs.

The PI is presently analyzing the 16mm color film, crew voice transcripts and copies of the downlinked TV. The PI has released a preliminary evaluation of the experiment runs performed on SL-3. The final PI report will be based upon the evaluation of the total run complement rather than on a mission basis.

F. Contamination

Two experiments were associated with the contamination in the spacecraft environs. Previous Gemini and Apollo flights had encountered window contamination that interfered with star sightings and lunar surface photography experiments. Sources of contaminant depositions were thruster firings and molecular evaporations from around the windows. With more advanced optical experiments on spacecraft, it is important that the effects of contamination on such instruments be evaluated. Experiment T027 dealt with deposited contaminants on optical surfaces and with the reflected light from particles in the contaminant cloud around the spacecraft. Experiment T025 used a coronagraph to also photograph the sunlit contaminant cloud. Experiment T025 also photographed the sunlit upper atmosphere and Comet Kohoutek.

Experiment T025 was planned for three performances all of which were accomplished during EVA's on SL-4. One performance on SL-2 for the surface deposition portion of the T027 experiment was planned and performed on SL-2. The reflected light portion of the T027 experiment was planned for 43 functional objectives in a joint observing program with experiment S073 of which 11 were performed on SL-2 and 6 on SL-3.

1. T025 Coronagraph Contamination Measurement.

The PI for Experiment T025 is Dr. J. Mayo Greenberg, Dudley Observatory, Albany, New York.

The experiment was originally planned to be deployed from the solar SAL; however, due to its unavailability, experiment operations were conducted during EVA on SL-4. The photographic film returned in the SL-4 CM was to, hopefully, provide altitude distribution of upper atmospheric particles, dust concentration, relationship of noctilucent clouds and effects of solar events on the upper atmosphere, and contamination measurements near the spacecraft. The Comet Kohoutek photographs were taken with special filters on EVA's on December 25th and 29th, 1973. These photographs and ATM observations were the only observations which could be made in this near-perihelion time frame.

Six frames (two white light, two at 2500 \AA and two at 3600 \AA) of atmospheric data were obtained during the first EVA, before a hardware problem occurred which prevented further photography. The Nikon camera was used during the near-perihelion EVAs. Unfortunately, the photographs taken with this camera were all out-of-focus. The Dudley Observatory personnel believe that the photographs which are in focus are unique and contain valuable information on the ozone structure.

They hope to prove the power of the coronagraph technique for aerosol monitoring. They further believe the out-of-focus data can be restored to a great extent. The 84 Comet Kohoutek frame images were greatly enlarged due to the out-of-focus condition but may be used to determine an upper limit on the comet's brightness.

2. T027 Contamination Measurement. The PI for Experiment T027 is Dr. J. Muscari of Martin Marietta Aerospace in Denver, Colorado.

Two different hardware systems were used to investigate the effects of contamination found about the orbital assembly and to measure the sky brightness background caused by solar illumination of particulate contaminants. One system was the Sample Array (SA) system which was performed on SL-2. The other was the Photometer System (PS) which was performed on SL-2 and SL-3.

a. Surface Deposition. [30] "The sample array system contained 248 optical surfaces and exposed outside the OWS did not collect any significant contaminants. Only trace amounts of surface deposited contaminants have been seen, in all cases the measurement was near the limiting sensitivity of the instrument. Unfortunate performance compromises and the relative cleanliness of the assembly (result of a rigorous NASA Skylab contamination control program) on the anti-solar side appeared to place the amount of available surface contaminants near the limiting sensitivity of the sample array. Mass spectroscopy on the trace contaminants show the presence of high molecular weight species, up to 773 amu. The data suggests the presence of condensed aromatics.

Surface deposition of contaminants on Skylab was very evident in the area of the EVA (extravehicular activity) quadrant of the airlock module. Photographs taken during each of the three missions show a darkening of the white surfaces into a yellow brown color. Several of the experiments performed in this area were affected by contaminants. Samples of contaminated surfaces from S230 principal investigator Dr. D. Lind, D024 principal investigator Dr. W. Lehn, S020 principal investigator Dr. R. Tousey, and S228 principal investigator Dr. P. Price, were studied in our laboratory.

Several S230 metal foil detector cuffs were exposed throughout the Skylab mission on the ATM strut deployment spools. The foil detector cuffs were retrieved and refurbished by EVA and returned to earth for analysis. Eleven small strips were measured for total reflectance from 0.25 μm to 2.5 μm and directional reflection with hemispherical incident infrared radiation from 1.2 μm to 20.5 μm . The foils were visibly contaminated with a film and the reflectance was significantly lower than the backup foils which remained on the

ground. The reflectance was used to calculate the solar absorptance of the foils and the observed interference bands throughout the visible wavelength region were used to calculate the thicknesses of the contaminant. Figure 57 shows an example of these bands.

Infrared absorption bands of the contaminant on the S230 foils were observed. "Because the Coolanol-15 (thermal control fluid) reservoirs are located behind the shroud of the airlock module and it was necessary to recharge the system because of a drop in pressure, Coolanol has been considered a prime candidate as the contaminant." Absorption bands for Coolanol-15 were obtained for comparison with the S230 contaminant. "While the absorption bands of the contaminant show some correlation to Coolanol-15, there is insufficient evidence to definitely point to contamination by this fluid."

"Selected thermal control coatings of D024 were exposed during the mission on the airlock module truss. The samples became progressively darker on the later missions, once again covered with a yellow-brown film. A section of one metal handle was measured in our laboratory to obtain the absorption bands of the contaminant. Very strong and broad absorption bands were seen from $9\text{ }\mu\text{m}$ to $11\text{ }\mu\text{m}$, suggesting a siliceous material. Although the composition of Coolanol-15 is proprietary, the transmission spectra indicates that it is a saturated alkyl silicone."

"The S020 UV/X-ray spectrograph mounted to a strut near the EVA hatch of the airlock module experienced a significant decrease in the transmission of their indium and beryllium thin film filters. Two main absorption bands were attributable to a contaminant, at $9.9\text{ }\mu\text{m}$ and $13.5\text{ }\mu\text{m}$. Once again there are too few bands to definitely determine the contaminant species.

Lexan plastic sheets of experiment S228 were clipped outside the airlock hatch and the aluminized tape used to hold the sheets showed no visual evidence of contaminant. There were no significant absorption bands in the infrared reflection spectra."

b. Particulate Scattering. "The T027 photometer system was designed to study the nature and extent of contaminants surrounding the OA. The expected information from the photometer data analysis will be:

- A. Brightness and polarization of scattered sunlight from the contaminant cloud,
- B. Spatial distribution and temporal variations of the cloud,
- C. Physical properties of the contaminant particles, and
- D. Guidelines for a model of spacecraft contamination.

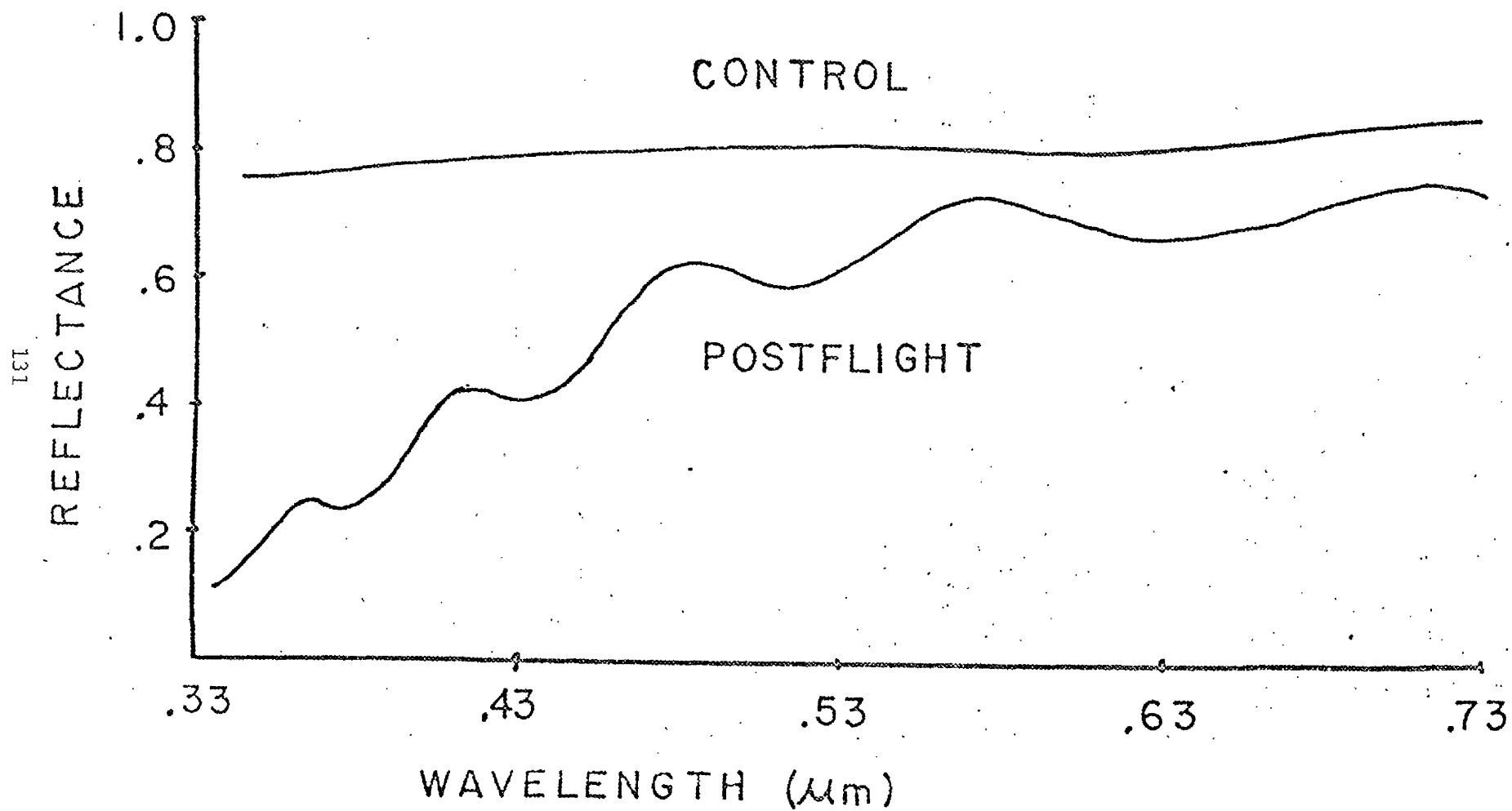


FIGURE 57. REFLECTANCE VERSUS WAVELENGTH FOR S230 ALUMINUM FOIL 4-2

The extendible mast deployed the photometer head through the anti-solar airlock on SL-2 and SL-3. The head was mounted on a gimbal system at the end of the mast allowing scans in elevation and azimuth through limits of 0° to 112.5° and 0° to 354° , respectively. The photometer head contains a Fabre optical train with a rotating polarizing disk, ten selectable filters, a variable field-of-view wheel, and a thermoelectric cooler/heater to regulate the temperature of the photomultiplier cathode. A radioactive low level light source was used to monitor the condition of the head. A 16mm camera recorded the objects in the field-of-view. Sunshields allowed data acquisition to within 18° of the sun or other bright sources. Twenty three telemetry channels monitored the photomultiplier voltage; polarizer wheel orientation pulse; temperatures of the cathode area, filter wheel, and light source; elevation and azimuth position; camera and photomultiplier shutters; photomultiplier gain; positions of the filter wheel and field-of-view wheel; and light source position. A programmer allowed automatic performance of any selected program from seven different operations. System monitor, fixed position, verticle circle scan, almucantar scan, detailed limited sky mapping, all sky mapping, and system retraction position were the seven programs to operate the photometer head.

The photometer was extended through the anti-solar airlock twice during SL-2 and eight of the fifteen minimum required programs were performed. Approximately 17.5 hours of data was taken on SL-2. As is the case of the sample array, the performance of the photometer on SL-2 was greatly reduced from the preflight planning. First the solar airlock was unusable, second the system was not performed early in the mission to study early contamination, third only two separate performances were done instead of three widely separated performances, and last only eight of the fifteen minimum programs were done. The photometer was extended through the anti-solar airlock once during SL-3. After performing six different programs, the crew was unable to position the head for retraction and the extended portion of the photometer was ejected from the airlock. Approximately 6.7 hours of data was taken before the head was ejected."

"Two different types of data has been available for the analysis of the photometer data. During the mission at Johnson Space Center strip chart recorders provided GMT, photomultiplier voltage, and polarizer position pulses in near real-time, along with a console video display of the remaining photometer telemetry parameters. Ground site coverage unfortunately was scarce during the times of photometer performance. However, first order estimates in contamination assessment was possible during the mission."

"Processing of the raw telemetry data tapes has been a long and difficult process. It now appears that the experiment user tapes being furnished by Marshall Space Flight Center are correct and the needed tapes are rapidly being delivered. As each tape arrives the photomultiplier voltage data is decompressed by a subroutine called BERNARD which regenerates the data points eliminated by the Skylab telemetry compression scheme. To remove unwanted noise from the decompressed signal, a narrow filter is used on the fast Fourier transform of the original signal. The Fourier transform of the filtered signal in the frequency domain gives the regenerated clean signal. The noisy spikes and the false peaks and valleys which would give erroneous calculations of the percent polarization and azimuth of the polarization ellipse are reduced. Distortion of the information as a function of filter bandwidth has been studied and selection of bandwidth is not difficult. When the full processing plan is in operation, the data reduction will be displayed in the form of plots of radiance, brightness (in units of solar surface brightness B/B_0), polarization versus angle for each filter. After the sky background is removed, a series of isoline plots of brightness for the cloud in polar coordinates at different times in the mission will be used to develop the spatial and temporal variations of the cloud. The physical properties of the contaminant particulates will be determined by applying scattering theory to all the data obtained from the various scanning and fixed position programs."

"The processed data at this time is still too minimal to draw any conclusions. However, the near real-time data combined with the small amounts of processed magnetic tapes does indicate that scattered light levels of the order of zodiacal light to two orders of magnitude above that have been measured. The amount of particulates appears transient, for the scattered light levels change within minutes.

Once all the data is processed, the scattered light values will be compared to theoretical values predicted by Mie theory. A FORTRAN program (MIESCA) has been constructed to calculate the total brightness and the ratio of polarization intensities in two perpendicular planes. The column density and size distribution will be determined by comparing the brightness and polarization measured in flight with the theoretical calculations. By assuming the composition of the particulates and varying the size distribution the model should converge to the measured flight values. The size distribution function used in our model is a Zeroth order logarithmic distribution (ZOLD)."

REFERENCES

1. Skylab Mission Report, First Visit. JSC-08414, Revision A., June 1974.
2. Skylab Mission Report, Second Visit. JSC-08662. January 1974.
3. Skylab Mission Report, Third Visit. JSC-08963. July 1974.
4. Potter, A.E.; Grandfield, A.L. and Williams, C.K.: "Flight Performance of the Skylab Earth Resources Experiment Package". NASA Lyndon B. Johnson Space Center, Houston, Texas, AAS74-141.
5. Houston, R.S. and Marrs, R.W.: "Use of Skylab S190A and S190B Photographs in Wyoming Earth Resources Studies". University of Wyoming, Laramie, Wyoming, AAS74-142.
6. Eagleman, J.R. and Ulaby, F.T.: "Remote Sensing of Soil Moisture by Skylab Radiometer and Scatterometer Sensors". University of Kansas, Lawrence, Kansas, AAS74-146.
7. Mission Requirements, First Skylab Mission, SL-1/SL-2. 1-MRD-001F, Volume I, February 1, 1973.
8. Mission Requirements, Second Skylab Mission, SL-3. 1-MRD-001F, Volume II, June 1, 1973.
9. Mission Requirements, Third Skylab Mission, SL-4. 1-MRD-001F, Volume III, August 27, 1973.
10. Siebel, M.P.L.: "Introduction to Space Processing". Proceedings of the Third Space Processing Symposium - Volume I. - NASA M-74-5. June 1974.
11. Kimzey, J.H.: "Skylab Experiment Zero Gravity Flammability". Proceedings of the Third Space Processing Symposium - Volume I. NASA M-74-5. June 1974.
12. McKannan, E.C. and Poorman, R.M.: "Skylab M551 Metals Melting Experiment". Proceedings of the Third Space Processing Symposium - Volume I. NASA M-74-5. June 1974.
13. Williams, J.R.: "Skylab Experiment M552 Exothermic Brazing". Proceedings of the Third Space Processing Symposium - Volume I. NASA M-74-5. June 1974.

14. Larson, D.J.: "Skylab M553 Sphere Forming Experiment". Proceedings of the Third Space Processing Symposium - Volume I. NASA M-74-5. June 1974.
15. Wiedemeier, H.; Klaessig, F.C.; Wey, S.J. and Irene, E.A.: "Vapor Growth of GeSe and GeTe Single Crystals in Micro-Gravity".
16. Reger, J.L.: "Experiment No. M-557 Immiscible Alloy Compositions". Proceedings of the Third Space Processing Symposium - Volume I. NASA M-74-5. June 1974.
17. Ukanwa, A.O.: "M558 Radioactive Tracer Diffusion". Proceedings of the Third Space Processing Symposium - Volume I. NASA M-74-5. June 1974.
18. Voltmer, F.W.: "Influence of Gravity-Free Solidification on Microsegregation". Proceedings of the Third Space Processing Symposium - Volume I. NASA M-74-5. June 1974.
19. Walter, H.U.: "Seeded, Containerless Solidification of Indium Antimonide". Proceedings of the Third Space Processing Symposium - Volume I. NASA M-74-5. June 1974.
20. Kawada, Tomoyoski: "Preparation of Silicon Carbide Whisker Reinforced Silver Composite Material in a Weightless Environment". Proceedings of the Third Space Processing Symposium - Volume I. NASA M-74-5. June 1974.
21. Witt, A.F.; Gatos, H.C.; Lichtensteiger, M.: "Steady State Growth and Segregation Under Zero Gravity: In Sb". Proceedings of the Third Space Processing Symposium - Volume I. NASA M-74-5. June 1974.
22. Yee, James F.; Sen, Sanghamitra; Samra, Kalluri; Lin, Mu-Ching; Wilcox, William R.: "Directional Solidification of InSb - GaSb Alloys". Proceedings of the Third Space Processing Symposium - Volume I. NASA M-74-5. June 1974.
23. Yue, A.S., Yu, J.G.: "Halide Eutectic Growth". Proceedings of the Third Space Processing Symposium - Volume I. NASA M-74-5. June 1974.
24. Deruyttere, A.; et al.: "Silver Samples Melted in Space". Proceedings of the Third Space Processing Symposium - Volume I. NASA M-74-5. June 1974.
25. Hasemeyer, Earl A.; Lovoy, Charles V.; Lacy, L.L.: "M566 Copper-Aluminum Eutectic". Proceedings of the Third Space Processing Symposium - Volume I. NASA M-74-5. June 1974.

26. Lehn, William L.: First Interim Status Report, Air Force Materials Laboratory, W-PAFB September 1973.
27. Randle, Robert J.: "Summary Results of Skylab Experiments T002 on SL-3". NASA ARC, Moffett Field, California. LTI-239-3, Dec. 1973.
28. Powers, Stanley W.: "Preliminary Results from Skylab Experiment T002". U.S. Air Force Academy, Colorado. May 1974.
29. Randle, Robert J.: "Summary Results of Skylab Experiment T002 on SL-4". NASA. ARC, Moffett Field, California. LTI-239-3, April 1974.
30. Muscari, J.A.; Jambor, B.J.; Westcott, R.A.: "Preliminary Results Skylab Experiment T027 Optical Contamination in Space". International Conference Space Environment Effects on Materials. Toulouse, France. June 17-22, 1974.

APPROVAL

TM X-64881

MSFC INTEGRATED EXPERIMENTS

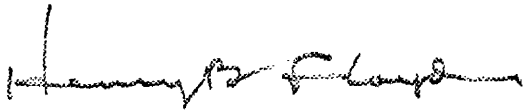
PRELIMINARY REPORT

BY

EXPERIMENT DEVELOPMENT AND PAYLOAD EVALUATION
PROJECT OFFICE

The information in this report has been reviewed for security classification. Review of any information concerning Department of Defense or Atomic Energy Commission programs has been made by the MSFC Security Classification Officer. This report, in its entirety, has been determined to be unclassified.

This document has also been reviewed and approved for technical accuracy.



Henry B. Floyd, Manager
Experiment Development and
Payload Evaluation Project Office



Rein Ise
Manager, Skylab Program Office